STELLINGEN

behorende bij het proefschrift van

V. BRANDWIJK

I.

Het zou van groot nut zijn, als enkele essentiële begrippen in de kristalchemie, zoals dichtstgepakte laag, stapeling, perovskietstructuur, duidelijker werden gedefinieerd.

Dit proefschrift.

II.

Het is niet nodig kation-kation binding in te voeren om de $BaNiO_3$ h-, $BaRuO_3$ hhc- en $BaTiO_3$ hcc-structuurtypen te verklaren.

L. Katz en R. Ward, Inorg. Chem. **3**, 205 (1964)
Dit proefschrift.

III.

In de afleiding van de kristallografische puntgroepen, zoals die door Buerger is gegeven, is een fout geslopen, zodat er slechts 31 werden gevonden.

M.J. Buerger, Elementary Cristallography, John Wiley, New York, 1956, pg. 52.

IV.

De verandering in de isomerenverdeling in de tijd bij de thallering van tolueen met thallium triacetaat moet worden toegeschreven aan het optreden van transthallering.

J.M. Briody en R.A. Moore, J. Chem. Soc. Perkin II, 179 (1972)
A.V. Huygens, Proefschrift, Leiden, 1972
A.V. Huygens, J. Wolters en E.C. Kooyman, Tetrahedron Letters 3341 (1970)
J. Spierenburg, Proefschrift, stelling 7, Leiden, 1970

V.

Een goede synthese van tetrafenylmethaan lijkt mogelijk via (trifenylmethyl)-trifenyllood.

L.C. Willemsens en G.J.M. van der Kerk, Investigations in the Field of Organolead Chemistry, Inst. Org. Chem. TNO, Utrecht, ILZRO, New York, p. 44

VI.

Zoals blijkt uit de magnetische gegevens van $RbFeCl_3$ moet men voorzichtig zijn een verband te leggen tussen de magnetische structuur en de paramagnetische susceptibiliteit van ketenverbindingen.

V.J. Minkiewicz, D.E. Cox en G. Shirane, Solid State Comm. **8**, 1001 (1970)
A. Epstein, J. Makovsky en H. Shaked, Solid State Comm. **9**, 249 (1971)
N. Achiwa, J. Phys. Soc. Japan, **27**, 561 (1969)
G.R. Davidson, M. Eibschütz, D.E. Cox en V.J. Minkiewicz, Magnetism and Magnetic Materials Conference, Chicago, 1971

VII.

Het is niet juist in de uitdrukkingen voor $\chi_{//}$ en $\chi_{\perp}$ van het 1-dimensionale Ising model een gemiddelde waarde voor de exchange constante J en de g-factor te gebruiken, omdat dit strijdig is met het anisotrope karakter van het Ising model.

K. Takeda, S. Matsukawa en T. Haseda, J. Phys. Soc. Japan **30**, 1330 (1971)

VIII.

De redenen die Scott en Remeika aanvoeren voor de voorspelling dat $SmAlO_3$ nog een fase overgang dichtbij het smeltpunt zou kunnen hebben, zijn onvoldoende gegrond.

J.F. Scott en J.P. Remeika, Phys. Rev. **1B**, 4182 (1971)
J.F. Scott, Phys. Rev. **183**, 823 (1969)
S. Geller en P.M. Raccah, Phys. Rev. **2B**, 1167 (1970)

IX.

Het begrip 'onrijpheid' in het oeuvre van Witold Gombrowicz (1904-1969) is een niet te onderschatten aanval op de hedendaagse Westerse beschaving.

Derivation and discussion of crystal structures of compounds ABX_3 and A_2BX_6

Derivation and discussion of crystal structures of compounds ABX_3 and A_2BX_6

PROEFSCHRIFT
TER VERKRIJGING VAN DE GRAAD VAN DOCTOR IN DE WISKUNDE EN NATUURWETENSCHAPPEN AAN DE RIJKSUNIVERSITEIT TE LEIDEN, OP GEZAG VAN DE RECTOR MAGNIFICUS DR. A.E. COHEN, HOOGLERAAR IN DE FACULTEIT DER LETTEREN, VOLGENS BESLUIT VAN HET COLLEGE VAN DEKANEN TE VERDEDIGEN OP WOENSDAG 22 NOVEMBER 1972 TE KLOKKE 16.15 UUR

DOOR

VAS BRANDWIJK

GEBOREN TE BRANDWIJK IN 1943

DRUK: elve/labor vincit, leiden

PROMOTOR: PROF.DR. E.W. GORTER †
CO-PROMOTOR: PROF.DR. G. BLASSE

in het bijzonder voor mijn vader en moeder

ik zit op een pier aan de haven, één van de talloze havens die ik heb bezocht, en kijk uit over de zee. het drukke gedoe van mensen die als mieren bezig zijn in en uit te laden. grote, fiere schepen, wrakken van houten vissersschepen waarvan de planken grotendeels zijn weggerot en langzaam oplossen in het bruine water.
soms wandelt er een zonderling over de pier. zijn ogen staan er niet naar dat hij snel moet gaan werken of eten of met iemand praten. evenmin ziet het er naar uit dat hij iets anders nuttigs heeft te doen wat iedereen kan begrijpen. zijn ogen staan dromerig, alsof hij het niet meer zo begrijpt en alleen maar wat tussen het leven door wil voortdobberen. hij behoort niet tot de mensen en ook niet tot de goden. misschien is hij te groot voor de mensen en te klein voor de goden, misschien ook wel te klein voor de mensen en te groot voor de goden, want wie zou de volgorde vaststellen. misschien is er wel helemaal geen orde en is hij gewoon geen mens en geen god maar een zwerver.
ik zit op de pier en kijk uit over de zee. de golven spatten uiteen op de rotsen, donkerblauw is de zee in de verte, dichtbij is hij lichtblauw. soms loopt er opeens een veel lichtere streep doorheen. naast me zit een vrouw met twee kinderen.
– bent u van deze stad – , vraagt ze.
– nee – , is mijn antwoord.
en ze praat niet verder, want hoe zou ze kunnen praten met iemand die niet van deze stad is. zwijgend tuur ik verder over het water. in de verte tegen de zon in ligt een andere pier. een jongen staat er te vissen. de zon glijdt over zijn naakte lichaam. soms komt er een grote golf aanrollen vanuit de zee. hij slaat kapot op de stenen en werpt een mensenhoge stortvloed van water over de jongen heen. druipend komt hij even later weer te voorschijn in de zon. zijn lichaam staat gebogen naar de hengel. de beeldhouwers probeerden hem uit steen te slaan. ook zij leefden van de zon, de zee en de aarde. gewone zwervers. geen mensen, ook geen goden. zwervers. toevallig beeldhouwers. er zijn al eindeloze rijen zwervers daarna geweest, ook beeldhouwers. er zijn eindeloze rijen jongens daarna geweest, ook uitgehouwen. maar je kunt ze de hele dag zien, niet uitgehouwen. waarom zou je niet een mens worden of een god. geen zwerver. geen zwerver die beeldhouwt. geen zwerver die schrijft. misschien alleen maar om een beetje te zien, om de mensen een beetje te laten kijken, en de goden. alleen maar, omdat ze er van houden.

CONTENTS

INTRODUCTORY REMARKS

CHAPTER I DERIVATION AND DISCUSSION OF CRYSTAL STRUCTURES OF COMPOUNDS ABX_3 AND A_2BX_6

PART I DERIVATION OF THE STRUCTURES

Abstract

I.1. Introduction

I.2. Derivation of ideal structures

I.2.1. Derivation of AX_3 structures

I.2.2. Derivation of ABX_3 and A_2BX_6 structures

I.2.3. Selection of A_2BX_6 structures by means of space-filling polyhedra of the anions

I.2.3.1. A_2BX_6 structures based on AX_3-layers with T-pattern

I.2.3.2. A_2BX_6 structures based on AX_3-layers with T_mR_n-patterns

I.2.4. Removal or substitution of anions in the ideal structures

I.3. Deviations from the ideal structures

I.3.1. Deformations of the ideal structures due to a difference in size between A and X ions

I.3.2. Deformations of the ideal structures due to deformed BX_6-octahedra

References

CHAPTER II DERIVATION AND DISCUSSION OF CRYSTAL STRUCTURES OF COMPOUNDS ABX_3 AND A_2BX_6

PART II STRUCTURAL CHEMISTRY OF ABX_3 HALIDES

Abstract

II.1. Introduction

II.2. Discussion of the derived ABX_3 structures

II.3. The structure types found for ABX_3 halides

II.3.1. Structures of ABX_3 halides in which the A ion is larger than the X ion

II.3.2. Structures of ABX_3 halides in which the A ion is smaller than the X ion

II.3.3. Deformations of the derived structures due to the electron configuration of the B ion

II.3.4. Structures of ABX_3 halides not derivable from AX_3-layers with T-pattern

II.4. Discussion of the experimental inter- and intralayer distances, reduced c/a-values and volumes per formula unit ABX_3

II.4.1. Inter- and intralayer distances and reduced c/a-values as a function of the radii of A , B and X ions

II.4.2. Volumes per formula unit ABX_3

II.5. Comparison of expected and reported structure types for ABX_3 halides

II.6. Structures of ABX_3 halides at non-ambient temperatures and pressures

II.6.1. Non-ambient temperatures

II.6.2. Non-ambient pressures

Conclusions

References

CHAPTER III THE EFFECT OF PRESSURE ON A_2BX_6 HALIDES, CONTRARY TO THE EFFECT OF PRESSURE ON ABX_3 HALIDES

Abstract

III.1. Introduction

III.2. Experimental

III.3. Results and discussion

References

SAMENVATTING

INTRODUCTORY REMARKS

In the present thesis an attempt is made to derive crystal structures of compounds ABX_3 and A_2BX_6 in a systematic way, using mainly qualitative electrostatic bonding rules (Chapter I) (1) (A represents a large cation that can replace an anion, B is a small interstitial cation, X is a halogen ion). In Chapter II the derived structures are compared with the structure data that are reported in the literature for ABX_3 halides (2). A paper in which the derived structures are compared with the structure data reported for A_2BX_6 halides is in preparation (3). In this paper it is predicted that the fraction of h-stacked AX_3-layers with T-pattern increases with pressure for A_2BX_6 halides contrary to the effect of pressure on ABX_3 halides. Since no data were available in the literature to prove this prediction, we investigated experimentally the effect of pressure on some A_2BX_6 halides (Chapter III) (4).

References

1. A.B.A. Schippers, V. Brandwijk and E.W. Gorter, to be published in the J. Solid State Chem., Volume **6**, Issue 4 (1973).
2. V. Brandwijk, A.B.A. Schippers and E.W. Gorter, to be published.
3. V. Brandwijk, A.B.A. Schippers and E.W. Gorter, to be published.
4. V. Brandwijk and D.L. Jongejan, Mat. Res. Bull. **7**, 635 (1972).

CHAPTER I

DERIVATION AND DISCUSSION OF CRYSTAL STRUCTURES OF COMPOUNDS ABX_3 AND A_2BX_6

PART I. DERIVATION OF THE STRUCTURES

A.B.A. Schippers, V. Brandwijk and E.W. Gorter.
Dept. of Solid State Chemistry, Gorlaeus Laboratories, P.O. Box 75, Leiden, The Netherlands.

Abstract

In this series of papers the crystal structures of compounds with compositions ABX_3 and A_2BX_6 are derived from a basic lattice, using mainly qualitative electrostatic bonding rules (Part I). (A represents a large cation that can replace an anion, B is a small interstitial cation, X is a halogen ion.)
In Part II a method will be outlined for selecting the appropriate structure for a particular compound. This method is tested on the experimental structure data of the ABX_3 halides in Part II, and applied to compounds A_2BX_6, A_2BX_{6-p}, Y_p, and $A_2BX_{6-p'-p''}Y_{p'}Z_{p''}$ in Parts III, IV and V, respectively (X=halogen; Y, Z=halogen, O, OH, H_2O, N or an anion vacancy).
In the present paper (Part I) we start with the derivation of the ideal structures (*i.e.* for A and X ions of equal diameter), for hypothetical compounds AX_3. It is shown that, if A-A contacts are not allowed in a stacking of trigonal nets (*viz.* in 'close packed' layers), each layer must have the composition AX_3 and the same type of order. This order can be one of two simple types ('T' and 'R') or any combination of these. From these AX_3 structures the ABX_3 and A_2BX_6 structures are derived. On the basis of mainly simple electrostatic considerations, structures with anion surroundings that are most unlikely are excluded. Use is made of the representation of anion surroundings by space-filling polyhedra (SFP). Finally, the deviations from the ideal ABX_3 and A_2BX_6 structures, resulting from variations in size of the A, B and X ions, are considered.

I.1. Introduction

In our laboratory a broad investigation is in progress into the possibility of predicting or deriving —fairly roughly— a crystal structure for any given compound ${}^aA_m{}^bB_n{}^xX_p$, where a, b and x represent the coordinations of the cations A and B and anions X, respectively. Having designed a structure, a compound —or compounds— must be selected that may show this crystal structure. When attempts to prepare these compounds succeed, the structure may prove to be different from the predicted one. This may mean either that we have chosen the wrong substance or that the compound may assume the predicted structure at a different temperature and/or applied pressure or that our model is wrong. Alternately, for all likely compounds another structure

may be more stable, even if slightly so. The calculation of small differences in stability will remain difficult for some time to come, in spite of the recent improvement of calculating facilities. If preparation of the selected compound fails, this may be due to the wrong choice of method, *i.e.* to our lack of industry, preparative skill or technical possibilities, or to the formation of other stable compounds, which together have the same overall composition. It is, therefore, difficult to know whether a certain structure will exist or not, and equally difficult to decide when to stop our attempts at preparing a particular compound. For these reasons it would be desirable to make the prediction of structures in a systematic way. This would also be of great help in indexing an X-ray powder diagram, since a rough structure prediction usually yields the correct space group and the rough cell dimensions and atomic parameters. As an example of such an approach we selected a class of compounds of composition A_2BX_6, on which little structural research has been done and which have structures closely related to a class of compounds of composition ABX_3, which have been the subject of extensive research.

In the present paper certain assumptions will be used, a.o. the concept of a 'basic lattice', some of Pauling's rules, and one of those used by Gorter. The greater part of these rules are derived from a simple electrostatic model, which has been shown to explain a great many structures of compounds $A_m B_n X_p$ (1,2). Other conditions will be imposed only in order to delimit the field of investigation.

The AX_3 structures formed by the positions of A and X ions in compounds ABX_3 and A_2BX_6 are derived first. These AX_3 structures need not (and do not) exist for ionic compounds, but they do exist in certain alloys. The method by which they are derived resembles that used by Beck for the derivation of structures for alloys AB_3 (3). Next, it has to be examined which of the interstices can be completely or partly filled by B ions. Finally, the deviations from these 'ideal' structures that result from a variation of the radii of A, B and X are derived.

The structures derived in the present paper will be compared with the structures of the ABX_3 halides in Part II. In the second paper (Part II) also semi-empirical rules will be derived for making the selection of a structure for a particular compound possible. These rules will be checked against the vast number of experimental structural data on ABX_3 halides. In the third, fourth and fifth papers of this series the method developed in Part I and tested in Part II will be applied to compounds A_2BX_6, $A_2BX_{6-p}Y_p$, and $A_2BX_{6-p'-p''}Y_{p'}Z_{p''}$, respectively (X=halogen; Y, Z=halogen, O, OH, H_2O, N, anion vacancy). Reviews concerning the properties of halides and their preparation (4,5,6,7), which were published recently, have been of great use to this investigation.

I.2. Derivation of ideal structures

It is our contention that most structures of inorganic compounds that may be described as ionic can be derived by placing that ion type —cations or anions—, of which a larger proportion is present, on a 'basic' lattice. Except in the so-called anti-structures these ions

are the anions. The cations are then inserted on part of the interstitial positions of this basic lattice. These ions will also form a basic lattice, as far as is possible for the given stoichiometry. We shall arbitrarily define the basic lattice as follows: Basic lattices are composed of trigonal nets and would have a 'packing density' of >50%, if the lattice points were occupied by spheres of equal size that are in contact with each other. Basic lattices are: face-centred cubic (f.c.c.), hexagonal 'close-packed' (h.c.p.)☆, '$MoSi_2$' ○, body-centred cubic (b.c.c.), simple cubic (s.c.), simple hexagonal (s.h.) *etc.* The arguments for choosing this definition can be related to the problem of finding the most likely distributions of charges in space that possess translation symmetry. Since the ions have a more or less variable size, the potential energy will reach a minimum at a certain distance between cations and anions.

If the ions do not fit exactly into the interstices of a certain basic lattice a structure with lower potential energy may be attained by deforming the structure either with or without complete preservation of the symmetry, or by choosing a different basic lattice. For an example of such a derivation, see Section I.3.

In addition to the above condition that charges of the same sign have to form a basic lattice, each charge has to be surrounded by equally spaced-out charges of opposite sign, *i.e.* isonomously. Requirements of isonomy as well as stoichiometry may cause the basic lattices to be only partly filled.

The above working rules have to be supplemented as follows:

a) Polarisation may cause the surrounding of large and polarisable ions to be less isonomous (1) and may cause a too low 'packing density' of the basic lattice of the interstitial ions.

b) Large cations may replace part of the anions in a basic lattice in an ordered manner, if their size makes them fit there.

When experimentally determined structures do not obey the rules discussed above, this must be traceable to effects like cation-cation or anion-anion bonding, lone electron pairs, *etc.* These effects must be treated starting from another more refined model.

In the present paper we have refrained from placing our ideas against the background of the work of other investigators. A historical introduction and a more extensive discussion of the rules will be given elsewhere (9).

☆ Together with the c (f.c.c.) and the h (h.c.p.) 'close-packed' lattices mixed c-h stackings can be mentioned; these are considered separately (Section I.3.).

○ By '$MoSi_2$' those lattices are meant in which each point has the same 10-coordination such as the lattices formed by metal and silicon ions together in $MoSi_2$, $CrSi_2$ and $TiSi_2$ (8).

For the derivation of the ideal structures for compositions ABX_3 and A_2BX_6, the following conditions are imposed only in order to delimit the subject:

a) The limitation of the stoichiometry $A_mB_nX_p$ to ABX_3 and A_2BX_6 we made already at the outset.

b) The large cations (A) together with the anions (X) form a three-dimensional lattice with over-all composition AX_3. These lattices consist of trigonal nets, stacked in such a way that each lattice point has twelve nearest neighbours at equal distances: these are the well-known 'close-packed' lattices.[☆] The choice of the close-packed lattices is also influenced by the fact that in most other lattices mentioned above no interstices with a regular surrounding of lattice points are available for the B ions.

c) The A ions, *i.e.* the large ions present in smaller number, shall not be adjacent to each other. This condition results from any difference in electronegativity between A and X and is also valid for certain classes of alloys.

I.2.1. Derivation of AX_3 structures

The close-packed lattices are composed of trigonal nets lying at a certain fixed distance from each other. For deriving structures of composition AX_3 we start by examining which of the ordered arrangements of A and X ions in a trigonal net (Fig. I.1.) of composition AX_3 satisfy the above condition (c). With these layers structures of composition AX_3 can be built, if restriction (c) is taken into account.

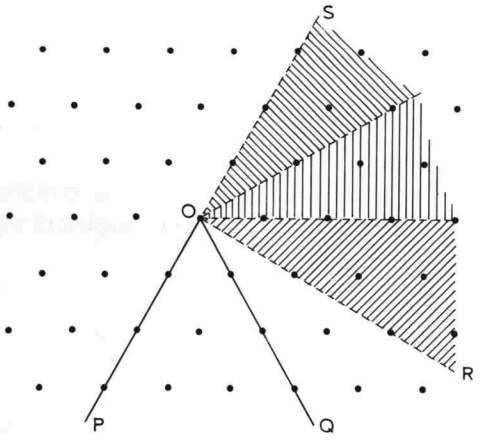

Fig. I.1.

Trigonal net. The positions of the lattice points in a trigonal net can be described by a hexagonal coordinate system. A translation vector is represented by the coordinates of the lattice point at the end of the vector. At the determination of all two-dimensional cells (Fig. I.2.) the first translation vector lies between OP and OQ. The second vector must make an angle $90^\circ \leqslant \beta \leqslant 120^\circ$ with the first, and must, therefore, lie between OR and OS.

A systematic way to find all types of order of A and X ions in a trigonal net is to determine all two-dimensional unit cells that may occur in such a net. Restrictions have to be imposed in order to prevent the number of unit cells from becoming infinite. The conventions concerning lattice description impose a restriction relating to the shape of the two-dimensional unit cell. The angle between the two translation vectors has to satisfy the condition $90° \leqslant \beta \leqslant 120°$ (11). A unit cell that would not fulfil this condition can be transformed into a cell with the same area, the angle of which does satisfy this condition. Now a unit cell may still contain an infinite number of lattice points. Therefore, we confine our attention to two-dimensional unit cells that do not contain more than twenty lattice points. This number is, of course, arbitrary, but even so rather large three-dimensional unit cells may occur[○]. In order to derive structures of alloys essentially the same approach was suggested by Beck (3)[△]. Because our approach deviates slightly from the procedure followed by Beck, we briefly summarize our calculation by means of a flow-chart (Fig. I.2.). For a more detailed description the reader is referred to Beck's paper (3).

In order to obtain layers of composition AX_3 one-quarter of the lattice points have to be occupied by A ions and the remaining ones by X ions. In other words, only those two-dimensional unit cells can be selected that contain four lattice points or a multiple of four. The most simple patterns, three in all, are derived from unit cells that contain only four lattice points. Of these, two remain when condition (c) is obeyed, *viz.* the well-known triangular (T) (Fig. I.3a.) and rectangular (R) (Fig. I.3b.) types of order..

Within certain delimitations on the size of the three-dimensional unit cell[□], we have found that only AX_3 structures of which the patterns in the layer are composed of T- and/or R-motifs are in agreement with restriction (c). We should have liked to give a rigorous proof, also for all larger cells, but we have not been able to do so. Instead we shall give a simple reasoning that makes this seem plausible.

The ordered patterns that are not exclusively composed of T- and/or R-motifs can be derived from the larger two-dimensional unit cells and can be described in terms of parts (or motifs) of more simple[◇] patterns (See, *e.g.* Fig. I.3d.). In order to obtain the composition AX_3, motifs of composition $AX_{3+\delta}$ have to be combined with motifs of composition $AX_{3-\epsilon}$ in the correct proportion. However, restriction (c) sets a lower limit to the anion-cation

☆ We prefer to avoid the term 'close-packing', since it is often interpreted too literally. The large ions that constitute a close-packed lattice need not be in contact with each other (10,9). That is why we prefer the term 'trigonal net' to 'close-packed layer'.

○ The volume of the unit cell, if the smallest anions (F^-) are used, would be about 800 $Å^3$ (cubic stacking of layers).

△ Unfortunately, his paper came to our attention only after we had finished the calculation of the two-dimensional unit cells.

□ Only those three-dimensional structures were considered that do not contain more than six different layers and of which the two-dimensional unit cell does not contain more than 20 lattice points.

◇ Simple means that the smallest unit cell by means of which the AX_n-pattern can be described does not contain more than n+1 lattice points.

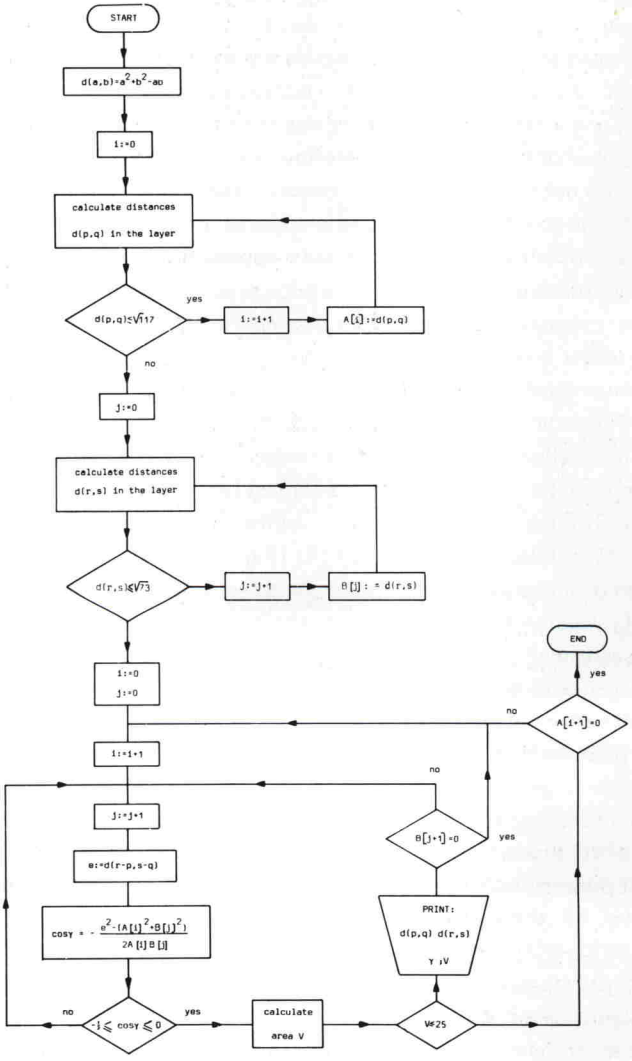

Fig. I.2.

Flow-chart for the calculation of two-dimensional unit cells. The coordinates and the length of the first translation vector are stored in the matrix A[i], these of the second translation vector in the matrix B[j] (Fig. I.1.). An upper limit is set to the maximal length of these vectors. In the course of the calculation a number of cells occurs more than once, but the abundant cells can be removed afterwards.

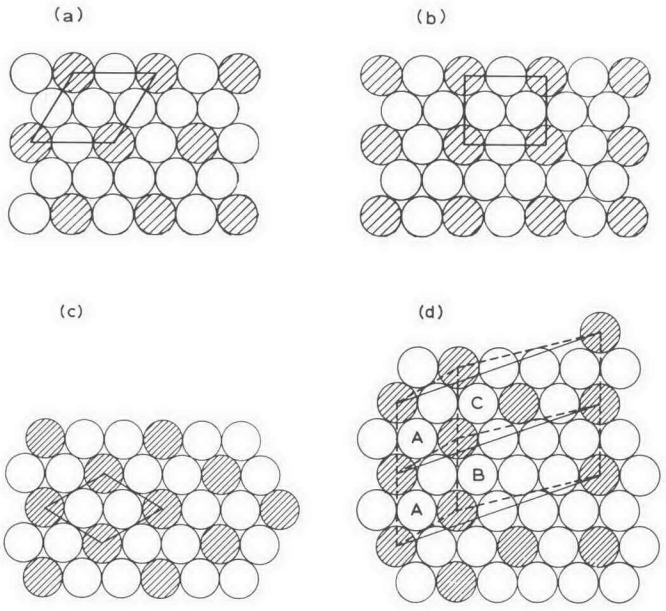

Fig. I.3.
Various types of order of A and X ions in a layer. The A ions are hatched.
a) AX_3-layer with triangular type of order: T-pattern.
b) AX_3-layer with rectangular type of order: R-pattern.
c) AX_2-layer, the honeycomb pattern.
d) Example of AX_3-layer formed by a combination of motifs AX_n, *viz.* AX_2 (denoted by A), AX_6 (denoted by B) and a combination of AX_3 (R-pattern) and AX_2 (denoted by C).

ratio in a layer and this determines the composition of the smallest motif. The limiting composition of an AX_n-layer satisfying, restriction (c) is AX_2. This composition can be realized in only one way, *viz.* the honeycomb pattern (Fig. I.3c.). Such an AX_2-layer can only be stacked with an X_3-layer (restriction (c)), so that the X/A-ratio is at least five. Locally the same holds for the *motif* of composition AX_2. Thus, all complex patterns of composition AX_3 that contain a motif of composition AX_2 cannot be stacked in a 'close-packing' to form an AX_3 structure without allowing A-A neighbours. It remains to be examined, therefore, whether patterns of composition AX_3 that are composed of motifs of composition AX_3 only, can be stacked with each other without violating restriction (c). An AX_3-layer with a pattern composed of T- and/or R-motifs can be stacked only if the pattern in the adjoining layers is identical. Thus, structures of composition AX_3, composed of layers with composition AX_3, meet our requirements only if the pattern in the layer is of the type $T_m R_n$ (m , n = 0,1,2. . .) and the patterns of adjoining layers are identical.

More structures of composition AX_3 can be derived by examining a less well-balanced distribution of the A ions over the layers. In other words, we have to determine if layers of composition $AX_{3+\delta}$, mixed with layers of composition $AX_{3-\epsilon}$ in the proper ratio, may give rise to a structure of composition AX_3. The same arguments as given above can be used here. The limit for a layer of composition $AX_{3-\epsilon}$ is reached for $\epsilon=1$. Such an AX_2-layer can only be stacked with a layer completely filled with anions, giving rise to a composition AX_5. Layers with compositions intermediate between AX_3 and AX_2 must have patterns that are partly composed of the motif of the honeycomb pattern. Layers of this type cannot be stacked with layers of composition $AX_{3+\delta}$ to form an AX_3 structure, without violating restriction (c). Thus, if the composition of the layer deviates from AX_3, no structure of composition AX_3 can be derived that meets our requirements.

I.2.2. Derivation of ABX_3 and A_2BX_6 structures

When trigonal nets occupied by large ions are stacked to form a lattice in the manner of close-packed spheres (condition (b)) interstitial positions of various types are left. The two largest of these sites☆ are surrounded by six and four large ions: when all of these are anions, the interstitial positions, called octahedral and tetrahedral sites, respectively, may be occupied by small cations.

For structures AX_3 that are composed of identical layers with T_mR_n-patterns (Section I.2.1.), the number of available octahedral and tetrahedral sites is as follows:

- Between two T-motifs only one interstitial position, *viz.* an octahedral site, can be occupied by a small cation.
- Between two R-motifs neither octahedral nor tetrahedral sites are available for B ions.

This means that for various patterns T_mR_n the composition for complete occupation of octahedral sites by B ions is $A_{m+n}B_mX_{3(m+n)}$. Only one pattern, T, exists from which structures for the composition ABX_3 can be derived. Structures of composition A_2BX_6 can be derived by complete occupation of the octahedral sites in all AX_3 structures that are composed of TR- or generally T_nR_n-patterns, and by partial occupation of octahedral sites in structures composed of T-, T_2R- or generally T_mR_n-patterns with $m > n$. Before investigating these possibilities of cation-vacancy order in the octahedral sites, we must examine whether restrictions, as mentioned in Section I.2., may also be applied to this case, in order to reduce the number of possible structures. No restrictions as a result of Coulomb repulsion between the cations will be imposed on the type of order *in* the layer of octahedral sites, because the smallest distances between the octahedral sites in this layer in structures of compositions ABX_3, $A_3B_2X_9$, *etc.* are at least twice the smallest X-X distances in the AX_3-net.

☆ Three-coordinated sites will not be taken into account nor will square-pyramidal 5-coordinations. Trigonal-bipyramidal holes can only be filled if the two face-sharing tetrahedra of which they are composed can be occupied.

Since we made the arbitrary restriction that the largest two-dimensional cell in a trigonal AX_3-net does not contain more than twenty particles (Section I.2.), we shall confine ourselves in this case to cells that do not contain more than five positions over which small cations and vacancies can be ordered. The Coulomb repulsion *between* two layers of octahedral sites will not be influenced very much either by the type of order of cations and vacancies in these layers. Therefore, we have maintained the arbitrary limit to the number of layers (see note on page 17): the translation period in the stacking direction does not contain more than six layers[○] with a different type of order of cations and vacancies. Although the number of possible types of order in one layer is small, a large number of structures arises in three dimensions, because the stacking order of the layers of octahedral sites is arbitrary. The number of possible A_2BX_6 structures derived from structures of compositions ABX_3, $A_3B_2X_9$, *etc.*, irrespective of the stacking sequence of the AX_3-layers, has been calculated. Within the geometrical delimitations we made, 147 structures are obtained by leaving half of the octahedral sites empty in an ABX_3 structure, and distributing the B ions equally over all layers. If a less well-balanced distribution of the B ions is considered, another 70,000 structures are added to this number. By leaving some of the octahedral sites vacant in structures of compositions $A_3B_2X_9$, $A_4B_3X_{12}$, *etc.*, about 7,000 structures for the composition A_2BX_6 can be found[☆].
A small part of this large number of A_2BX_6 structures remains if only these structures are permitted, in which the cation arrangement around all anions is isonomous. Of these structures only those are allowed in which most and preferably all anions have the same coordination (Pauling's rule of parsimony (12)). The anion coordination will be investigated in Section I.2.3. with the aid of the space-filling polyhedra (SFP's) of the anions.

I.2.3. Selection of A_2BX_6 structures by means of space-filling polyhedra of the anions

The SFP's of the anions are the smallest polyhedra formed by constructing midway planes between an anion and all anions surrounding it (1). The cations can generally be found on the corners, edges and faces of these polyhedra, or even inside them. Although the term SFP, according to the name, suggests that all SFP's in the whole structure are of the same type, this need not be the case. If the anions are spread over more than one crystallographic position, there is one different SFP for each crystallographic position[△]. The SFP's of the anions, constructed as mentioned above, for the c- and h-stackings of AX_3-layers with T- and R-patterns are drawn in Fig. I.4. Not more than these four different space-filling polyhedra

○ *I.e.*, irrespective of the stacking of the AX_3-layers that can be hexagonal (h), cubic (c) or mixed hexagonal-cubic (hhc , hc , hhcc , hcc , *etc.*).

☆ More detailed information is available on request.

△ The concept SFP is used in a more general sense than Niggli's 'Wirkungsbereich'. The latter is constructed in the same way as a SFP, but the midway planes are between one point of a crystallographic position and its neighbouring points. For a more extensive discussion see Ref. 9.

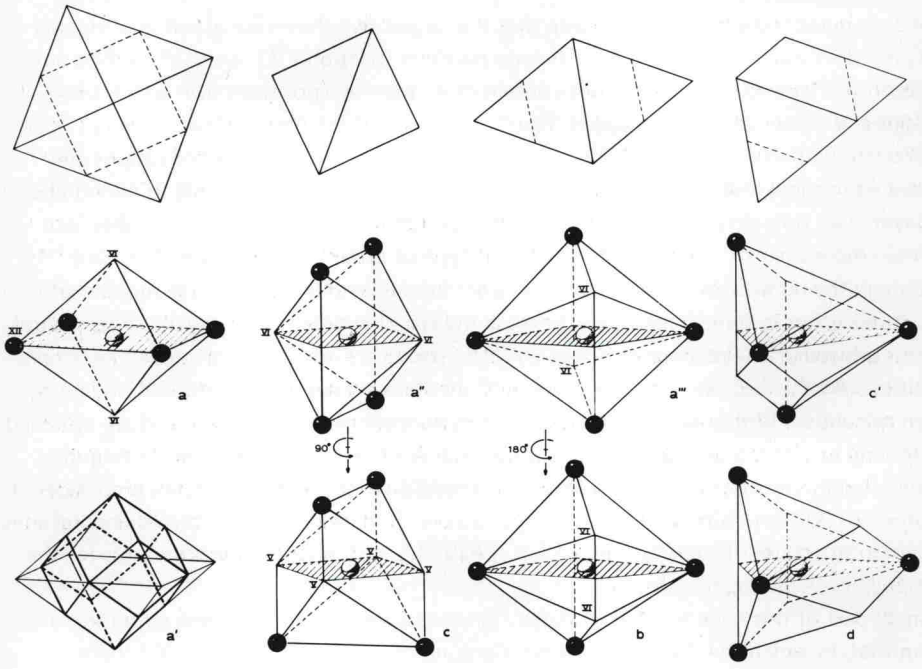

Fig. I.4.

The anion coordination in 'close-packed' structures composed of AX_3-layers with T_mR_n-pattern, indicated by means of their space-filling polyhedra (SFP). Black spheres are A ions, white spheres X ions. In the first column the relation between the anion coordination in a f.c.c. anion lattice (denoted by a') and that in a f.c.c. AX_3 structure (denoted by a). The remaining primes denote different orientations of the polyhedra. In a c-stacked T-motif only the anion-polyhedron denoted by (a) occurs and in a h-stacked T-motif only the SFP denoted by (b). The anion coordinations in both the h- and c-stacked R-motif are of two different kinds: c-stacking: 1 x (a) and 2 x (c) and h-stacking: 1 x (b) and 2 x (d). The number of anions by which the corners of the SFP's are coordinated are indicated by a Roman figure (in the text by a Roman superscript to the left of the symbol of the ion). The equatorial plane in each SFP is hatched. The SFP denoted by (d), can be derived from the SFP denoted by (c') by replacing the bottom half by its mirror image.

(SFP) occur for the anion when the occupation of interstitial positions available for smaller cations is not taken into account. 'Close-packed' structures with other types of order in the AX_3-layers and/or mixed cubic-hexagonal stackings do not give rise to new types of SFP's, but consist of a mixture of these four SFP's.

I.2.3.1. A_2BX_6 structures based on AX_3-layers with T-pattern

In the structures that result when the stacking sequence of AX_3-layers with T-pattern is cubic, hexagonal or mixed cubic-hexagonal, only two different anion coordinations occur, when a possible occupation of the octahedral sites by the smaller cations is not taken into account (Figs. I.4a. and b.). The smaller cations in the $^{XII}A^{VI}B^{VI}X_3$ structures are located on the 6-coordinated positions indicated as VI in the figures. In order to derive structures of composition A_2BX_6 from the ABX_3 structures half of these smaller cations have to be removed. Only six different SFP's result in this way: one with two cations, one with one cation and one with no cation in the octahedral positions, both in the c- (Fig. I.4a.) and in the h- (Fig. I.4b.) stacking. The anion coordination, as shown by the SFP for the c-stacking with vacant octahedral sites, will not occur in A_2BX_6 compounds, since the coordination of the anion by a square of A ions is very unfavourable even when the polarizability of the anion is large☆. This SFP can only be expected if the anion in the centre is replaced by a water molecule or also perhaps by a hydroxyl ion, because the H^+ ions then complete the anion coordination in such a way that the coordination becomes more isonomous. This is also valid for the anion coordination shown by the SFP of the h-stacking with vacant octahedral sites. If the SFP's without B ions are not allowed, the SFP's with two octahedral sites occupied cannot occur either in A_2BX_6 structures, so that only the two SFP's with one octahedral site occupied are left.
Stacking of the SFP's with one octahedral site occupied leads to a number of A_2BX_6 structures, in which the AX_3-layers can form a cubic, a hexagonal and any mixed cubic-hexagonal stacking.

c-stacking

The SFP of Fig. I.4a. with one octahedral site filled can be stacked in only one way as will be obvious from the following reasoning. If one octahedral position is chosen to contain a B ion, the choice for six other octahedral positions is fixed. Three out of these are situated in the layer with octahedral positions immediately above the first one and the remaining three are situated in the layer below. Each of these six positions in turn fixes the choice for the octahedral sites immediately surrounding it. The structure that results will have B ion layers alternately filled and empty. This is the structure of K_2PtCl_6 (13).

h-stacking

The SFP of Fig. I.4b. with one octahedral site occupied can be stacked in several ways. The only restriction is that, if one octahedral position is chosen to contain a B ion, the choice for all octahedral positions on one row parallel to the c-axis is fixed. The octahedral sites on this row will be alternately filled and empty. In other words: the pattern in one layer is repeated

☆ In the structures of alloys of composition AB_3 the coordination of the B atom by a square of A atoms can occur, because the electrons are not localized like, *e.g.* in the structure of Cu_3Au.

Table I.1.

Structures of composition A_2BX_6 derived by removing half of the B ions from the h-stacked ABX_3 structure. In all structures only one anion coordination occurs, *viz.* the SFP of Fig. I.4b. with one octahedral site occupied.

two-dimensional unit cell [a]				occupation of octahedral sites in the		space group	cell parameters, expressed in the shortest X-X distance				number of units A_2BX_6 in the cell
area	a	b	γ	1st layer	2nd layer						
1	1	1	120°	1	0	$P\bar{3}m1$; D^3_{3d}	a=2		c=2/3√6		Z=1
2	1	2	120°	1/2	1/2	Pnnm; D^{12}_{2h}	a=2√3	b=2/3√6	c=2		Z=2
4	2	√3	90°	1/2	1/2	Pbcn; D^{14}_{2h}	a=2/3√6	b=4	c=2√3		Z=4
4	4	1	120°	1/2	1/2	Pnma; D^{16}_{2h}	a=4√3	b=2	c=2/3√6		Z=4
3	3	1	120°	1/3	2/3	C 2/m; C^3_{2h}	a=6√3	b=2	c=2/3√6	β=90°	Z=6
3	√3	√3	120°	1/3	2/3	$P\bar{3}1m$; D^1_{3d}	a=2√3		c=2/3√6		Z=3
4	2	2	120°	1/4	3/4	$P\bar{3}m1$; D^3_{3d}	a=4		c=2/3√6		Z=4
4	2	√3	90°	1/4	3/4	P 2/m; C^1_{2h}	a=2√3	b=4	c=2/3√6	β=90°	Z=4
4	4	1	120°	1/4	3/4	P 2/m; C^1_{2h}	a=4√3	b=2	c=2/3√6	β=90°	Z=4
5	√3	√7	109°6′	1/5	4/5	C 2/m; C^3_{2h}	a=2	b=10√3	c=2/3√6	β=90°	Z=10
5	1	5	120°	1/5	4/5	C 2/m; C^3_{2h}	a=2√3	b=10	c=2/3√6	β=90°	Z=10
5	√3	√7	109°6′	2/5	3/5	C 2/m; C^3_{2h}	a=2√3	b=10	c=2/3√6	β=90°	Z=10
5	√3	√7	109°6′	2/5	3/5	C 2/m; C^3_{2h}	a=2√3	b=10	c=2/3√6	β=90°	Z=10
5	1	5	120°	2/5	3/5	C 2/m; C^3_{2h}	a=10√3	b=2	c=2/3√6	β=90°	Z=10
5	1	5	120°	2/5	3/5	C 2/m; C^3_{2h}	a=10√3	b=2	c=2/3√6	β=90°	Z=10

[a] The area is expressed in the number of B ions in the two-dimensional unit cell, the axes a and **b** are expressed in the shortest B-B distance (= two times the shortest X-X distance).

in the next layer, but now the positions of B ions and vacancies are interchanged. Thus, only, the type of order *in one layer* can be varied independently. The number of structures that can thus be derived is fifteen.

The space groups and the cell dimensions of these structures are given in Table I.1. Only one of these fifteen structures has each kind of ions in only one crystallographic position, *viz.* the structure in which the layers with octahedral sites are alternately vacant and occupied by B ions. This structure is adopted by K_2GeF_6 (14). The remaining fourteen structures have been excluded, since they do not follow so well the rule of parsimony.

Mixed cubic-hexagonal stackings

It is clear that for each of the mixed cubic-hexagonal stackings only one structure will be found, because one c-stacked AX_3-layer determines the type of order in the two surrounding layers of octahedral sites: one layer is filled with B ions and the other is empty. All these structures with mixed stackings, therefore, have layers of octahedral sites that are alternately occupied and empty.

I.2.3.2. A_2BX_6 structures based on AX_3-layers with T_mR_n-patterns

A disadvantage of the structures containing the SFP's of Figs. I.4a. and b. with only one octahedral site occupied may be that the surrounding of the anion is rather irregular. This is true to a greater extent for the anion coordination in the c- than for that in the h-stacking. Choosing AX_3-layers with TR-pattern this irregular anion coordination can be partly avoided. In a structure derived by stacking AX_3-layers with TR-pattern various types of anion coordination occur. In the c-stacking the SFP of Fig. I.4a. with two B ions, that with one B ion and the SFP of Fig. I.4c. occur in the proportion 1:1:1. In the h-stacking the SFP of Fig. I.4b. with two B ions, that without B ions and the SFP of Fig. I.4d. occur in the proportion 3:1:2. The SFP of Fig. I.4b. without B ions will most probably not occur for ionic compounds because of its non-isonomous anion coordination. Therefore, the hexagonal stacking and thus the mixed hexagonal-cubic stackings of the AX_3-layers with TR-pattern and with more complicated T_mR_n-patterns are not expected for A_2BX_6 compounds. A_2BX_6 structures based on the c-stacking of AX_3-layers with T_2R_2-pattern are not expected either, since they contain a non-isonomous anion coordination, *viz.* the SFP of Fig. I.4a. without B ions. The same argument is used to exclude A_2BX_6 structures derived from all other T_mR_n-patterns in which at least two successive R-motifs occur. In structures composed of AX_3-layers with T_nR-patterns, $(n-1)/2$ octahedral positions must remain empty to attain the composition A_2BX_6. The anion coordination of Fig. I.4a. without B ions can be avoided only, however, if not more than $(n-2)/2$ octahedral positions remain empty. Therefore, these A_2BX_6 structures can also be excluded. For the same reason A_2BX_6 structures derived from a c-stacking of more complex patterns like T_2RTR can be excluded. Therefore, A_2BX_6 structures can be built only from AX_3-layers with T-pattern and c-stacked AX_3-layers with TR-pattern. The conditions which determine whether a particular compound A_2BX_6 will have a structure based on the TR-pattern or one of the structures based on the T-pattern, will be discussed in greater detail in Part III of this series of papers.

I.2.4. Removal or substitution of anions in the ideal structures

By removing some anions from structures of compositions A_2BX_6, $A_3B_2X_9$, *etc.*, new structures arise with compositions $A_2BX_5\diamondsuit$, $A_2BX_4\diamondsuit_2$, $A_3B_2X_7\diamondsuit_2$, *etc.*☆. From the SFP's of the anions (Fig. I.4.) it is evident where the anion vacancies in these structures might occur. In the structures derived in this paper anions may be removed most easily from those positions that are surrounded by cations with a low charge and/or by a small number of cations☆. This conditions is fulfilled for the anions of the SFP's of the R-pattern (Figs. I.4c. and d.) and for

☆ The coordination of the cations must also be taken into account, especially when their charge is high and/or their coordination is low (the inverse application of Pauling's second rule). The above-mentioned structures are in accordance with this condition.

☆ $\diamondsuit$ denotes an anion vacancy.

the anions of the SFP's of the T-pattern if the two octahedral sites were vacant (Figs. I.4a. and b.). A more extensive discussion of A_2BX_6 structures in which the X ions are partly removed will be given in Parts IV and V of this series of papers.

In the foregoing, structures have been derived for compounds of compositions ABX_3 and A_2BX_6. It would be a logical extension to examine how the anions would arrange themselves in these structures if they are of a different kind, in other words, to derive structures of compositions $ABX_{3-p}Y_p$ and $A_2BX_{6-p}Y_p$, in which X may differ from Y both in size and charge. These types of order of X and Y can be determined in at least two ways:

- For each type of anion the most suitable SFP may be selected and these SFP's can be stacked in such a way that the desired composition is obtained.
- Instead of starting from the SFP of the anion it is possible to determine the ways in which the various types of $BX_{6-p}Y_p$ octahedra can be joined. This has been investigated by Smirnova (15) for a more general class of compounds.

Deriving structures with ordered arrangements of X and Y, the ABX_3 and A_2BX_6 structures derived above may be used to set limits to the number of possible structures. In order to select from the derived structures those that are the most suitable for a certain compound, rules have to be derived.

A more extensive discussion of structures of A_2BX_6 compounds with different types of anions will be given in Parts IV and V of this series of papers.

I.3. Deviations from the ideal structures*

Starting from a basic lattice we derived structures with compositions ABX_3 and A_2BX_6. Among these, those structures are 'favourable' that meet the following requirements as far as possible:

a) The surrounding of each of the anions, as well as of the cations, by ions of opposite sign, has to be as isonomous as possible, when its polarizability is low or, if not, also when the coordination of the ion is high (1).

b) The charge of each of the anions has to be compensated by the sum of the charges of the cations immediately surrounding it, divided by their respective coordination numbers. It is preferable to correct these coordination numbers for variations in the cation-anion distances (See, *e.g.* Baur's paper (16) on Pauling's second rule, also for refs.).

c) Pauling's first rule (12): 'A coordinated polyhedron of anions is formed about each cation, the cation-anion distance being determined by the radius sum and the coordination number of the cation by the radius ratio'. For the ABX_3 and A_2BX_6 structures that are derived here, the fact that the starting point was the basic lattice, limits the number of different cation coordination polyhedra. The radius ratio rule may be used as a first approximation to find

* In this section deformations of the ideal ABX_3 and A_2BX_6 structures as a result of the electronic structure of the B ions, *e.g.* Cu^{2+}, Sn^{2+}, will be left out of consideration.

out whether the interstices in the basic lattice are too large or too small. When this is the case, such deformation will take place that yields a gain in potential energy so large that any possible loss in isonomy is outweighed.

d) Pauling's fifth rule (12): 'The number of essentially different kinds of constituents in a crystal tends to be small'. We prefer a more restrictive formulation (9): 'The same ions will prefer to have the same coordination, as regard number and polyhedron shape, of oppositely charged ions, if this can be achieved for the given stoichiometry and if the structure meets the requirements (a-c). This may mean that chemically identical ions prefer to occupy an identical crystallographic position☆, with the above restrictions. We have found no justification from electrostatic theory so far, neither for Pauling's fifth rule nor for either of the other formulations.

The ABX_3 structure with c-stacked AX_3-layers is completely in accordance with the above requirements. In the ABX_3 structure with h-stacked AX_3-layers the surrounding of the anion is less isonomous than in the case of the c-stacking, but this disadvantage can be overcome by the polarization energy. For the composition A_2BX_6 the structure derived from the h-stacking of the T-pattern has a more isonomous anion coordination than the structure with the c-stacking of these AX_3-layers. This anion coordination of the c-stacking (Fig. I.4a.) becomes more regular when the anion is moved from the centre of the SFP towards the octahedral position occupied by the B ion. ABX_3 and A_2BX_6 structures derived from mixtures of the h- and c-stackings do not conform to requirement (d), but a gradual change of radius ratios of the ions and the anion polarization stabilizes these structures. In the c-stacked A_2BX_6 structure derived from the TR-pattern the anions do not meet the requirements (b) and (d), but the coordinations of two-thirds of the anions are more isonomous than in the c-stacked A_2BX_6 structure derived from the T-pattern.

So far the third of the above requirements was irrelevant to the derivation of the structures, because our restriction to the 'close-packed' lattices means that the A ion is 12-coordinated, and since in the course of the derivation it appeared that the only interstitial position that can be occupied by a small cation is a position surrounded by an octahedron of anions. When we wish to select compounds that may have one of these structures, requirement (c) has to be taken into account. For, if a choice is made for the ions A, B and X, the A ions will generally not be of the same size as the X ions and the B ions will not fit exactly into the octahedral holes. Since the structures derived above are very favourable, they will have a fair tolerance for deviations from the ideal size ratios. How large this tolerance exactly is, will depend on the difference in energy between the ideal structure and a deformed structure with a lower potential energy. When the mutual size ratios of the A, B and X ions deviate too strongly from the ideal values, the structures will adjust themselves, *i.e.* they deform to make the cations fit into the interstices. These deformations are discussed by introducing a difference in size between A and X ions (Section I.3.1.) or by varying the r_B/r_X-ratio (Section I.3.2.), both between certain limits.

☆ *I.e.* the same crystallographic position with only one value for each of the parameters.

I.3.1. Deformations of the ideal structures due to a difference in size between A and X ions

We have started by assuming that the A and X ions together constitute a basic lattice and limited ourselves to 'close-packed' lattices. When the difference in size between A and X ions becomes so large that the ideal structures have to deform, those deformations are most likely in which the A ions fit best. The stability of various deformations applied to make the A ions fit may be roughly compared by calculating the space-filling, *i.e.* the percentage of space filled by hard spheres. A similar approach is usual for deriving structures of alloys (See, *e.g.* Ref. (17)) and was used by Van Vucht (18) for structures of alloys AB_3[☆]. It is, however, a rather difficult problem to find that deformation of the three-dimensional AX_3 structure that possesses the best space-filling. We ought to consider, however, that the ideal structures were very favourable and the 'advantages' of these ideal structures —*i.e.* in how far they meet the requirements (a-d) enumerated above— have to be preserved as much as possible. Consequently, in designing deformed structures we must maintain the symmetry of the ideal structures, *i.e.* preserve the threefold and/or fourfold axes as long as possible.

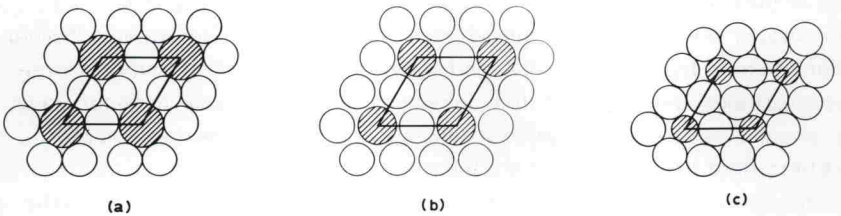

Fig. I.5.
Deformations of AX_3-layers with T-pattern, due to a too large A ion (T(1)-layer, Fig. I.5a.) or to a too small A ion (T(3)-layer, Fig. I.5c.). A T(2)-layer is equally expanded in all directions, so that the full cubic symmetry is preserved (Fig. I.5b.).

ABX_3 structures

First those deformations will be derived in which *the threefold axis* is maintained. A necessary condition for a three-dimensional structure to possess trigonal symmetry is that the layers possess trigonal symmetry.
In order to maintain the trigonal symmetry in the AX_3-layer, when the A ion is **larger** than the X ion, the layer has to deform as given in Fig. I.5a. (T(1)-layer). When this layer is stacked hexagonally, the densest packing is obtained when the large ion of the adjoining layer fits in the large X_3-triangle. Besides, this structure conforms equally well to the requirements (a-d)

☆ His assertion that the space-filling for the h-stacking of deformed AX_3-layers with R-pattern is better than that for the h-stacking of the deformed AX_3-layers with T-pattern (Fig. I.5a.) appeared to be in error, as he communicated to us.

as the ideal structure. The cubic stacking of these T(1)-layers gives rise to two different structures: a structure with two different types of octahedral holes and a structure with equal but much deformed octahedral holes. In both structures the advantages of the ideal structure as regards requirements (a, c and d) are lost for the greater part. Therefore, we consider it unlikely that one of these deformations will be realized, and the ideal structure has to expand equally in all directions with preservation of the symmetry. The AX_3-layers forming this structure are shown in Fig. I.5b. (T(2)-layer). This subject is discussed more extensively in Part II of this series of papers.

When the A ion is **smaller** than the X ion, the threefold axis will be maintained when the AX_3-layer is deformed as shown in Fig. I.5c. (T(3)-layer)○. Only the c-stacking of these layers is expected, for in the h-stacking the anion coordination is non-isonomous.

The fourfold axis is present only in the structure with c-stacked AX_3-layers.

When the A ion is **larger** than the X ion, no irregular deformation in which the fourfold axis is maintained is probable, for in the structure the BX_6-octahedra are joined by all corners and these can only expand in all directions to make room for the large A ion.

When the A ion is **smaller** than the X ion, an irregular deformation of the BX_6-octahedra cannot occur either, because requirement (b) is then violated. The potential energy can only be decreased by turning the octahedra around the fourfold axis. When the rotation around this axis is so large that the A ions have to shift from their original positions, their coordination number is lowered from 12 to 8 and the symmetry of the structures may be lowered. The A ions can be displaced in more than one way, of which the most simple case is realized in the $GdFeO_3$ structure (20). More details are given in Part II.

A_2BX_6 structures

In the A_2BX_6 structures derived from the T-pattern the most likely deformations can be determined easily with the aid of the deformations derived for the ABX_3 structures. When the A ion is larger than the X ion, the c-stacking of T(1)-layers (Fig. I.5a.) is also allowed now, since only one-half of the octahedral positions are occupied. So the full symmetry of the ideal structure is preserved. When the A ion is smaller than the X ion, T(3)-layers (Fig. I.5c.) will be formed. However, for these A_2BX_6 structures not the h-stacking, but the c-stacking of these layers is unfavourable, due again to a non-isonomous anion coordination. Rotation around the fourfold axis results in the same framework of twisted octahedra as for the ABX_3 structures. This time the deformation is not carried forward by corner sharing of the octahedra, but by anion-anion repulsion. Here again the A ions can be displaced in various ways. The c-stacked A_2BX_6 structure derived from the TR-pattern has tetragonal symmetry. It has to be deformed first in order to be able to compete with the other ideal A_2BX_6 structures and afterwards deformations due to the differences in size of A and X ions have to be considered. The value of the parameters of the A and X ions for which this structure is more

○ This deformation can also be described by a rotation of the X_3-triangles around the threefold axes, as has been done by H.D. Megaw (19).

favourable have not been calculated as far as we know☆. No conclusions can yet be made, therefore, as to whether the parameters of a particular compound may be influenced by a difference in size between A and X ions or not. A more extensive discussion of these deformations is given in Part III.

I.3.2. Deformations of the ideal structures due to deformed BX_6-octahedra

Most of these deformations are the same as when the A and X ions differ in size. An increase in size of the BX_6-octahedron has the same effect as a decreasing r_A/r_X-ratio, and *vice versa.*

When the B ion is too **large** for the octahedral position, an expansion of the BX_6-octahedra can occur either equally along all B-X directions or by preserving only the threefold axis. When the BX_6-octahedra are expanded by preserving only the threefold axis, the deformation of the AX_3-layers may be similar to T(1)-layers or T(3)-layers. For ABX_3 compounds only the h-stacking of T(1)-layers is allowed (Section I.3.1.) and in this stacking the B ions are now situated above the large X_3-triangles. Such a structure is not very probable, because the X ion moves in the direction of the A ions (Fig. I.4b.). For A_2BX_6 compounds both the c- and th h-stackings of T(1)-layers are allowed (Section I.3.1.) and in this stacking the B ions are situated now above the large X_3-triangle. The c-structure thus derived is not expected to occur, since the B ion prevents the anion coordination from adjusting itself. The h-structure may occur for particular compounds, as will be discussed in Part III. Structures derived from T(3)-layers for ABX_3 compounds can only occur when the stacking of the layers is cubic (Section I.3.1.). Structures of composition A_2BX_6 are expected only when the stacking of the T(3)-layers is hexagonal (Section I.3.1.). Increase in size of the BX_6-octahedra with preservation of the fourfold axis gives rise to the same deformations of ABX_3 and A_2BX_6 structures as in the case of a decreasing r_A/r_X-ratio.

When the B ion is too **small** for the octahedral hole, a contraction of the BX_6-octahedra occurs. When this contraction is equal in all directions, the effect resembles the effect of an increasing r_A/r_X-ratio. The same is true for a contraction of the BX_6-octahedra in which only the threefold axis is maintained.

In order to extend our understanding of structures ABX_3 and A_2BX_6 in which the radii of A and B gradually approach each other, we must probably start from other basic lattices. Examples of such types are $LuMnO_3$ (22), Y_2O_3 (23) and β-Rh_2O_3 (24). An experimental and theoretical investigation on ABX_3 halides of this type has been started in our laboratory, but the results are not yet available. Nevertheless, using the above reasoning the structures of a vast number of compounds reported in the literature can be classified and the structures of new compounds can be predicted as will be shown in the following parts.

☆ H.G. von Schnering pointed out (21) that the value of the parameters must be adjusted in order to make the structure more favourable.

References

1. E.W. Gorter, J. Solid State Chem. **1**, 279 (1970).
2. A.E. van Arkel, 'Moleculen en Kristallen' (in Dutch), W.P. van Stockum, 's-Gravenhage, 1961.
3. P.A. Beck, 'Close-packed Ordered Alloys' in 'Advances in X-ray Analysis' (C.S. Barrett *et al.*, Eds.), Vol. 12, Plenum Press, New York, 1969. See also the references in this paper.
4. D. Babel, 'Structural Chemistry of Octahedral Fluorocomplexes of the Transition Elements', in 'Structure and Bonding' (C.K. Jørgensen *et al.*, Eds.), Vol. 3, p. 1-87, Springer-Verlag, Berlin/Heidelberg/New York, 1967.
5. R. Colton and J.H. Canterford, 'Halides of the First Row Transition Metals', Wiley-Interscience, London/New York/Sydney/Toronto, 1969.
6. J.H. Canterford and R. Colton, 'Halides of the Second and Third Row Transition Metals', Wiley-Interscience, London/New York/Sydney/Toronto, 1969.
7. D. Brown, 'Halides of the Lanthanides and Actinides', Wiley-Interscience, London/New York/Sydney, 1968.
8. A.F. Wells, 'Structural Inorganic Chemistry', third ed., Clarendon Press, Oxford, England, 1962.
9. A.B.A. Schippers and E.W. Gorter, to be published.
10. G.O. Brunner, Acta Cryst. **A27**, 388 (1971).
11. M.J. Buerger, Z. Krist. **109**, 48 (1957).
12. L. Pauling, J. Am. Chem. Soc. **51**, 1010 (1929).
13. G. Engel, Z. Krist. **90A**, 341 (1935).
14. J.L. Hoard and W.B. Vincent, J. Am. Chem. Soc. **61**, 2849 (1939).
15. N.L. Smirnova, Soviet Phys. Cryst. **8**, 131 (1963).
16. W.H. Baur, Trans. Amer. Cryst. Assoc. **6**, 129 (1970).
17. F. Laves, 'Factors Governing Crystal Structure' in 'Intermetallic Compounds' (J. Westbrook, Ed.), Chapter 8, John Wiley, New York/London/Sydney, 1967.
18. J.H.N. van Vucht, J. Less-Common Metals **11**, 308 (1966).
19. H.D. Megaw, Acta Cryst. **A26**, 235 (1970).
20. S. Geller, J. Chem. Phys. **24**, 1236 (1956).
21. H.G. von Schnering, Z. Anorg. Allgem. Chem. **353**, 13 (1967).
22. H.L. Yakel, W.C. Köhler and E.F. Bertaut, Acta Cryst. **16**, 957 (1963).
23. B.H. O'Conner and T.M. Valentine, Acta Cryst. **B25**, 2140 (1969).
24. R.D. Shannon and C.T. Prewitt, J. Solid State Chem. **2**, 134 (1970).

CHAPTER II

DERIVATION AND DISCUSSION OF CRYSTAL STRUCTURES OF COMPOUNDS ABX_3 AND A_2BX_6

PART II. STRUCTURAL CHEMISTRY OF ABX_3 HALIDES

V. Brandwijk, A.B.A. Schippers and E.W. Gorter.
Dept. of Solid State Chemistry, Gorlaeus Laboratories, P.O. Box 75, Leiden, The Netherlands.

Abstract

In Part I of this series of papers the crystal structures of compounds with compositions ABX_3 and A_2BX_6 were derived from a basic lattice, using mainly qualitative electrostatic bonding rules (A represents a large cation that can replace an anion, B is a small interstitial cation, X is a halogen ion). In the present paper the crystal structures of compounds with composition ABX_3 are derived in greater detail and compared with the experimentally determined structure types for ABX_3 halides. Calculated inter- and intralayer distances, reduced c/a-values and volumes per formula unit did not agree satisfactorily with the experimental values, so that these are discussed only qualitatively. The structures reported in the literature for ABX_3 halides, also those adopted at non-ambient temperatures and pressures, appear to lie within the stability regions that are roughly indicated for them.

II.1. Introduction

As an example to derive crystal structures in a systematic way we selected a class of compounds of composition A_2BX_6, of which the structures are known to be closely related to those of compounds of composition ABX_3 (A represents a large cation that can replace an anion, B is a small interstitial cation, X is a halogen ion). In Part I of this series of papers (1) ABX_3 and A_2BX_6 structures were derived by starting from structures AX_3 in which A-A contacts were excluded in a stacking of 'close-packed' layers. Only AX_3 structures that are composed of identical AX_3-layers of which the types of order of A and X ions consist of the well-known T (= triangular) and/or R (= rectangular) motifs, appeared to be in accordance with our requirements. From these AX_3 structures the ABX_3 and A_2BX_6 structures were derived. On the basis of mainly simple electrostatic considerations☆, structures with anion surroundings that are most unlikely were excluded. Use was made of the representation of anion surroundings by space-filling polyhedra (SFP) (2). Finally, the deviations from the ideal ABX_3 and A_2BX_6 structures, resulting from variations in size of the A , B and X ions, were considered.

☆ We could not find an electrostatic justification for the rule of parsimony (1).

In the present paper (Part II) the ABX_3 structures are derived in greater detail (Section II.2.) and compared with the structure types found for ABX_3 halides (Section II.3.). Since a calculation of the inter- and intralayer distances, reduced c/a-values and volumes per formula unit ABX_3 with the aid of the Shannon & Prewitt radii did not lead to a sufficient agreement with the experimental data, only a qualitative discussion of these values is given (Section II.4.). The structures reported in the literature for ABX_3 halides are collected in plots of the radii of the A ions against the radii of the B ions in order to determine the stability region for a particular structure type. These regions are compared with those that are expected (Section II.5.). Finally, the expected and reported structures at non-ambient temperatures and pressures are discussed☆ (Section II.6.).

II.2. Discussion of the derived ABX_3 structures

As was demonstrated in Section I.2.○ the structures of compounds with composition ABX_3 can only be built by stacking AX_3-layers having the triangular type of order (T-pattern). In these AX_3 structures the B ions occupy all available octahedral sites. In deriving ABX_3 structures only the hexagonal and cubic stackings of AX_3-layers were discussed and not the more complex stacking types: hhc , hc , hcc , *etc.* Structures with such a mixed hexagonal-cubic stacking are considered to arise from a gradual change of the properties of the ions and not to prefer exclusively the advantages of the cubic or those of the hexagonal structure. Which are the advantages of the h-stacking in comparison with the c-stacking? The only way up till now in which a large number of structures can be discussed, is by making use of a

☆ Throughout the whole series of papers the effective ionic radii of Shannon & Prewitt (3,4) are used. These were derived from the structures of oxides and fluorides and corrected for both the anion and the cation coordination and also for the spin states of certain transition metal ions.
In the present paper the radius of the B ions is that for 6-coordination. We take the A ion in 12-coordination with the exception of Na , which is taken in 8-coordination, since it is generally 8-coordinated in $NaBF_3$ compounds. For the radius of the X ion is taken that for 6-coordination. Shannon & Prewitt do not report radii either for Ag^+ and NH_4^+ in 12-coordination, or for Ge^{2+} and Sn^{2+} in 6-coordination, or for Cl^- , Br^- and I^- in 6-coordination. Shannon & Prewitt could not calculate a radius for Ag^+ in 12-coordination because of lack of accurate experimental data. We use an estimated radius of 1.3 Å . For NH_4^+ a radius of 1.73 Å , equal to the radius of Rb^+ , is used because the cell volumes of the $RbBF_3$ and NH_4BF_3 compounds are almost equal for B = Cu , Co , Zn , Fe , Cr , Mn (Fig. II.13.). For Ge^{2+} and Sn^{2+} radii of 1.0 and 1.1 Å , respectively, are estimated from a comparison of the volumes at room temperature of all known $CsBCl_3$ compounds. Since the free electron pair of these ions usually distorts the regular octahedral coordination, more accurate calculation of these radii is not possible. For Cl^- , Br^- and I^- the Ahrens radii of 1.81 , 1.96 , 2.20 Å are used.
In all tables in this paper we shall tabulate the B ions from the left to the right and the A ions downwards in the order of increasing radii.

○ Section I.2. indicates: Section 2 of Part I of this series of papers (1). This notation is used in the whole paper.

modified electrostatic[☆] picture (2). The following differences between the c- and the h-stackings then become obvious from the space-filling polyhedra (SFP)[○] of the anions in these ideal structures (Figs. II.1a. and b.):

– The Coulomb repulsion between nearest B ions is much larger for the h- than for the c-stacking.
– The contribution of polarization to the lattice energy is much larger for the h- than for the c-stacking. It is assumed that only the contribution from the polarization of the X ions to the lattice energy is sufficiently large and that these X ions are only polarized by the nearest four A ions and two B ions.

Since the ideal ABX_3 structure with c-stacked AX_3-layers has the most isonomous coordinations of all ions, this structure is most likely to occur. However, the presence of large polarizable anions will favour the ABX_3 structure with h-stacked layers, if the polarization energy can outweigh the loss of isonomy, *i.e.* the B-B repulsion. The difference between the h- and c-stackings discussed above were mentioned by other authors, *e.g.* by Katz & Ward (6) and by Blasse (7).

However, when such an ideal structure is realized for a particular compound, the mutual size ratios of the A , B and X ions will seldom have the ideal values. When the deviations from these values are too large, the structures will deform in order to decrease the potential energy. These deformations are a compromise between the favourable ideal structures and less favourable structures in which the ions fit better (Section I.3.). This compromise can be attained by preserving the symmetry as much as possible, *i.e.* preserve the threefold and/or fourfold axes as long as possible. In deriving the deformations of the ideal structures in Part I , we confined our attention to those deformations that are due to either a difference in size between A and X ions or to a non-ideal r_B/r_X-ratio[△]. These deformations are now discussed in greater detail.

We saw that when the A ion is **larger** than the X ion, the *fourfold axis* can only be preserved be preserved by expanding the c-stacked structure equally in all directions (*i.e.* the ideal symmetry is maintained), since irregular BX_6-octahedra were ruled out[□]. Expansion results in an increase of the potential energy and when it becomes too large, a deformed structure with a lower total potential energy will occur, which does not contain a fourfold axis but in which the threefold axis is preserved.

☆ A non-ionic approach of a large but limited number of structures is given by E. Parthé (5).

○ The space-filling polyhedron of an ion in a structure is obtained by constructing midway planes between this ion and its nearest neighbours of the same kind (2).

△ Discussing size differences between the various ions, the radius ratio rule cannot be used, for it is our contention that the derivation of structures must start with a 'basic lattice' (1,8). This lattice will tolerate small deviations from the ideal radius ratios.

□ In the BX_6-octahedron the B-X distances must remain equal. Since the coordination of each anion contains two B ions, a noticeable change in a part of the B-X distances would disturb the local charge compensation.

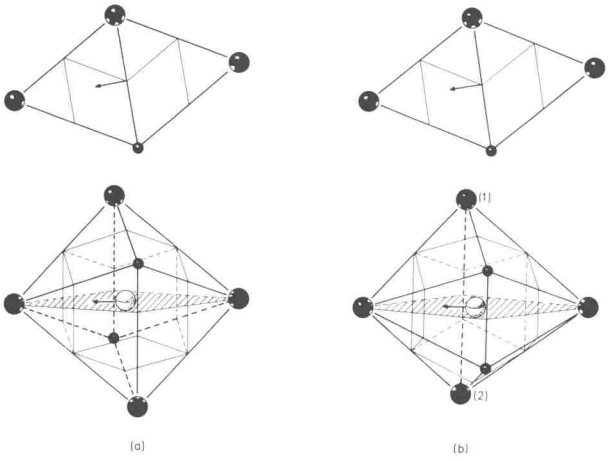

Fig. II.1.
Space-filling polyhedra (SFP) of the anion in the ideal ABX_3 structures with cubic (Fig. II.1a) and hexagonal (Fig. II.1b.) stacking of AX_3-layers. The SFP's of the anion in the 'close-packed' anion lattices are indicated by light lines. Black spheres represent A ions, white spheres X ions, and small black spheres B ions. The equatorial plane is shaded.

The *threefold axis* can only be preserved when the AX_3-layers are deformed as given in Fig. II.2a. (T(1)-layer). A h-stacking of these T(1)-layers can be achieved in two ways: the A ion of the adjoining layer can be situated either above the large or above the small X_3-triangle (Fig. II.2a.). The former structure (Fig. II.3.) occurs when the A ion is larger than the X ion, for then the packing of A and X ions is as dense as possible (*i.e.* the A ions fit as well as possible between the X ions) and this deformed structure conforms equally well to the requirements (a-d) (1) as the ideal structure. Moreover, the polarization energy increases, because the X ion is forced by the large A ions to move in the direction of the two B ions. The latter deformation might occur when the B ion is too large for the octahedral site. The occurrence of T(1)-layers is caused then by the B ions instead of by the A ions. In this structure the anion is displaced from its position in the ideal structure (Fig. II.1b.) in the direction of the A_1 and A_2 ions. In other words, the contribution to the polarization energy decreases (*i.e.* the factor that causes the h-stacking to exist disappears), so that this structure cannot be expected.

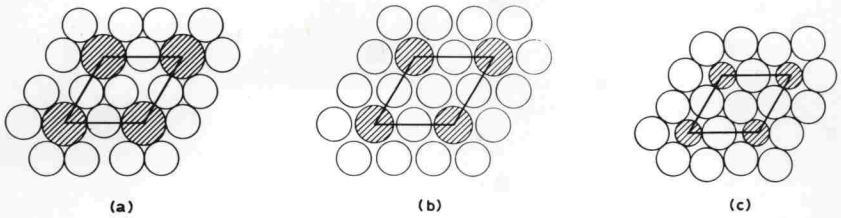

Fig. II.2.
Deformations of AX_3-layers with T-pattern, due to a too large A ion (T(1)-layer,Fig. II.2a.) or a too small A ion (T(3)-layer, Fig. II.2c.). A T(2)-layer is equally expanded in all directions, so that the full cubic symmetry is preserved in a cubic stacking of these layers (Fig. II.2b.).

A c-stacking of these T(1)-layers can be realized again in two ways as shown in the (110)-sections of the structures (Fig. II.3.). The structures that can be built from these deformed layers are less dense than for the h-stacking (9). Moreover, the B ions are distributed over two different types of octahedral sites in one of these c-structures: a small and a large one, whereas the anion coordination in the other structure is irregular without causing a significant gain in polarization energy. Moreover, all ions in both structures have a less isonomous coordination than in the ideal structure. Because no favourable deformation of the ideal structure with c-stacking of the layers is available, the structure has to expand equally in all directions, so that T(2)-layers are formed (Fig. II.2b.). Since no deformation of the ideal c-structure was found that met our requirements, it will have a larger tolerance for differences in size between A and X ions than an ideal structure that has favourable deformations.
The stacking types intermediate between the c- and h-stackings will be adopted when the A ions are too large for the c-stacking. The less isonomous anion coordination can then be compensated by a gain in polarization energy and a better fitting of the A ions into the structure. The h-stacked layers in these mixed stackings are T(1)-layers in order to make the A ions better fit and to screen the field of the B ions (B-B repulsion) as much as possible. The c-stacked layers are T(2)-layers, so that chemically identical ions are as much as possible in the same coordination (Pauling's rule of parsimony (10,8)). These mixed stacking types are further discussed in Section II.3.1.

When the A ion is **smaller** than the X ion, the *threefold axis* can only be preserved when the AX_3-layers are deformed as given in Fig. II.2c. (T(3)-layer). In the h-stacking of T(3)-layers the anion coordination is less isonomous than in the ideal h-stacked structure. Moreover, the contribution to the polarization energy is decreased by the displacement of the X ion from its ideal position (arrow in Fig. II.1b.) owing to a stronger polarization by three A ions at a shorter distance from the X ion which counteracts the polarization by the B ions. Con-

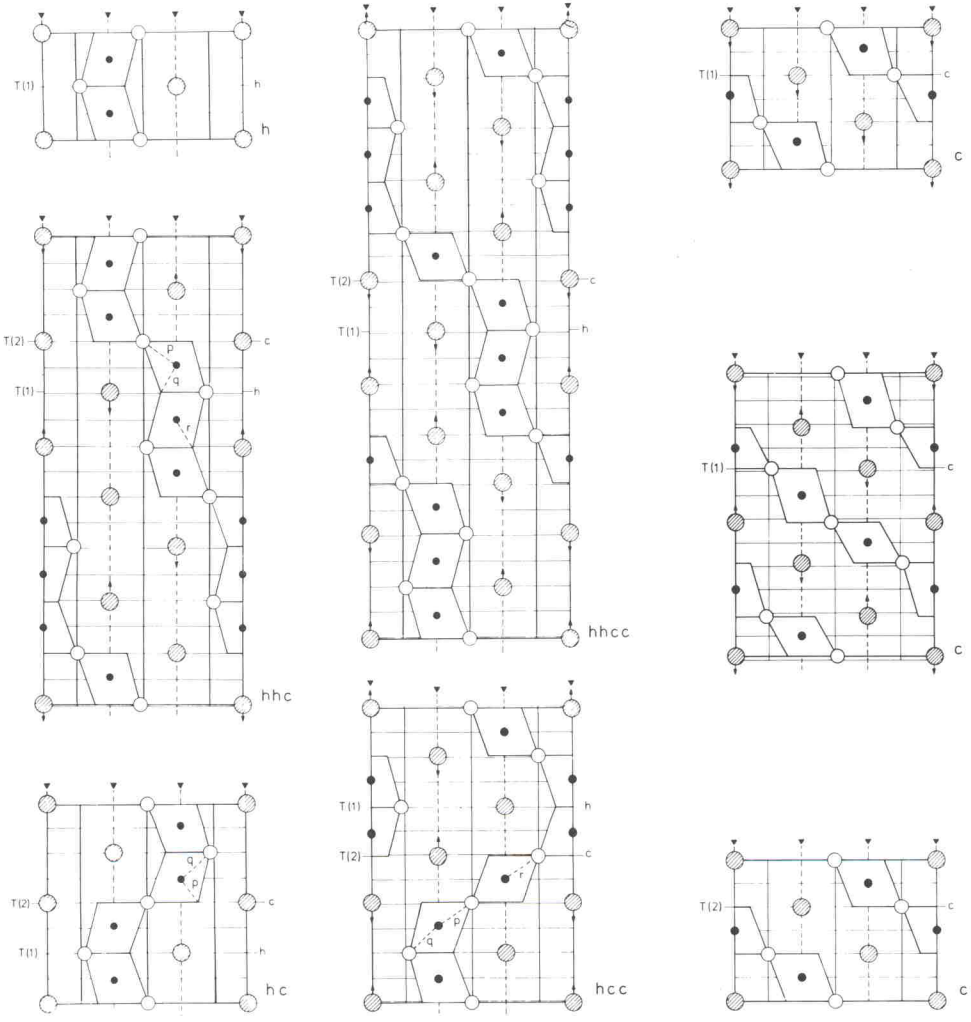

Fig. II.3.

(110)-sections of the unit cells of the derived ABX_3 structures composed of AX_3 layers with T-pattern, viz. the hexagonal (h) stacking of T(1)-layers (the $BaNiO_3$ h-structure), the hhc- (the $BaRuO_3$ hhc-structure), hc-, hhcc- and hcc- (the $BaTiO_3$ hcc-structure) stackings of T(1)- and T(2)-layers, two c-stackings of T(1)-layers and the c-stacking of T(2)-layers ($SrTiO_3$ c-structure). Shaded circles represent A ions, open circles X ions, and black circles B ions. The light horizontal lines indicate the ideal positions of the h- or c-stacked AX_3-layers at (m/2n)c (m = 0 , 1 ... 2n , n = number of AX_3-layers, c = length of the c-axis). Arrows indicate the displacement of the A ions out of the AX_3-layers. The BX_6-octahedra are denoted by heavy lines.

Table II.1.

Symmetry, cell dimensions and atomic parameters of the derived deformations of the ideal c-stacked ABX_3 structure when the space available for the A ion is too large. The edges of the unit cells are expressed in the edge of the unit cell of the ideal c-stacked ABX_3 structure. δ represents the deviation from the ideal parameter caused by the rotation of the octahedra around the threefold or fourfold axis. $0 \leqslant \delta \leqslant 1/6$ for the trigonal structure and $0 \leqslant \delta \leqslant (2-\sqrt{3})/4$ for the other structures. ϵ and ϵ' denote an adjustment of the X(1)-position for the orthorhombic structure of Fig. II.4b. ϵ is also the displacement of the A ion as indicated in Figs. II.4c. and d.

1. *Trigonal structure* composed of T(3)-layers					
Space group $R\bar{3}c$ (D^6_{3d})	^{IX}A	(6a)	0	0	1/4
$\sqrt{2} \leqslant a \leqslant \sqrt{66}/6$ and $60° \leqslant \alpha \leqslant 53°55'$	^{VI}B	(6b)	0	0	0
or: $\sqrt{2} \leqslant a_{hex} \leqslant \sqrt{6}/2$ and $c_{hex} = 2\sqrt{3}$	^{V}X	(18e)	$1/2 \pm \delta$	0	1/4
$c/a = 2\sqrt{6}/\sqrt{1/(3\delta^2 + 1/4)}$					
$Z = 6$					
2. *Tetragonal structure* of Fig. II.4a.					
Space group I4/mcm (D^{18}_{4h})	A	(4b)	0	1/2	1/4
$a = \sqrt{2/(16\delta^2 + 1)}$ and $c = 2$	B	(4c)	0	0	0
$c/a = 2\sqrt{2}/\sqrt{1/(4\delta^2 + 1)}$	X_1	(4a)	0	0	1/4
$Z = 4$	X_2	(8b)	$(1/4) + \delta$	$(3/4) + \delta$	0
3. *Orthorhombic structure* of Fig. II.4b.					
Space group Pbnm (D^{16}_{2h}) [a]	^{VIII}A	(4c)	−.015	.055	1/4
$a = \sqrt{2/(16\delta^2 + 1)}$	^{VI}B	(4b)	1/2	0	0
$b > a$ and $c < 2$	$^{IV}X_1$	(4c)	$-.017 + \epsilon$	$.523 \pm \epsilon'$	1/4
$Z = 4$	$^{V}X_2$	(8d)	.700	.300	.015
4. *Orthorhombic structure* of Fig. II.4c. (rough data)					
Space group $Cmc2_1$ (C^{12}_{2v})	$^{VIII}A_1$	(4a)	0	$(3/8) + \epsilon/2$	ϵ
$a = 2 \quad b < 2\sqrt{2} \quad c < \sqrt{2}$	$^{VIII}A_2$	(4a)	0	$(1/8) + \epsilon/2$	$(1/2) - \epsilon$
$Z = 8$	^{VI}B	(8b)	1/4	1/8	0
	$^{V}X_1$	(8b)	1/4	$0 + \delta/2$	$(1/4) + \delta$
	$^{V}X_2$	(8b)	1/4	$(1/4) + \delta/2$	$(1/4) - \delta$
	$^{III}X_3$	(4a)	0	1/8	0
	$^{V}X_4$	(4a)	0	5/8	0
5. *Orthorhombic structure* of Fig. II.4d. (rough data)					
Space group Pnma (D^{16}_{2h})	$^{VIII}A_1$	(4c)	0	1/4	ϵ
$a < 2 \quad b = 2 \quad c < 2$	$^{VIII}A_2$	(4c)	$-\epsilon$	1/4	1/2
$Z = 8$	^{VI}B	(8d)	1/4	0	1/4
	$^{V}X_1$	(8d)	$(1/4) - \delta\sqrt{2}$	0	0
	$^{V}X_2$	(8d)	0	0	$(1/4) + \delta\sqrt{2}$
	$^{V}X_3$	(4c)	1/4	1/4	1/4
	$^{III}X_4$	(4c)	1/4	1/4	3/4

[a] A non standard orientation of Pnma was chosen in order to facilitate comparison with experimentally determined structures.

sequently, this structure is not expected. In the c-stacking of T(3)-layers the anion coordination remains fairly isonomous, so that the potential energy is decreased without loss of the advantages of the ideal structure (arrow in Fig. II.1a.). The structure data are given in Table II.1.

If an irregular deformation of the BX_6-octahedra is excluded (see note on page 34), the *fourfold axis* can only be preserved by rotating the BX_6-octahedra around this axis in such a way that the space available for the A ion decreases. Because all octahedra are joined by six corners this deformation can only be realized in one way, resulting in a tetragonal structure. In order to obtain a favourable structure the octahedra along this axis are rotated alternately in opposite directions, which decreases the anion-anion repulsion and keeps the coordination of the A ions as isonomous as possible (Fig. II.4a.). The deviation from the ideal value of the parameter of the X(2) ion (δ) (Table II.1.) and the c/a-value of the tetragonal unit cell are determined by the angle over which the BX_6-octahedra are rotated.

When the octahedra are rotated around the fourfold axis over a larger angle, much more space is available for the A ion if the adjacent octahedra along this axis rotate in the same direction and if the A ion moves as denoted in Fig. II.4b., so that it is then coordinated by eight anions at more equal distances. This displacement of the A ions can be realized in two opposite directions. Of course, the displacements of adjacent A ions along the previous fourfold axis are opposite in order to reduce the A-A repulsion. In a plane perpendicular to this axis neighbouring A ions can be displaced in various ways, giving rise to a large number of structures. Again, only those are selected in which the anion coordination is as isonomous as possible and in which the number of different coordinations for each type of ions is as small as possible (the rule of parsimony). All these deformed structures contain at least two types of anion coordinations:

- The anions in the plane perpendicular to the previous fourfold axis and containing the B ions are coordinated by five ions, *viz.* three A and two B ions, irrespective of the direction in which the A ions move.
- The coordination of the anions in the plane perpendicular to the previous fourfold axis and containing the A ions, may vary from six (four A and two B ions) to two (two B ions), but the average coordination must be four. (From $^{VIII}A^{VI}B^{V}X_2^{x}X$ it follows that x equals IV.) The number of this type of anions is one-half of the number of the first type.

In order to be in good agreement with the rule of parsimony, only the following combinations of coordinations of anions of the second type will be allowed: 4 or 5 + 3 or 5 + 5 + 2 . The last named possibility can be excluded, because no charge distribution over A and B ions can be found that is in accordance with Pauling's second rule of local charge compensation, modified for distance (11).

An equal number of 5- and 3-coordinated anions of the second type can be realized in various structures. None of them can be realized for an $A^{+}B^{2+}X_3^{-}$ halide, since the deviations from the local charge compensation become too large. The rough structure data of the two simplest structures (Figs. II.4c. and d.) are given in Table II.1. As far as we know, these structures have never been found. They might occur for compounds of compositions

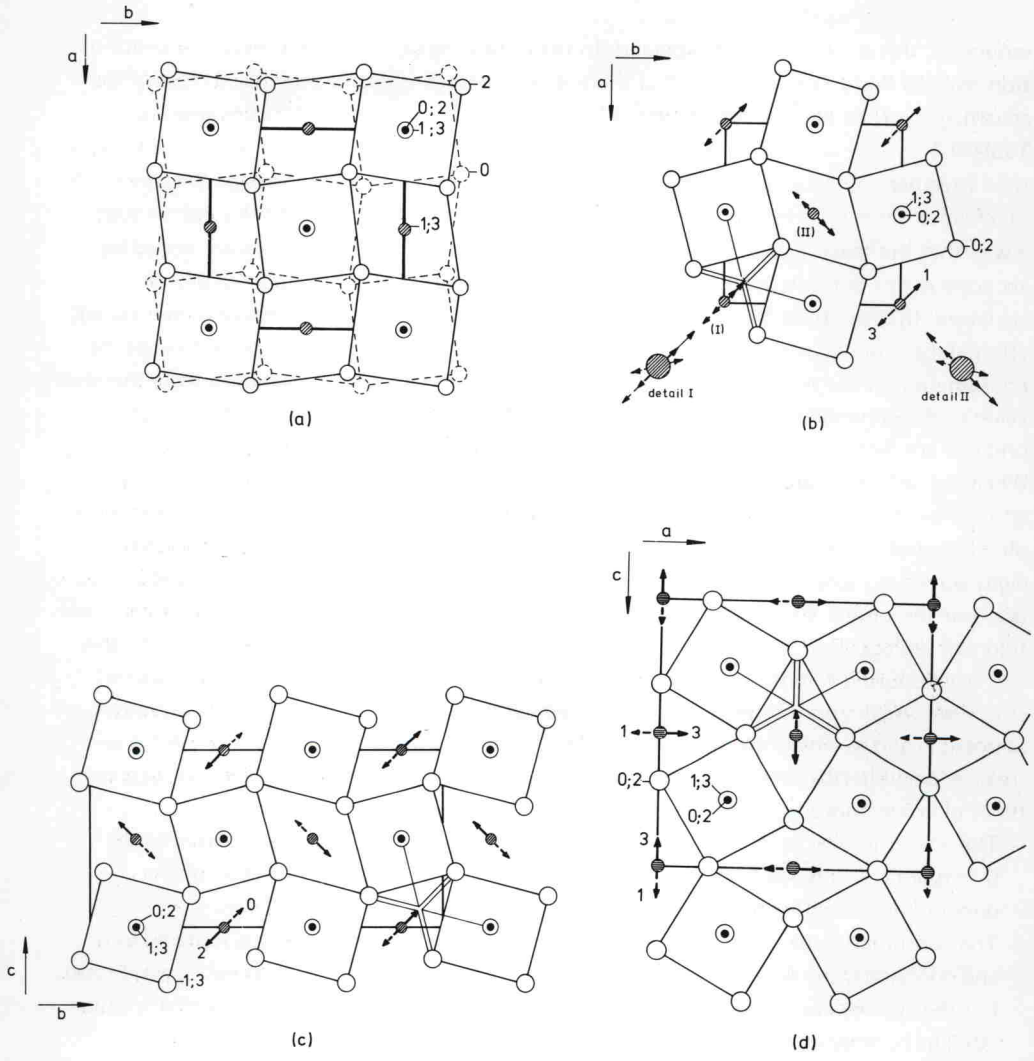

Fig. II.4.

Deformations of the ideal c-stacked ABX_3 structure when the space available for the A ion is too large: the tetragonal structure (Fig. II.4a.), the orthorhombic structure with 4-coordinated anions of the second type (Fig. II.4b.) and the two simplest orthorhombic structures with 5 + 3 coordination for the anions of the second type (Figs. II.4c. and d.). Shaded circles represent A ions, open circles X ions, and black circles B ions. Figures indicate the heights of ions above the plane of the paper in quarters of the axis perpendicular to the plane of the paper. The unit cells are indicated by very heavy lines. The arrows indicate the displacement of the A ions from their ideal positions. The 8-coordination of the A ions is marked in Figs. II.4b., c. and d.

$A^+B^{5+}O_3$ or $A_2B_2O_5F$. A compound of composition $A_2B_2O_5F$ is not easy to prepare, because the number of different ions is rather large and the charge of the A ions has to be high in order to be in good agreement with Pauling's second rule. In an $A^+B^{5+}O_3^{2-}$ compound the deviations from Pauling's second rule may be compensated by decreasing the A-X distances of the 3-coordinated anions with regard to the A-X distances of the 5-coordinated anions. If this adjustment can be realized, these structures still have anions that are situated in more crystallographic positions☆ than in the structure with 5-, 5- and 4-coordinated anions (Figs. II.4b. and Table II.1.). It is questionable whether these structures will ever be more favourable than the structure with 5-, 5- and 4-coordination of the anions, derived below.

If the anions of the second type are 4-coordinated, only one structure can be derived (Fig. II.4b.). These anions are indicated by X(1) in Table II.1. This structure has to be adjusted in order to improve the coordinations of the ions. The direction in which the A ion has to move is evident, but how large the displacement has to be is not clear immediately. There are two possibilities: the A ion may be shifted to the centre of the deformed trigonal prism of anions (large arrows in Fig. II.4b.) or to the centre of the two nearest equiplanar anions and four anions of the deformed trigonal prism (heavily drawn small arrows in Fig. II.4b.). The last named possibility is most likely, because the space available for the A ion is larger and the distances between the nearest A ions in the xy-plane are larger. The shortest and almost shortest A-A distances in the xy-plane will become more alike by rotating the shift vector of the A ion in the direction of the b-axis (indicated by the weakly drawn small arrows in Fig. II.4b) and by making the b-axis larger than the a-axis. When doing so, the X(2) ions have to move out of the xy-plane in order to keep the A-X distances equal○. For the same reason the X(1)-position has to be adjusted. The atomic parameters of this structure, calculated for a displacement of the X(2) ion $\delta = 0.05$ (due to rotation of the BX_6-octahedra) and a rotation over 30° of the shift vector of the A ion (A-A repulsion) are given in Table II.1. We refrained from a further adjustment of the X(1)-position (necessary to improve the coordination of this anion), because geometrical considerations, as used above, did not lead to an unambiguous result. A further adjustment of the X(1)-position is therefore indicated by ϵ and ϵ' in Table II.1. More accurate atomic parameters may be obtained, a.o., by minimizing the Madelung energy.

When the A ion is smaller than the X ion three deformations of the ABX_3 structures thus arise: a trigonal, a tetragonal and an orthorhombic structure. Which of these structures is likely to occur for the ABX_3 halides may be indicated by considering the possible charges of A and B ions. In the trigonal structure ($0 \leqslant \delta \leqslant 1/6$) the position of the anion reached by the geometrical adjustment of the ideal structure is more favourable when the charge distribution is A^{3+} , B^{3+} or A^{4+} , B^{2+} than when the charge distribution is A^{2+} , B^{4+} or A^+ , B^{5+} .

☆ *I.e.* crystallographic positions with only one value for each of the parameters.

○ Adjustment of the A-X distances by a displacement of the X(2) ion *in* the xy-plane leads to a less isonomous anion coordination.

On the other hand, the positions of two-thirds of the anions in the tetragonal structure ($0 \leqslant \delta \leqslant (2-\sqrt{3})/4$) are more favourable when the charge distribution is A^{2+}, B^{4+} or A^{+}, B^{5+} than when the charge distribution is A^{3+}, B^{3+} or A^{4+}, B^{2+}. This expected correlation between the deformed structures and the charge distribution might be tested by experiment or by calculation of the Madelung energy[△]. Since not all atomic parameters of the orthorhombic structure could be fixed by geometrical arguments, no decision can be made whether a certain charge distribution is favoured in this structure or not. From geometrical arguments it can be concluded that the orthorhombic structure occurs when the r_A/r_X-ratio becomes too small for the tetragonal or trigonal structure.

Deformations of the ideal ABX_3 structures due to the bad fit of the B ion into the BX_6-octahedron are often the same as when the A and X ions differ in size (Section I.3.2.). An increase in size of the BX_6-octahedron may be equivalent to a decreasing r_A/r_X-ratio, a decrease to an increasing r_A/r_X-ratio. The only exception to this simplification occurs when the B ion is too large for the BX_6-octahedron and the threefold axis is preserved, but this deformation is not expected, as was discussed above.

The results of the discussion given above can be summarized as follows:

- The structure with c-stacked layers is generally most likely to occur.
- When the anion is large and polarizable or when the A ion is larger than the X ion, the structure with h-stacked layers will become more favourable than that with c-stacked layers.
- When the anion is not very polarizable and the A ion is smaller than the X ion, deformations of the structure with c-stacked layers will occur (Table II.1.). For the $A^{+}B^{2+}X_3$ halides the tetragonal structure is expected when the difference in size between A and X ions is small and the orthorhombic structure when this difference is larger.
- Only when the anion is polarizable and the A ion is smaller than the X ion, no favourable structure could be derived within the delimitations made in this series of papers. It would be worth while trying to derive such structures by starting from one of the other basic lattices.

II.3. The structure types found for ABX_3 halides

II.3.1. Structures of ABX_3 halides in which the A ion is larger than the X ion

When the A ion is larger than the X ion the potential energy of the structure decreases when the fraction of h-stacked layers increases (Section II.2.). For ABX_3 halides only the structures

△ A simple consideration like charge distribution might be correlated with the parameters b and e in the model of Thomas and Müller (12).

with h- , hhc- , hcc- and c-stackings of AX_3-layers with T-pattern have been reported in literature☆. Apart from these also the hc-stacking found for oxides is discussed in the present section, so that only the most simple mixed hexagonal-cubic stacking types are regarded.

The ABX_3 structure with h-stacked layers only consists of T(1)-layers as derived in Section II.2. For $BaNiO_3$ (13) this structure is realized (Fig. II.3.). The X ions are in the 6(h) position of which the x-parameter would be 5/6 (0.833) if the AX_3-layers are T(2)-layers, and > 5/6 if T(1)-layers are formed. This x-parameter is expected to increase with r_A , to be nearly independent of r_B and to decrease with increasing r_X . In Table II.2. the known x-parameters for the ABX_3 halides with *$BaNiO_3$ h-structure* are listed. Although the lack of data prevents to test the rules with any degree of certainty, the influence of r_A and r_B is found to be very weak, whereas the rule for r_X is confirmed.

Table II.2.

The x-parameter of the X ion in ABX_3 halides with $BaNiO_3$ h-structure. The standard deviations are given in parentheses. The data are taken from the references reported in Tables II.9., 10. and 11.

	Ni	Co	Fe	Cr	Ti
$CsBF_3$	.8569(28)				
$RbBCl_3$	.8434(3)	.839(2)	.84(1)	5/6	
$CsBCl_3$	.844	.8455(3)	.842(1)		
$RbBBr_3$	.843(1)				.844
$CsBBr_3$					.844

☆ In the literature the term 'perovskite structure' was originally attributed to the structure of $CaTiO_3$. Afterwards the term 'cubic perovskite structure' was used for the c-stacking of T(2)-layers, the term 'hexagonal perovskite structure' for the h-stacking of T(1)-layers and the hcc-stacking of Fig. II.3. We indicate a structure type, also distinguishing stacking type and symmetry, as follows: the chemical formula of the compound for which the structure type was found first; h , hhc , hcc , c , *etc.* for the stacking type when the symmetry of the structure is as high as possible for the pertinent structure type; h′ , hhc′ , hcc′ , c′ , *etc.*, when the symmetry is lowered. Therefore, the c-stacking of T(2)-layers is called the $SrTiO_3$ c-structure, the c-stacking of T(3)-layers the $LaAlO_3$ c′-structure, the structure of Fig. II.4a. the $KMnF_3$ c′-structure (in order to prevent confusion with the $SrTiO_3$ c-structure, for this structure type was also found first for $SrTiO_3$) , the h-stacking of T(1)-layers the $BaNiO_3$ h-structure, the hcc-stacking of Fig. II.3. the $BaTiO_3$ hcc-structure, *etc.*

The hhc-stacking of T(1)- and T(2)-layers. In this structure two types of A ions occur: those in h-stacked and those in c-stacked AX_3-layers. The T(2)-layer will not be replaced by a T(1)-layer, because there are then two types of A ions in the h-stacked layers and this conflicts with the rule of parsimony. In the hhc-stacking of Fig. II.3. two-thirds of the A ions move in the directions as indicated by the arrows in order to decrease the B-A repulsion and to improve their coordination by the X ions.
This structure is known as the *$BaRuO_3$ hhc-structure* (14) and is also realized for $CsCoF_3$ (15). The shifts of the A and X ions in the direction of the c-axis and the shifts of two-thirds of the X ions in the xy-plane are in accordance with the expected structure. Two-thirds of the B ions are also shifted in the direction of the c-axis in order to keep all B-X distances equal (Table II.3.).

Table II.3.
Symmetry, cell dimensions and atomic parameters for compounds with $BaNiO_3$ hhc- and $BaTiO_3$ hcc-structure. The standard deviations are given in parentheses.

$BaRuO_3$ hhc-structure (Fig. II.3.)						atomic parameters for: $BaRuO_3$	$CsCoF_3$	derived structure
Space group $R\bar{3}m$ (D^5_{3d})	A_1	(3a)	0	0	0			
	A_2	(6c)	0	0	z	.2181(2)	$.219_2$	$2/9 - \delta$
a = 5.75 Å and c = 21.60 Å	B_1	(3b)	0	0	1/2			
for $BaRuO_3$ (14)	B_2	(6c)	0	0	z	.3819(3)	$.377_6$	$7/18 - \delta'$
a = 6.19_4 Å and c = 22.61 Å	X_1	(9e)	1/2	0	0			
for $CsCoF_3$ (15)	X_2	(18h)	x	$\bar{x}$	z	.156(4) .558(1)	.142 $.561_6$	$1/6 - \epsilon''$ $5/9 + \delta''$

$BaTiO_3$ hcc-structure (Fig. II.3.)						atomic parameters for: $BaTiO_3$	$CsMnF_3$	$RbNiF_3$	derived structure
Space group $P6_3/mmc$ (D^4_{6h})	A_1	(2b)	0	0	1/4				
	A_2	(4f)	1/3	2/3	z	.097(10)	.0986(2)	.0948(1)	$1/12 + \delta$
a = 5.735 Å and c = 14.05 Å	B_1	(2a)	0	0	0				
for $BaTiO_3$ (19)	B_2	(4f)	1/3	2/3	z	.845(30)	.8498(4)	.8453(1)	$5/6 + \delta'$
a = 6.213(3) Å and c = 15.074(4) Å	X_1	(6h)	x	2x	1/4	.522(60)	.522(2)	.5172(7)	$1/2 + \epsilon$
for $CsMnF_3$ (20)	X_2	(12k)	x	2x	z	.836(30) .076(30)	.835(2) .078(1)	.8328(7) .0798(3)	5/6 $1/12 - \delta''$
a = 5.840(2) Å and c = 14.308(4) Å for $RbNiF_3$ (21)									

In the hc-stacking of AX_3-layers, composed of T(1)- and T(2)-layers, the space for the A ions in the c-stacked layers is appreciably larger than for these in the h-stacked layers (Fig. II.3.). This difference in space for the A ions cannot be compensated, for the A ions cannot move out of the planes of the X ions. This structure will therefore be unfavourable for ABX_3 compounds with one type of A ions. If the T(2)-layers are replaced by T(1)-layers either the A or the B ions occupy an additional crystallographic position, contrary to the rule of parsimony.

For $BaMnO_3$ the hc-stacking is reported (16), but all AX_3-layers are of the T(2)-type. An other peculiarity of the reported structure is the large difference between the B-X distances with lengths of 1.94 and 2.10 Å , due to the displacement of the B ions from their ideal positions. As was pointed out before (note p. 34) such large deviations in the B-X distances are not very probable. Negas *et al.* (17) suggested, however, that $BaMnO_3$ (16) is oxygen-deficient. The hc-structure has so far not been found for ABX_3 halides (see, *e.g.* Ref. 18)°.
Another stacking of AX_3-layers with an equal fraction of h- and c-stacked layers, *viz.* the hhcc-stacking, will not occur, because the B ions are distributed over three different types of octahedral sites, contrary to the hhc- , hc- or hcc-stackings (Fig. II.3.).
On the basis of the qualitative rules used here the hc-structure cannot be excluded, but the stability range of this structure will be very small.

In the ABX_3 structure with hcc-stacking of T(1)- and T(2)-layers again two different coordinations occur for both the A and the B and the X ions. In this structure the A ions will move out of the T(2)-layers in order to decrease the B-A repulsion and to improve their coordination by the X ions. The number of crystallographic positions occupied by chemically identical ions remains the same, if the T(2)-layers are replaced by T(1)-layers. Such a replacement, however, causes a larger difference between the coordination of either the A or the B ions on the two crystallographic positions. Since the rule of parsimony does not rest on any term of the lattice energy, no conclusion can be drawn as to whether the B or the A ions have a stronger preference for a more similar coordination. Therefore, the T(2)-layers cannot be replaced by T(1)-layers.
Compounds that crystallize with the hcc-structure are the hexagonal modification of $BaTiO_3$ (19), $CsMnF_3$ (20) and $RbNiF_3$ (21). The structure data of these compounds are collected in Table II.3. In compounds with the *$BaTiO_3$ hcc-structure* shifts of the A and X ions in the direction of the c-axis occur, but the shifts of the X ions in the xy-plane for $BaTiO_3$ and $CsMnF_3$ are not in agreement with the hcc-structure, as derived by us. In the derived structure two-thirds of the anions have to be situated in T(2)-layers and in $BaTiO_3$ and $CsMnF_3$ the x-parameter of the anion deviates from its ideal value, although this deviation is amply within the standard deviation in the case of $BaTiO_3$ and just within the standard deviation in the case of $CsMnF_3$.

The c-stacking of AX_3-layers, consisting of T(2)-layers only, results in a favourable structure, since all ions are isonomously surrounded and the A , B and X ions separately have only one type of coordination. For $SrTiO_3$ (22) (Fig. II.3.) this structure was found. In this *$SrTiO_3$ c-structure*, which has been reported for a large number of ABX_3 halides, no displacement of the ions from their ideal positions occurs.

° Recently, Negas *et al.* (17) described a number of other, more complicated stacking types for $BaMnO_3$ prepared at elevated temperatures in air. They suggest that these are not stoichiometric phases that tend to be oxygen-deficient. These structures are therefore not discussed here.

Finally, let us summarize the results of the comparison between experimentally determined and derived structures:

- *h-stacked layers are T(1)-layers.* The only exception occurs in the $BaMnO_3$ hc-structure. Since increasing fraction of h-stacked layers is caused by increasing radius of the A ion and/or increasing contribution to the polarization energy, the deviation of the x-parameter from its ideal value is also expected to increase. The latter conclusion cannot be checked because of lack of sufficient and accurate experimental data.
- *c-stacked layers are T(2)-layers.* This is also valid for the hcc-structure, since the deviations from the ideal x-parameter reported for $BaTiO_3$ and $CsMnF_3$ are within the standard deviations.
- *Deviations in the A-X and B-X distances.*
  We did not expect appreciable variations in these distances, since all anions are surrounded by four A ions and two B ions and are, therefore, completely in accordance with Pauling's modified second rule. Variations may arise, however, from B-B and B-A repulsion and other small adjustments of the structures. The variations will be larger between the A-X than between the B-X distances, since the charge of the A ion is lower and its coordination number is higher. For the h- and c-structures all B-X distances in the structure are equal by symmetry. In compounds with hhc- and hcc-structures only small variations occur in the B-X distances (Table II.4.). An exception is the $BaMnO_3$ hc-structure.

Table II.4.
B-X distances in ABX_3 compounds with hhc-, hc- and hcc-stacking. The standard deviations are given in parentheses.

compound	B-X (p) [a]	B-X (q) [a]	B-X (r) [a]	sum of the Shannon & Prewitt radii (in Å)	reference
$BaRuO_3$ (hhc)	1.96(1)	2.02(1)	2.00(1)	2.02	14
$CsCoF_3$ (hhc)	2.05	2.05	2.06	2.075	15
$BaMnO_3$ (hc)	1.94	2.10		1.94	16
$BaTiO_3$ (hcc)	2.02(8)	1.96(8)	1.95(8)	2.005	19
$RbNiF_3$ (hcc)	1.993(8)	2.036(7)	2.041(8)	2.02	21
$RbNiF_3$ (hcc)	2.03	2.15	2.01	2.02	15 [b]
$CsMnF_3$ (hcc)	2.12(2)	2.16(2)	2.12(2)	2.16	20

[a] These distances (in Å) correspond to those indicated by p , q and r in Fig. II.3.
[b] Babel's data (15) do not permit the degree of accuracy attained by Weidenborner *et al.* (21).

II.3.2. Structures of ABX_3 halides in which the A ion is smaller than the X ion

When the space available for the A ion in the ideal c-structure becomes too large, three deformations can be derived (Section II.2.): a trigonal structure (composed of c-stacked T(3)-layers), a tetragonal structure and an orthorhombic structure. The two last mentioned structures were obtained by rotation of the BX_6-octahedra around a fourfold axis.
Of these possible deformations the trigonal structure (reported for $LaAlO_3$ (23,24) (Tables II.1. and 5.)) was not expected for $A^+B^{2+}X_3$ halides and has not been found so far for one of these compounds.
When the space available for the A ion in the ideal structure is too large, the tetragonal structure is expected first and the orthorhombic structure next.
The tetragonal deformation is found for $SrTiO_3$ below 110°K (26) and for $KMnF_3$ below 184°K (27). The cell edges and the atomic parameters of $KMnF_3$ (Table II.5.) are not determined at the same temperature, so that the interdependence of the rotation parameter δ and the c/a-value, which we derived (Table II.1.), cannot be checked.
The orthorhombic structure of Fig. II.4b. (Table II.1.) is known as the $GdFeO_3$ structure type (29) and has been reported for a vast number of ABX_3 halides and oxides. The structure

Table II.5.
Symmetry, cell dimensions and atomic parameters of the $LaAlO_3c'$-, $KMnF_3c'$- and $GdFeO_3c'$-structures.
No standard deviations were reported in the literature.

1. $LaAlO_3$ (25,23)					
Space group $R\bar{3}c$ (D_{3d}^6)	La	(6a)	0	0	1/4
a = 5.365 and c = 13.11 Å	Al	(6b)	0	0	0
	O	(18e)	.53	0	1/4
2. $KMnF_3$ (27,28)					
Space group I4/mcm (D_{4h}^{18})	K	(4b)	0	1/2	1/4
a = 5.900 and c = 8.330 Å	Mn	(4c)	0	0	0
	F_1	(4a)	0	0	1/4
	F_2	(8h)	.21	.71	0
3. $NaCoF_3$ *with* $GdFeO_3c'$*-structure* (30)					
Space group Pbnm (V_h^{16})	Na	(4c)	−.0169	.0481	1/4
a = 5.428 b = 5.607	Co	(4b)	1/2	0	0
and c = 7.790 Å	F_1	(4c)	.0974	.4552	1/4
	F_2	(8d)	−.3066	.3006	.0584

data of one of these compounds, $NaCoF_3$, are given in Table II.5. The $c/(a\sqrt{2})$- and $c/(b\sqrt{2})$-values for ABX_3 halides with *$GdFeO_3$ c'-structure* are listed in Table II.6. The former value is > 1 (NH_4SnF_3 excepted), the latter is < 1 ($KMgCl_3$, $RbCaCl_3$ and $CsHgCl_3$ excepted). The two values are nearly independent of the size of the B ion for $NaBF_3$ compounds.

Table II.6.
$c/(a\sqrt{2})$- and $c/(b\sqrt{2})$-values for ABX_3 halides with $GdFeO_3$ c'-structure. The data are taken from the references reported in Tables II.9. and 10.

	Ni	Mg	Co	Zn	Fe	Mn	Ca	Hg	Sn	Sr
$NaBF_3$	1.017 0.986	1.012 0.988	1.017 0.984	1.013 0.983	1.015 0.984	1.016 0.982				
KBF_3								1.005 0.992		
NH_4BF_3									0.981 0.981	
$KBCl_3$		1.009 1.006					1.018 0.978			
$RbBCl_3$							1.010 1.000			1.017 0.979
$CsBCl_3$								1.003 1.000		

II.3.3. Deformations of the derived structures due to the electron configuration of the B ion

The *$CsCuCl_3$ h'-structure* (31) is the $BaNiO_3$ h-structure with a deformation caused by the non-spherical symmetry of the environment of the Cu^{2+} ion. If we assume that this so-called Jahn-Teller effect distorts the BX_6-octahedron in such a way that two collinear B-X distances are longer than the other four —as reported for most compounds with a Cu^{2+} ion—, an attempt can be made to derive the ideal h-stacked ABX_3 structure with Jahn-Teller distortion. An elongation of two collinear B-X distances in the BX_6-octahedron can be realized in three directions, *i.e.* along the three fourfold axes. Since the octahedra are sharing faces, the displacement of the X ions in any shared face is that resulting from the elongation of the two octahedra. In the three most simple deformations the *successive* face-sharing octahedra will have an elongation in one, two or three different directions. Of these three possibilities that deformation is expected in which the coordinations of the A and X ions are deformed as less as possible and in which the structure remains fairly dense. The elongation

of the BX_6-octahedra causes a displacement of one or two anions in an AX_3-layer. An elongation of the BX_6-octahedra can also be obtained by displacing adjacent AX_3-layers with respect to each other, resulting in a more dense structure. The B ion must keep a central position between the six anions. If the three most simple deformations are built by displacing adjacent AX_3-layers with respect to each other (Figs. II.5a., b. and c.), the structure in which the face-sharing BX_6-octahedra are successively elongated in the three different directions (Fig. II.5c.), turns out to be the most likely one, because:

- the A ion keeps a rather high and isonomous coordination.
- the contribution as a result of polarization to the lattice energy is only slightly decreased.
- the coordination of the B ion closely resembles an octahedron with two longer collinear B-X distances.

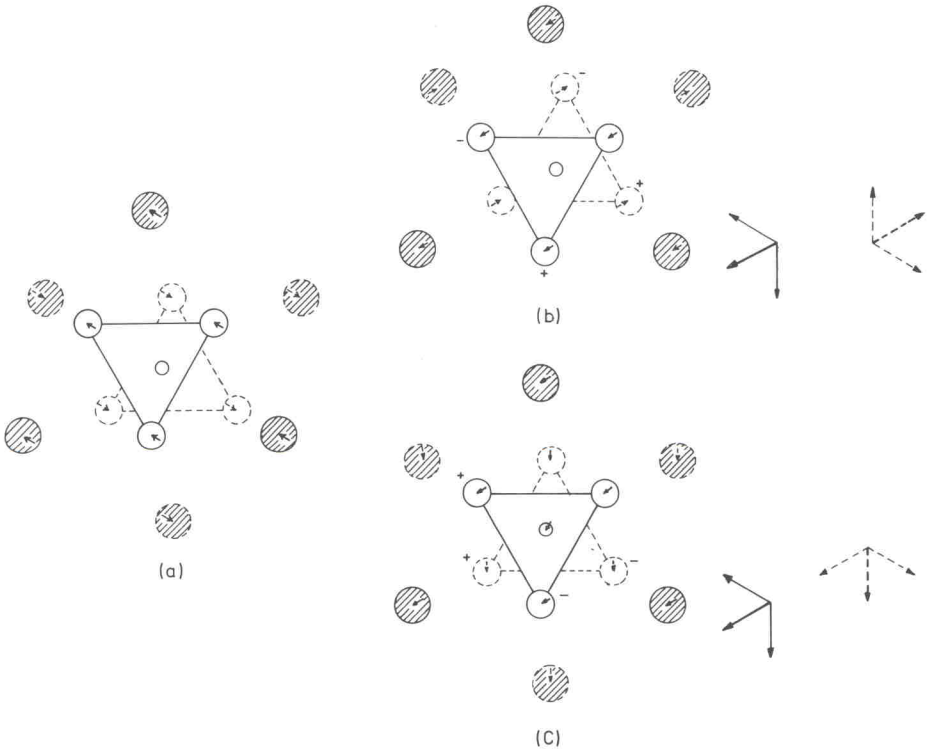

Fig. II.5.

Deformations of the ideal h-stacked ABX_3 structure as a result of elongation of the BX_6-octahedra due to the Jahn-Teller effect. Elongation occurs by displacing AX_3-layers with respect to each other. Successive face-sharing octahedra have an elongation in one (Fig. II.5a.), two (Fig. II.5b.) or three (Fig. II.5c.) different directions. Shaded circles represent A ions, open circles X ions, and small open circles B ions. The AX_3-layer below the plane of the paper is dotted. The B ion lies between the two AX_3-layers. The arrows indicate the displacements of the ions, resulting from the elongation of *two* adjacent octahedra. The plus and minus signs denote positions above and below the plane of the AX_3-layer.

This result is in accordance with the assumption that only those deformations are expected in which the symmetry of the ideal structure is preserved as much as possible (Section I.3.). The agreement between the structure data, derived in the way as discussed above and the experimentally determined values (Table II.7.) is rather bad. Both the shift of the Cu^{2+} ion and the displacement of the Cl(1)-position from the ideal position in the $BaNiO_3$ h-structure are larger than expected. The ratio between the shift along the z-axis and the shift in the xy-plane for the Cl(2)-position does not agree very well either with the expected value. More accurate data are not to be expected from such a qualitative approach, since the contribution of polarization to the lattice energy cannot be evaluated and the allowed difference between the two types of short Cu-Cl distances is not known.

Table II.7.

Symmetry, cell dimensions and atomic parameters for the realized and derived $CsCuCl_3$ h'-, $KCuF_3$ c'- and $CsGeCl_3$ c'-structure. The cell dimensions are expressed in the cell edge of the unit cell of the ideal c-stacked ABX_3 structure for the derived structures. Standard deviations are given in parentheses. δ , ϵ and ϵ' indicate the expected deviations from the ideal parameters as a result of the electron configuration of the B ion.

						atomic parameters for: realized structure	atomic parameters for: derived structure
1. *$CsCuCl_3$ h'-structure* (31)							
Space group $P6_122$ (D_6^2)	A	(6b)	x	2x	1/4	.35458(10)	$1/3+\delta$
	B	(6a)	x	0	0	.0616(3)	δ
$a=\sqrt{2}$ and $c=2\sqrt{3}$	X_1	(6b)	x	2x	1/4	.8877(3)	$5/6+\delta$
						.3540(5)	$1/3+\delta$
$a=7.2157(5)$ and $c=18.1777(10)$ Å	X_2	(12c)	x	y	z	.2095(5)	$1/6+2\delta$
						.2418(2)	$1/4-\delta/2$
2. *$KCuF_3$ c'-structure* (32)						atomic parameters for: r. s.	atomic parameters for: d. s.
Space group I4/mcm (D_{4h}^{18})	A	(4a)	0	0	1/4		
	B	(4d)	0	1/2	0		
$a>\sqrt{2}$ $c=2$ $c/a<\sqrt{2}$	X_1	(4b)	0	1/2	1/4		
$a=5.855(2)$ and $c=7.852(4)$ Å	X_2	(8h)	x	1/2+x	0	.228(8)	$1/4-\delta$
$c/(a\sqrt{2})=$ .948 .930 .903 .914 ($ACuF_3$) .938 .930 .902 .921 ($ACrF_3$) for A = K , Rb , NH_4 , Tl[a]							
3. *$CsGeCl_3$ c'-structure* (33)						atomic parameters for: r. s.	atomic parameters for: d. s.
Space group R3 (C_3^4)	A	(3a)	0	0	0		
$a=\sqrt{2}$ and $c=\sqrt{3}$	B	(3a)	0	0	z	.481(3)	$1/2-\epsilon$
						.1459	$1/6-\delta$
$a=7.67$ and $c=9.48$ Å	X	(9b)	x	y	z	.2876	$1/3-2\delta$
						.3515	$1/3+\epsilon'$
Ge-Cl distances 2.32 Å (3x) and 3.13 Å (3x)							

[a] For references, see Table II.9.

The *$KCuF_3$ c'-structure* has been described as the $SrTiO_3$ c-structure with Jahn-Teller distortion (32). If the Jahn-Teller effect is assumed to distort the BX_6-octahedra in such a way that two 'opposite' B-X distances are larger than the other four, the deformation of the c-structure can be derived by preserving its symmetry as much as possible. Since the BX_6-octahedra join each other by their six corners, it is unlikely that a deformation can be found in which a threefold axis or a threefold screw axis is maintained (See the $CsCuCl_3$ h'-structure). The two most probable deformations in which the fourfold axis is maintained are:

- All BX_6-octahedra are elongated in the same direction.
- The BX_6-octahedra are alternately elongated in two perpendicular directions in the xy-plane (Fig. II.6.).

The former deformation can be rejected by taking into account the coordination of the anions: One of the two different anion coordinations consists of a square of A ions and of two B ions that are farther away than in the ideal structure. Such a non-isonomous anion coordination does not occur in the second deformation. This deformation, however, gives rise to three different B-X distances if the c/a-ratio would be kept constant. Since we started from the assumption that only two B-X distances tend to be larger than the other four, the c/a-ratio has to be decreased. The diminution of the c/a-ratio and the shift (δ) of the anion parameter depend on the increase of two of the B-X distances (due to the Jahn-Teller distortion) and the tolerance in the differences among the other four B-X distances and the A-X distances. The rough parameters of the second deformation and those of the experimentally determined structure are listed in Table II.7.

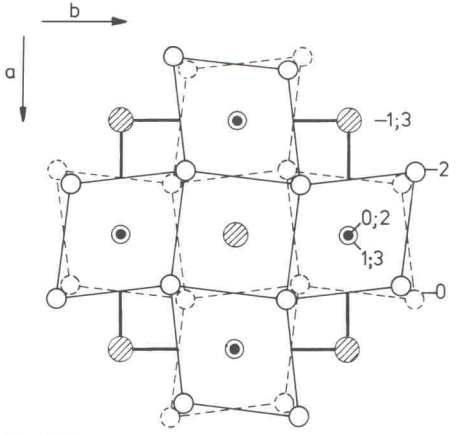

Fig. II.6.

Deformation of the ideal c-stacked ABX_3 structure as a result of elongation of the BX_6-octahedra due to the Jahn-Teller effect. The BX_6-octahedra are alternately elongated in two perpendicular directions in the xy-plane. Shaded circles represent A ions, open circles X ions, and black circles B ions. Figures indicate the heights of ions above the plane of the paper in quarters of the c-axis. The unit cell is indicated by very heavy lines.

The *$CsGeCl_3$ c'-structure* (33) is a $SrTiO_3$ c-structure with a deformation due to the $d^{10}s^2$-electron configuration of the Ge^{2+} ion having a free electron pair. It is experimentally found that the BX_6-octahedron is deformed in such a way that three short and three long B-X distances are formed. The free electron pair is assumed to be between the B ion and the three X ions at the larger distance from the B ion. These BX_6-octahedra are realized in one of the c-stackings of T(1)-layers (Fig. II.3.). Each B ion is sandwiched between a small and a large X_3-triangle and is displaced in the direction of the small X_3-triangle. So three much larger B-X distances are formed allowing for the free electron pair. The A ion moves in the direction of the large X_3-triangle in order to make the structure more dense and to increase the attraction by the free electron pair. The structure data of the hexagonal setting of the structure are given in Table II.7.

II.3.4. Structures of ABX_3 halides not derivable from AX_3-layers with T-pattern

Some experimentally determined structures for ABX_3 halides could not be derived within the delimitations made in Section I.2. and are neither deformations of the ideal structures caused by electronic effects of the B ions (Section II.3.3.). These structures and deformations of them that are due to the electronic configuration of the B ion will be discussed in this section.

The *NH_4CdCl_3 structure* (34,35) (Fig. II.7.) consists of double-chains of $CdCl_6$-octahedra with the NH_4^+ ions between these double-chains in a fairly isonomous nine-coordination of Cl^- ions. The sharing octahedron (2) of this structure is drawn in Fig. II.8. The nine-coordination of the NH_4^+ ion consists of a trigonal prismatic coordination and an intraplanar triangular coordination. The interionic distances and the coordination of the anions are listed in Table II.8.

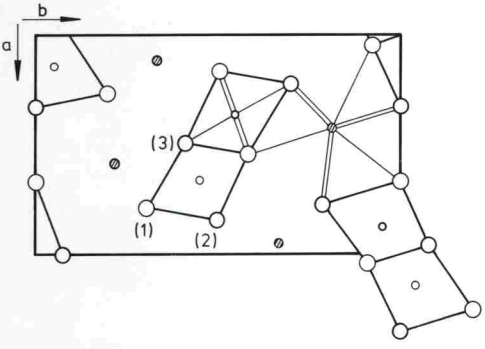

Fig. II.7.
Projection of the crystal structure of NH_4CdCl_3 (34,35) along the c-axis. The shaded circles represent A ions, the open circles X ions, and the small open circles B ions. Ions at heights 1/4 and 3/4 are distinguished as light and heavy circles. The cation coordinations are marked by light lines. The figures indicate the three types of X ions listed in Table II.8.

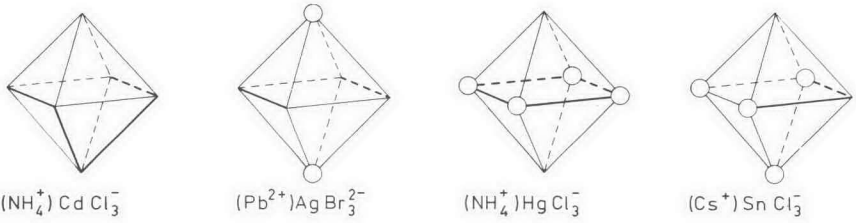

Fig. II.8.

Idealized sharing octahedra (2) in the structures of NH_4CdCl_3, $PbAgBr_3$ (if derivable from the $PuBr_3$ structure), NH_4HgCl_3 and $CsSnCl_3$. Heavy full and broken lines indicate the edges, and circles indicate the vertices that the octahedra share with other octahedra in the structure.

Table II.8.

A-X and B-X distances (in Å) and anion coordinations in the crystal structures of NH_4CdCl_3 (34), NH_4HgCl_3 (38) and $CsSnCl_3$ (41).

	NH_4CdCl_3	NH_4HgCl_3	$CsSnCl_3$
A-X distances	3.27(4x) \ prism 3.40(2x) / 3.34; 3.47 3.82	3.39(8x) 3.97(2x)	3.41; 3.55 3.59(4x) 3.63 3.85; 3.94; 4.14
B-X distances	2.60(2x) 2.62; 2.64 2.72(2x)	2.33(2x) 2.96(4x)	2.50; 2.52; 2.55 3.21; 3.45; 3.77
Anion coordination:			
X_1	4A 3.27(4x) 1B 2.62	4A 3.39(4x) 1B 2.33	4A 3.55; 3.59; 3.85; 4.14 2B 2.52; 3.45
X_2	3A 3.47; 3.40(2x) 2B 2.60(2x)	2A 3.97(2x) 4B 2.96(4x)	3A 3.41; 3.59(2x) 1B 2.50
X_3	2A 3.34; 3.82 3B 2.64; 2.72(2x)		3A 3.59; 3.63; 3.94 3B 2.55; 3.21; 3.77

The *$KCuCl_3$ structure* (36) can be considered as a NH_4CdCl_3 structure with Jahn-Teller distortion due to the Cu^{2+} ion.

Recently, the X-ray powder diagram of *$PbAgBr_3$* was reported to be very similar to that of $PuBr_3$, and it was indexed with the lattice constants a = 13.46 Å, b = 4.21 Å and c = 9.88 Å (37). If the structure of $PbAgBr_3$ is indeed a substitution of the $PuBr_3$ structure the sharing octahedron is of the type drawn in Fig. II.8.

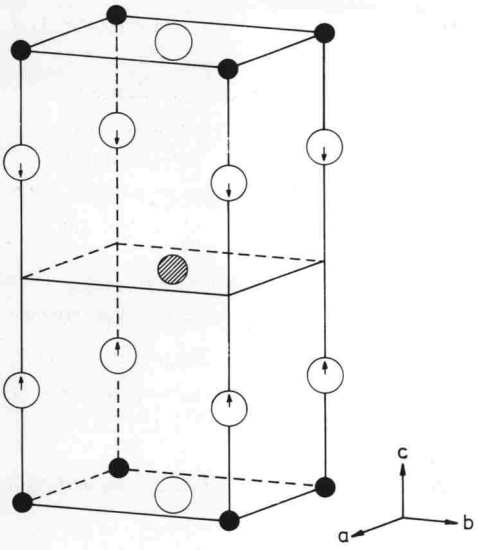

Fig. II.9.
Idealized crystal structure of NH_4HgCl_3 (38). Shaded circles represent A ions, open circles X ions, and black circles B ions. Arrows indicate the displacement of the X ions from their idealized positions.

In the *NH_4HgCl_3 structure* (38) the A and X ions constitute a lattice, intermediate between a b.c.c. and a '$MoSi_2$' lattice☆ (c/a(b.c.c.) = 1 , c/a('$MoSi_2$') = 0.8165 , c/a(NH_4HgCl_3) = 0.947). The structure can be obtained by placing two b.c.c. cells on top of each other (Fig. II.9.). One of these cells contains one A and one X ion and the other one two X ions. The Hg^{2+} ion lies in the compressed octahedral hole of the b.c.c. structure. Although the Hg^{2+} ion seems to prefer a two-coordination○, the compression of the octahedron is decreased by a displacement of the X ions from their ideal positions. By this displacement and a slight compression of the b.c.c. lattice along the c-axis the coordination of the NH_4^+ ion resembles the ten-coordination of a lattice point in the '$MoSi_2$' lattice of which two lattice points are put at a longer distance. Another distribution of NH_4^+ and Cl^- ions over the lattice positions of the b.c.c. lattice in which the NH_4^+ ions are more equally spaced out is less probable, because the Hg^{2+}-coordination cannot be adjusted as above without making the coordination of the NH_4^+ ion unfavourable. The sharing octahedron of this structure is given in Fig. II.8. and the interionic distances are listed in Table II.8. The stability of this structure has not only to be attributed to the specific coordination of the Hg^{2+} ion but also to the tetragonal surrounding of the NH_4^+ ion, which allows for 'hydrogen-chlorine' interaction.

☆ By '$MoSi_2$' lattice that lattice is meant that is constituted by the Mo and Si positions in the $MoSi_2$ structure (39).

○ A two-coordination, often found for Cu^+ , Ag^+ , Au^+ and Hg^{2+} compounds, was explained by Orgel (40), who attributed it to the small energy difference between the d^{10} and d^9s-electron states of these ions.

The *$CsSnCl_3$ structure* (41) could not be derived from AX_3-layers with T-pattern either. The Sn^{2+} ion like the Ge^{2+} ion has a $d^{10}s^2$-electron configuration and is often coordinated by three anions at a smaller and three at a larger distance. This deformed six-coordination is generally attributed to the presence of a free electron pair that is assumed to constitute a tetrahedral coordination together with three anions[△]. If the $CsSnCl_3$ structure is considered to be a deformation of a structure with regular octahedra like $CsGeCl_3$ (Section II.3.3.), the sharing octahedron is of the type as drawn in Fig. II.8. The interionic distances and the coordinations of the anions are listed in Table II.8.

The structures, briefly described in this section, have in common that the BX_6-octahedra do not exclusively share corners and/or faces, like in the derived structures, but also edges and that they occur for compounds with polarizable anions. Some of these structures are derived by Gorter (45) by constructing structures with nine-coordinated cations. These structures might also be derived by starting from another basic lattice.

II.4. Discussion of the experimental inter- and intralayer distances, reduced c/a-values and volumes per formula unit ABX_3

Since the derived structures are in good agreement with the real structures (Section II.3.), an attempt was made to calculate c_{red}-, a_{red}-, $(c/a)_{red}$-values[☆] and the volumes per formula unit for ABX_3 halides with $BaNiO_3$ h-, $BaRuO_3$ hhc-, $BaTiO_3$ hcc- and $SrTiO_3$ c-structures. The c_{red}-, a_{red}- and $(c/a)_{red}$-values calculated with the aid of the ionic radii of Shannon & Prewitt (3,4) roughly agreed with the experimental data but, generally, they were too high (0.1 Å and sometimes even 0.2 Å). We therefore restrict ourselves to a brief qualitative discussion of the experimental data. The experimentally determined structures and the references to the papers in which the structure data are reported are tabulated in Tables II.9., 10., 11. and 12. for the ABF_3, $ABCl_3$, $ABBr_3$ and ABI_3 compounds, respectively.

△ This tetrahedral coordination of the Sn^{2+} ion is also found for $SnCl_2$, SnS, SnSe, $SnCl_2.2H_2O$, $K_2SnCl_4.H_2O$, $SnSO_4$ (42), $NaSn_2F_5$ (43) and Sn_2S_3 (44).

☆ c_{red} = the mean distance between two nearest AX_3-layers, the interlayer distance.
a_{red} = half the shortest distance between two A ions in an AX_3-layer, the intralayer distance.
$(c/a)_{red} = c_{red}/a_{red}$ = the reduced c/a-value.

Table II.9.

Structure types and references for ABF_3 *compounds at ambient temperature and pressure.*

The structure types are denoted as follows: the crystal system is indicated by a capital letter and an index-letter indicates a characteristic ion of the first compound found with the respective structure or the stacking type of the AX_3-layers (the latter in the case of the 'undeformed' h-, hhc- and hcc-structures). H_h, H_{hhc}, H_{hcc}, **C** indicate the $BaNiO_3$ h-, $BaRuO_3$ hhc-, $BaTiO_3$ hcc- and $SrTiO_3$ c-structures, respectively. O_{Fe} indicates the $GdFeO_3$ c′-structure and T_{Cu} the $KCuF_3$ c′-structure. If the crystal system is indicated by small letters (c = cubic, t = tetragonal, o = orthorhombic, h = hexagonal, r = rhombohedral, m = monoclinic, a = triclinic (anorthic)) this means that it was determined by indexing the X-ray pattern or by optical measurements, but that the structure is not known. An asterisk indicates that the correctness of the structure determination is in doubt, *e.g.* because the specimen was not pure or because the volume per formula unit deviates strongly from the expected value (Section II.4.2.), or because the indexing is only tentative, *e.g.* in the case of 'pseudocubic' indexing. A plus sign indicates that the compound was prepared but that the X-ray pattern has not been indexed.

The references in which the most reliable and accurate structure data are reported are also given.

	Ni	Mg	Mg	Cu	Co	Zn	Fe	V	Cr	Mn	Pd	Cd	Cd	Ca	Ca	Ca	Ge	Hg	Sn	Sn	Sr	Eu	Pb
Na	O_{Fe} (46, 30)	O_{Fe} (47)		m (48)	O_{Fe} (50, 30)	O_{Fe} (49)	O_{Fe} (50)	C* (51)	m (52)	O_{Fe} (53)									m (54)				
Ag	C (55)	C (55)		m (55)	C (55)	C (55)				C (55)													
K	C (56)	m (57)	C (58)	T_{Cu} (32)	C (56)	C (59)	C (56)	C (51)	T_{Cu} (52)	C (28)		c* (60)	C (61)	m (57)	c* (62)	C (61)	+ (63)	O_{Fe} (64)	m (54)	a (65)			
Rb	H_{hcc} (21)	m (57)		T_{Cu} (48)	C (66)	C (67)	C (68)	C (51)	T_{Cu} (52)	C (67)		t (60)	C (52)	C (57)				C (64)	o (69)		c* (60)		+ (70)
NH_4	c* (46)	C (71)		T_{Cu} (67)	C (67)	C (67)	C (72)		T_{Cu} (52)	C (67)		t (73)							O_{Fe} (54)				
Tl	H_{hcc} (74)			T_{Cu} (48)	C (48)	H_{hcc} (52)	C (50)		T_{Cu} (52)	C (75)		C (52)											
Cs	H_h (15)	t* (57)		h* (76)	H_{hhc} (15)	t* (57)	H_{hcc} (68)			H_{hcc} (20)	+ (77)	C (60)		C (57)			o (63)	C (64)	o (69)		C (60)	C (78)	t (70)

Table II.10.

Structure types and references for $ABCl_3$ *compounds at ambient temperature and pressure.* H_h, H_{hhc}, H_{hcc}, **C** indicate the $BaNiO_3$ h-, $BaRuO_3$ hhc-, $BaTiO_3$ hcc- and $SrTiO_3$ c-structures, respectively. O_{Fe} indicates the $GdFeO_3$ c′-structure, H_{Cu} the $CsCuCl_3$ h′-structure, R_{Ge} the $CsGeCl_3$ c′-structure. The respective structures of NH_4CdCl_3, $KCuCl_3$, NH_4HgCl_3 and $CsSnCl_3$ are indicated by O_{Cd}, M_{Cu}, T_{Hg} and M_{Sn}. See also the caption of Table II.9.

	Ni	Mg	Cu	Co	Zn	Fe	V	Cr	Mn	Ti	Cd	Ca	Ge	Hg	Sn	Sr	Pb	Ba
Na		+ (79)			o (80)				h (81)	+ (82)				O^*_{Cd} (83)				
K	H_h (84)	O_{Fe} (85)	M_{Cu} (36)	H^*_h (86)	+ (87)	H_h (88)	H^*_h (89)	+ (90)	t (91)	+ (92)	O_{Cd} (93)	O_{Fe} (94)	+ (95)	+ (96)	+ (97)		+ (98)	
Rb	H_h (99)	+ (100)		H_h (101)		H_h (102)	+ (103)	H^*_h (90)	H_{hcc} (104)	+ (105)	O_{Cd} (35)	O_{Fe} (94)	+ (95)	C (84)	+ (97)	O_{Fe} (94)		
NH_4	H_h (94)	+ (106)	M_{Cu} (36)	H_h (94)	+ (107)		+ (103)				O_{Cd} (35)		+ (95)	T_{Hg} (38)				
Tl	H_h (84)			+ (84)					t (108)		+ (109)			O_{Cd} (110)	+ (111)			
Cs	H_h (112)	H_h (113)	H_{Cu} (31)	H_h (114)		H_h (102)	H_h (113)	H_h (90)	H_{hhc} (115)	H_h (113)	C (116)	C (113)	R_{Ge} (33)	O_{Fe} (94)	M_{Sn} (41)	t (94)	t (117)	+ (118)

Tables II.11. and 12.

Structure types and references for $ABBr_3$ *and* ABI_3 *compounds, respectively, at ambient temperature and pressure.* H_h , **C** , O_{Cd} and M_{Cu} indicate the $BaNiO_3$ h-, $SrTiO_3$ c-, NH_4CdCl_3 and $KCuCl_3$ structures, respectively. See also the caption of Table II.9.

	Ni	Mg	Cu	Ti	Cd	Hg	Sn	Pb
K		+ (119)	M_{Cu} (36)		+ (120)	+ (121)		+ (122)
Rb	H_h (99)			H_h (123)				
Tl					+ (124)	O_{Cd} (110)		
Cs	H_h (125)			H_h (123)	C (126)	c* (127)	C (128)	m (129)

	Cd	Hg	Pb
K	+ (130)		+ (131)
Tl	+ (124)		+ (132)
Cs	+ (133)	m (126)	O_{Cd} (134)

II.4.1. Inter- and intralayer distances and reduced c/a-values as a function of the radii of A , B and X ions

The c_{red}-, a_{red}- and $(c/a)_{red}$-values are calculated for the various structure types in the following manner:

- The $BaNiO_3$ h-structure consists of T(1)-layers only. The B ions are placed above and below the centres of the small X_3-triangles, so that they are in contact with the X ions. The values of c_{red} and a_{red} are therefore determined by the radii of B and X and by the radii of the A and X ions, respectively.
- In the $BaRuO_3$ hhc-structure one-third of the AX_3-layers are of the T(2)-type. These determine the a_{red}-value. The B ions are placed between the T(1)- and T(2)-layers as indicated in Fig. II.3., so that they are in contact with the X ions. c_{red} is determined by the A , B and X ions.
- In the $BaTiO_3$ hcc-structure two-thirds of the AX_3-layers are of the T(2)-type, in which the A ions lie above or below their ideal positions. We therefore consider the other one-third of the AX_3-layers, T(1)-layers to determine the a_{red}-value. The B ions are placed between the various X_3-triangles in the AX_3-layers, so that they are in contact with the X ions. c_{red} is determined by the A , B and X ions.
- The $SrTiO_3$ c-structure consists of T(2)-layers only. c_{red} and a_{red} are only determined by the B and X ions.

Table II.13.

The expected relation between the c_{red}-, a_{red}- and $(c/a)_{red}$-values and r_A, r_B, r_X for the $BaNiO_3$ h-, $BaRuO_3$ hhc-, $BaTiO_3$ hcc- and $SrTiO_3$ c-structures. The value of c_{red}, a_{red} or $(c/a)_{red}$ increases with (+), is independent of (0) or decreases with (−) increasing r_A, r_B or r_X.

structure	radius	c_{red}	a_{red}	$(c/a)_{red}$
$BaNiO_3$ (h)	r_A	0	+	−
	r_B	+	0	+
	r_X	+	+	−
$BaRuO_3$ (hhc)	r_A	−	+	−
	r_B	+	0	+
	r_X	+	+	+[a]
$BaTiO_3$ (hcc)	r_A	−	+	−
	r_B	+	0	+
	r_X	+	+	+
$SrTiO_3$ (c)	r_A	0	0	0
	r_B	+	+	0
	r_X	+	+	0

[a] increases weakly.

From the above, relations between the c_{red}-, a_{red}-, $(c/a)_{red}$-values and r_A, r_B, r_X can be derived for the various structure types. The results are listed in Table II.13. and will be compared with the experimental data (Figs. II.10., 11., 12.). The data for compounds at non-ambient temperatures and pressures are also included in Fig. II.12. These are, however, discussed in Section II.6.

- The experimental c_{red}-values of Fig. II.10. for compounds with $BaNiO_3$ h-structure are almost independent of r_A and increase with r_B. Exceptions are $KFeCl_3$ and $CsVCl_3$. The c_{red}-values of $CsMgCl_3$ and $CsCrCl_3$ are too high, compared with the values of the other compounds. The influence of r_X is confirmed for $CsNiX_3$ (X = F, Cl).
  The experimental a_{red}-values (Fig. II.11.) increase with r_A, increase slightly with (should be independent of) r_B and increase with r_X (one datum). The a_{red}-values of $CsMgCl_3$ and $KFeCl_3$ are too high in comparison with the other data.
  The experimental $(c/a)_{red}$-values (Fig. II.12.) decrease with increasing r_A and r_X (one datum). The relation between the $(c/a)_{red}$-values and r_B is not very clear.
- The predictions for the $BaRuO_3$ hhc-structure cannot be verified because of lack of data.
- The c_{red}-values of compounds with the $BaTiO_3$ hcc-structure (Fig. II.10.) are, contrary to our expectation, independent of r_A and increase with r_B. The influence of r_X cannot be verified because of lack of data.

The influence of r_A on the a_{red}-values (Fig. II.11.) is confirmed, but the influence of r_B is not as expected.

The experimental $(c/a)_{red}$-values of Fig. II.12. agree with our expectation for the influence of r_A , although the difference between the $(c/a)_{red}$-values of $RbNiF_3$ and $TlNiF_3$ is very small. The $(c/a)_{red}$-value of $CsBF_3$ compounds with the $BaTiO_3$ hcc-structure increases with r_B , but that for the $TlBF_3$ compounds is independent of r_B .

— The calculation of the c_{red}- and a_{red}-values for the ABX_3 halides with $SrTiO_3$ c-structure has particularly shown that these values cannot be calculated by a simple addition of the ionic radii. The calculated c_{red}- and a_{red}-values are not only larger than these determined experimentally (3), but the curves of Figs. II.10. and 11. are not flattened at the point where r_A determines the c_{red}- and a_{red}-values (For KBF_3 compounds at B = Mg ; for $TlBF_3$ and $RbBF_3$ compounds at B = Mn .). Moreover, when the c_{red}- and a_{red}-values are determined by r_B and r_X , the influence of r_A is clearly observable and the slope of the curve is less steep than expected.

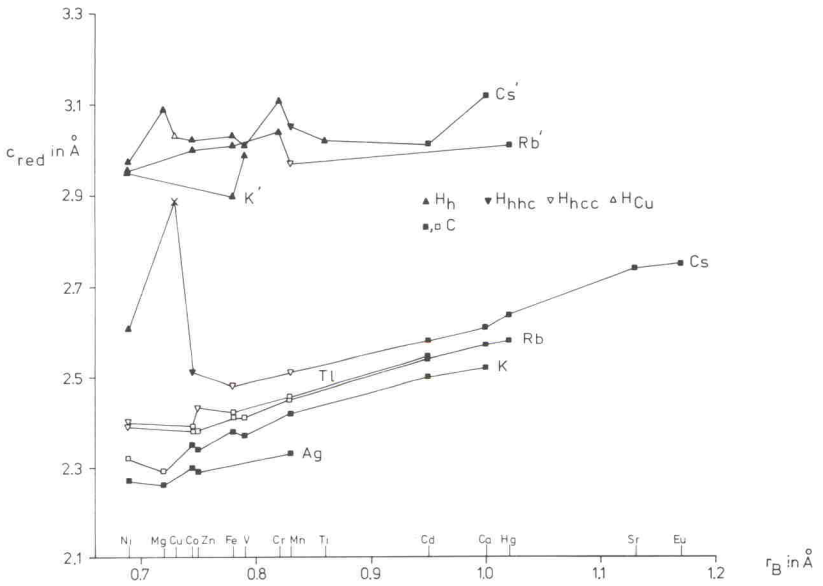

Fig. II.10.

Interlayer distances as a function of the radii of the B ions for ABF_3 and $A'BCl_3$ compounds at ambient temperature and pressure.

H_h = $BaNiO_3$ h-structure
H_{hhc} = $BaRuO_3$ hhc-structure
H_{hcc} = $BaTiO_3$ hcc-structure
H_{Cu} = $CsCuCl_3$ h'-structure
C = $SrTiO_3$ c-structure (indicated by black squares when the A ion 'rattles', by open squares when the B ion 'rattles').

A cross marks an unknown hexagonal structure type.

From the foregoing it is clear again that 'ionic radii' are neither 'radii' nor 'constants', even not if the ion has the same coordination in the same structure. The radius of an ion does not depend only on its coordination and electron configuration, but also on the sizes and charges of all remaining ions. These deviations from a constant value will become more apparent in structures with special positions and particularly in structures with cubic symmetry. Nevertheless, ionic radii will remain of great help at the comparison of the structures of different compounds and at the derivation of structures.

So far we only discussed the c_{red}-, a_{red}- and $(c/a)_{red}$-values as a function of r_A , r_B and r_X for constant structure type. The following can be expected for these values as a function of structure type for constant r_A , r_B and r_X:

- c_{red} decreases in the order h , hhc , hcc , c . It is, however, larger for the c-structure than for the other structures, when the r_B/r_X-value is large, which is nearly always the case.
- a_{red} is almost the same for the h- , hhc- and hcc-structures. For the c-structure a_{red} is larger than for the other structures when the r_B/r_X-value is large.
- $(c/a)_{red}$ decreases in the order h , hhc , hcc , c . The $(c/a)_{red}$-value for the h- , hhc- and hcc-structures, however, may become smaller than that for the c-structure, when the r_A/r_X-value is large and the r_B/r_X-value is small.

For compounds with constant r_A and r_X these expected effects are fairly well realized, as can be seen in Figs. II.10., 11. and 12.

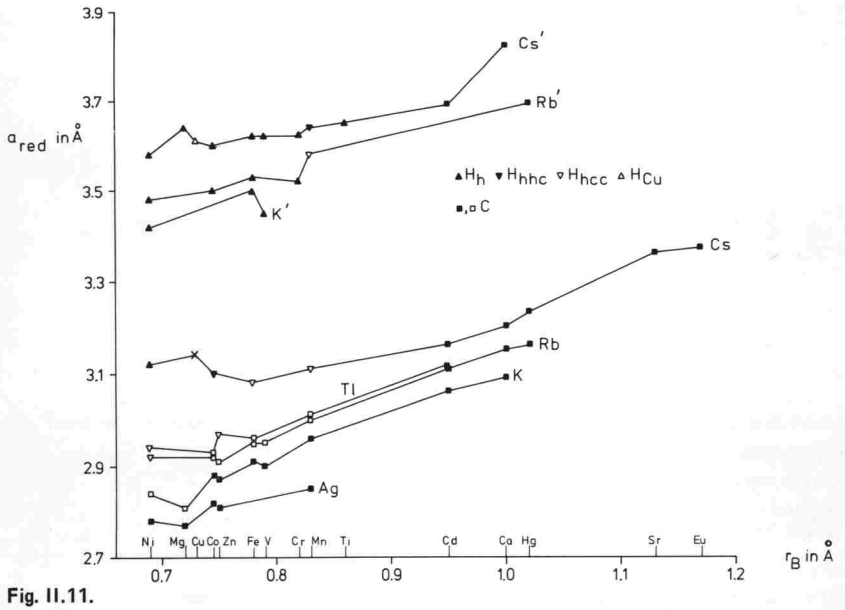

Fig. II.11.

Intralayer distances as a function of the radii of the B ions for ABF_3 and $A'BCl_3$ compounds at ambient temperature and pressure. See caption of Fig. II.10.

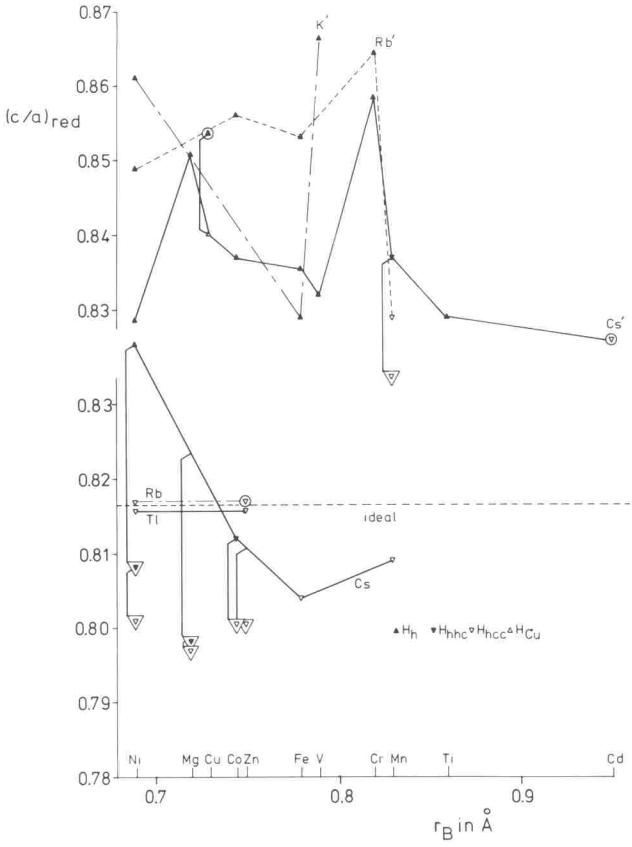

Fig. II.12.

Reduced c/a-values as a function of the radii of the B ions for ABF_3 and $A'BCl_3$ compounds.

H_h = $BaNiO_3$ h-structure

H_{hhc} = $BaRuO_3$ hhc-structure

H_{hcc} = $BaTiO_3$ hcc-structure

H_{Cu} = $CsCuCl_3$ h'-structure.

A symbol within a circle indicates a high-temperature, a symbol within a triangle a high-pressure modification.

II.4.2. Volumes per formula unit ABX_3

Calculation of the volumes per formula unit (V) for the $BaNiO_3$ h-, $BaRuO_3$ hhc-, $BaTiO_3$ hcc- and $SrTiO_3$ c-structures as described in Section II.4.1. leads to the following relations between V and r_A , r_B , r_X :

– V increases with r_A , r_B and r_X with one exception: V remains constant for the c-structure when r_A increases.

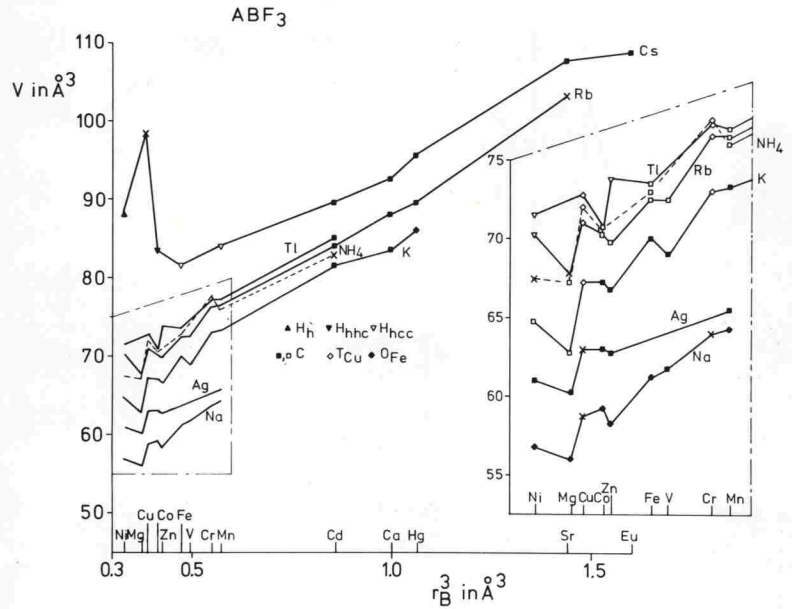

Fig. II.13.

Volumes per formula unit (V) for ABF_3 compounds at ambient temperature and pressure as a function of r_B^3.

H_h = $BaNiO_3$ h-structure

H_{hhc} = $BaRuO_3$ hhc-structure

H_{hcc} = $BaTiO_3$ hcc-structure

C = $SrTiO_3$ c-structure (indicated by black squares when the A ion 'rattles', by open squares when the B ion 'rattles')

T_{Cu} = $KCuF_3$ c'-structure

O_{Fe} = $GdFeO_3$ c'-structure

A cross marks an unknown structure type.

– V decreases in the order h , hhc , hcc , if r_A , r_B and r_X are constant. These small differences between the volumes of the h-, hhc- and hcc-structures are due to the influence of the B ion☆. The volume of the c-structure is larger than the volumes of the h-, hhc- and hcc-structures for constant r_A , r_B and r_X , except when the A and the B ions are very large.

In Figs. II.13. and 14. the volumes per formula unit are plotted against r_B^3 for ABF_3 and $ABCl_3$ compounds. The bromides and iodides were omitted because of lack of data and the ABX_3 halides with B = Ge , Sn were omitted because of the uncertainty of the radii of these ions. The volumes per formula unit for $KMgF_3$, $KCdF_3$, $KCaF_3$ and $RbCdF_3$ have only been

☆ If only T(1)-layers were stacked, the h-stacking would have the smaller volume (9).

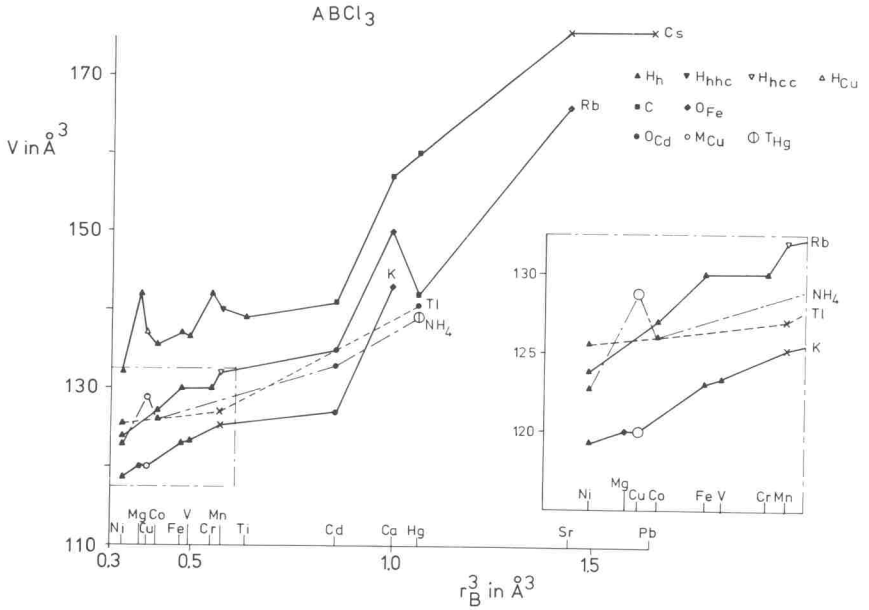

Fig. II.14.

Volumes per formula unit (V) for $ABCl_3$ compounds at ambient temperature and pressure as a function of r_B^3.

H_h = $BaNiO_3$ h-structure
H_{hhc} = $BaRuO_3$ hhc-structure
H_{hcc} = $BaTiO_3$ hcc-structure
H_{Cu} = $CsCuCl_3$ h′-structure
C = $SrTiO_3$ c-structure
O_{Fe} = $GdFeO_3$ c′-structure
O_{Cd} = NH_4CdCl_3 structure
M_{Cu} = $KCuCl_3$ structure
T_{Hg} = NH_4HgCl_3 structure
A cross marks an unknown structure type.

calculated for the phase with $SrTiO_3$ c-structure, although more structure types were reported for the room-temperature modification. $NaHgCl_3$ —omitted in Fig. II.14.— is reported to have a volume per formula unit of 180.92 Å^3. This volume is so large, *i.e.* larger than for $CsHgCl_3$, that the structure determination cannot be correct.

In the following the volumes per formula unit for ABX_3 halides with constant structure type are discussed as a function of r_A, r_B, r_X.

— For the $BaNiO_3$ h-structure V generally increases with r_A as expected. Exceptions occur for the $ABCl_3$ compounds with A = Rb, NH_4, Tl and with small B ions, but not all data in this region are equally reliable. A regular increase of the volume with r_B is not always

observed; the volumes of $CsMgCl_3$ and $CsCrCl_3$, for instance, are fairly large and the volume of $RbCrCl_3$ is rather small. The expected increase of V with r_X is observed for $CsNiX_3$ compounds.

- For the $BaRuO_3$ hhc-structure no relation can be verified because of lack of data.
- For the $BaTiO_3$ hcc-structure V increases with r_A or r_B as expected. An increase of V with r_X could not be verified because of lack of data.
- From the data for ABX_3 halides with $SrTiO_3$ c-structure it appears that the volume does depend on r_A, which was not expected for most compounds from a simple calculation with ionic radii. The same was found for the c_{red}- and a_{red}-values (Section II.4.1.). V increases fairly well with r_B or r_X as expected. The volumes of the $AHgCl_3$ compounds with A = Rb, Tl, NH_4 seem to be too small in comparison with the volumes of $ACaCl_3$ (A = K, Rb, Cs) and $CsHgCl_3$.

So far we discussed the relation between the volume of a compound and r_A, r_B and r_X for constant structure type. The expected relation between the volumes of the h-, hhc-, hcc- and c-structures is confirmed rather well, the volume of $TlCoF_3$ is too small. The volume of $CsMnCl_3$ may also be an exception: it is smaller than the large volume of $CsCrCl_3$ (according to our expectation), but larger than the volume of $CsTiCl_3$. The volumes of ABF_3 compounds with B = Mg, Zn are smaller than the volumes of the other ABF_3 compounds. Comparison of the data of ABF_3 and $ABCl_3$ compounds shows a remarkable fact. The volumes of the $TlBF_3$ compounds are somewhat larger than those of $RbBF_3$ and NH_4BF_3 compounds, but the volumes of $TlBCl_3$ compounds are smaller than these of $ABCl_3$ compounds with A = Rb, NH_4.

Although the qualitative results of Section II.2. are in good agreement with the experiments (Section II.3.), we did not succeed in obtaining good quantitative results in this section.

II.5. Comparison of expected and reported structure types for ABX_3 halides

Most experimentally determined structure types are in good agreement with the derived structures. Exceptions are the structures due to the electron configuration of the B ions and those of NH_4CdCl_3 and $PbAgBr_3$. The latter two may be derived from another basic lattice. Before discussing all experimentally determined structures of ABX_3 halides we shall briefly summarize which structure type may roughly be expected for a particular ABX_3 halide (Sections II.2. and 3.).

For the ABF_3 compounds we expect:

- the $SrTiO_3$ c-structure when the A ion has about the same size as the X ion and the B ion fits more or less into an octahedral hole°.

° An increase in the r_B/r_X-ratio is equivalent to a decrease in the r_A/r_X-ratio and *vice versa* (Section II.2.).

– the $BaTiO_3$ hcc-, $BaRuO_3$ hhc-, $BaNiO_3$ h-structures in the order of increasing r_A/r_B-ratio when the A ion is larger than the X ion and the B ion is not too large.
– the $KMnF_3$ c'- or the $GdFeO_3$ c'-structure when the A ion is smaller than the X ion or the B ion is large△.

For compounds with more polarizable anions, *viz.* $ABCl_3$, $ABBr_3$ and ABI_3, we expect:
– the $SrTiO_3$ c-structure when the A ion has about the same size as the X ion and the B ion is slightly too large to fit into an octahedral hole.
– the $KMnF_3$ c'- or the $GdFeO_3$ c'-structure when the A ion has about the same size as the X ion and the B ion is very large.
– the $BaTiO_3$ hcc-, $BaRuO_3$ hhc-, $BaNiO_3$ h-structures in the order of increasing r_A/r_B-ratio when the A ion has about the same size or is larger than the X ion and the B ion is not too large.
– the NH_4CdCl_3 structure when the A ion is smaller than the X ion and the B ion is slightly too large to fit into an octahedral hole□.
– no particular structure type when the A ion is smaller than the X ion and the B ion fits into an octahedral hole. The NH_4CdCl_3 structure becomes less favourable in this region by a decrease of the polarization energy and a less isonomous coordination of the A ion (Fig. II.7.). The $KMnF_3$ c'- and $GdFeO_3$ c'-structures are less favourable, because their contribution to the polarization energy is small. The $BaNiO_3$ h-structure is less favourable, because an adjustment of this structure to improve the coordination of the A ion leads to a decrease of the polarization energy (Section II.2.).

In order to obtain an insight into the structural chemistry of compounds with composition ABX_3 it is useful and customary to study the structures as a function of the various ratios of the radii of the A , B and X ions, *e.g.* r_A/r_X , r_B/r_X , r_A/r_B . For ABX_3 compounds the tolerance factor t☆ is generally used for this purpose. We do not use this particular ratio of r_A , r_B and r_X , because we prefer to use ratios that are also applicable to compounds having structures and/or stoichiometries other than those with $SrTiO_3$ c-structure. Moreover, the r_A/r_B-ratio, for instance, is more sensitive to variation in the radii than the tolerance factor.

The structure types at ambient temperature and pressure and the references to the papers on the structural data are tabulated in Tables II.9., 10., 11. and 12. for the ABF_3, $ABCl_3$, $ABBr_3$ and ABI_3 compounds, respectively. In Figs. II.15. and 16. the structures of the ABF_3 and $ABCl_3$ compounds are plotted as a function of the r_A/r_X- and r_B/r_X-ratios. Because of the scarcity of data the $ABBr_3$ and ABI_3 compounds are not plotted. The $AgBX_3$, $AGeX_3$ and $ASnX_3$ compounds are not plotted because of the uncertainty of the radii.

△ It has not been examined whether a more favourable structure than the $GdFeO_3$ c'-structure can be derived from another basic lattice.

□ Other structure types may exist in this region.

☆ The tolerance factor $t = (r_A + r_X)/(r_B + r_X)\sqrt{2}$ was derived by Goldschmidt (135) from the ideal $SrTiO_3$ c-structure. If the radii of A and X ions are equal and the B ion fits exactly into the octahedral hole $t = 1$.

ABF_3 compounds

The regions A , B , C , D , E in Fig. II.15., in which the $BaNiO_3$ h-, $BaRuO_3$ hhc-, $BaTiO_3$ hcc-, $SrTiO_3$ c- and $GdFeO_3$ c'-structures occur, respectively, agree with our expectations for the various structures. The more or less unexpected structures in the various regions are discussed now.

In region B ($BaRuO_3$ hhc-structure) the tetragonal indexing for $CsMgF_3$ and $CsZnF_3$ seems strange, but the stoichiometry of these compounds may be incorrect: a stoichiometry $Cs_4B_3F_{10}$ has been suggested (15,18). The structure of $CsCuF_3$ is not known.

In region C ($BaTiO_3$ hcc-structure) for NH_4NiF_3 (not indicated in Fig. II.15.) a 'pseudocubic' indexing has been given. This compound might have one of the mixed hexagonal-cubic structures (46).

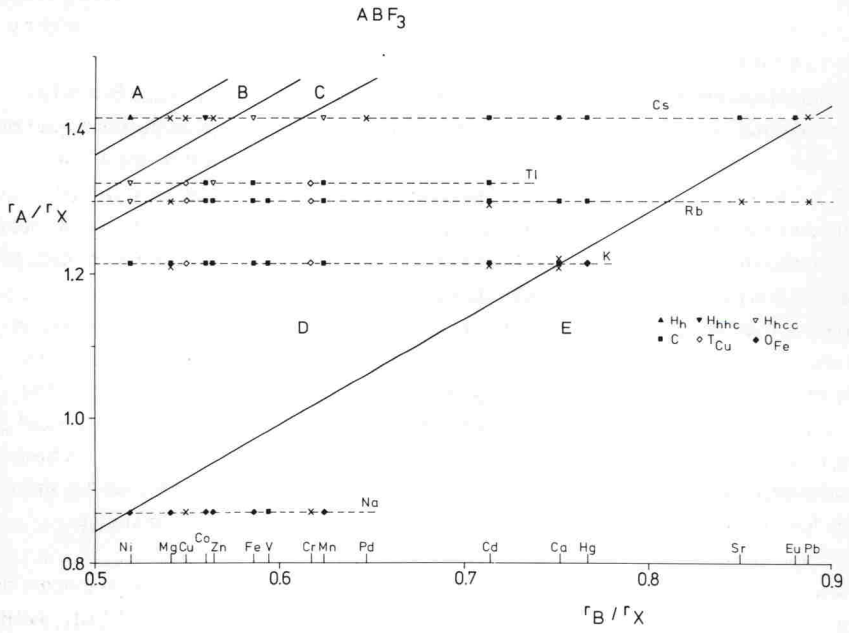

Fig. II.15.

Structure types for ABF_3 compounds at ambient temperature and pressure as a function of r_A/r_X- and r_B/r_X-ratios.

H_h = $BaNiO_3$ h-structure
H_{hhc} = $BaRuO_3$ hhc-structure
H_{hcc} = $BaTiO_3$ hcc-structure
C = $SrTiO_3$ c-structure
T_{Cu} = $KCuF_3$ c'-structure
O_{Fe} = $GdFeO_3$ c'-structure
A cross marks an unknown structure type.
The choice of the regions A , B , C , D and E is explained in the text.

In region D ($SrTiO_3$ c-structure) for the Cr and Cu compounds a deformation due to the Jahn-Teller effect is found, the $KCuF_3$ c'-structure. It is remarkable that the indexing of $KMgF_3$ and $RbMgF_3$ is monoclinic, that the indexing for $RbCdF_3$ and NH_4CdF_3 (not indicated in the figure) is tetragonal and that the $BaTiO_3$ hcc-structure has been reported for $TlZnF_3$ and $CsMnF_3$. The latter two compounds are, however, not far from region C . For $KCdF_3$ and $KCaF_3$ various structure types are given, because it is not clear from the literature which of them is the room-temperature modification. $CsPdF_3$ could not be indexed.
In region E ($GdFeO_3$ c'-structure) a monoclinic deformation of the $GdFeO_3$ c'-structure caused by the Jahn-Teller effect is reported for $NaCuF_3$ and $NaCrF_3$. The unexpected $SrTiO_3$ c-structure reported for $NaVF_3$ may be due to impurities or to high-temperature. $RbSrF_3$ is reported to be monoclinic, $CsPbF_3$ to be tetragonal.

$ABCl_3$ compounds

The polarizability of the X ion and the inaccuracy of the structure data complicate the division into regions in which the various structure types are expected as is apparent from Fig. II.16.
In region A the $BaNiO_3$ h-structure is expected and for smaller r_A/r_B-ratio, the $BaRuO_3$ hhc-structure (found for $CsMnCl_3$) and the $BaTiO_3$ hcc-structure (found for $RbMnCl_3$). NH_4CuCl_3 (not drawn in the figure) has the NH_4CdCl_3 structure with Jahn-Teller distortion. $CsCuCl_3$ has the $BaNiO_3$ h-structure with Jahn-Teller distortion. The tetragonal indexing for $TlMnCl_3$ is unexpected in this region and $CsTiCl_3$ was expected to have a mixed hexagonal-cubic stacking instead of a h-stacking.
In region B the $SrTiO_3$ c-structure occurs as expected.
For region C we could not derive a favourable structure, but the NH_4CdCl_3 structure, found for $ACdCl_3$ compounds with A = K , Rb , NH_4 and for $TlHgCl_3$, seems to be a favourable structure for $ABCl_3$ compounds with large B ions. The $GdFeO_3$ c'-structure found for various $ABCl_3$ compounds seems to be possible for those with large B ions in which the polarization plays a less important role, but it is also found for $KMgCl_3$. $RbHgCl_3$ with $SrTiO_3$ c-structure is probably a metastable high-temperature modification. It is doubtful whether all $KBCl_3$ compounds which are reported to have the $BaNiO_3$ h-structure really have this structure. $KCuCl_3$ has the NH_4CdCl_3 structure with Jahn-Teller distortion. The $NaBCl_3$ compounds are not plotted in Fig. II.16., because the structure of none of these compounds is certain. The NH_4CdCl_3 structure reported for $NaHgCl_3$ cannot be correct, since the confirmed parameters of NH_4CdCl_3 are very different (136) and since the volume per formula unit ABX_3 is much too large (Section II.4.2.). The structure of $NaMnCl_3$ has not been solved, but it is reported to have no relation to the perovskite structures (81), which on the basis of the r_A/r_X-value seems a likely assumption☆. $NaZnCl_3$ is reported to be orthorhombic.

☆ In the course of the preparation of this series of papers the structure of $NaMnCl_3$ was solved in our laboratory. It appeared to have the ilmenite structure (137).

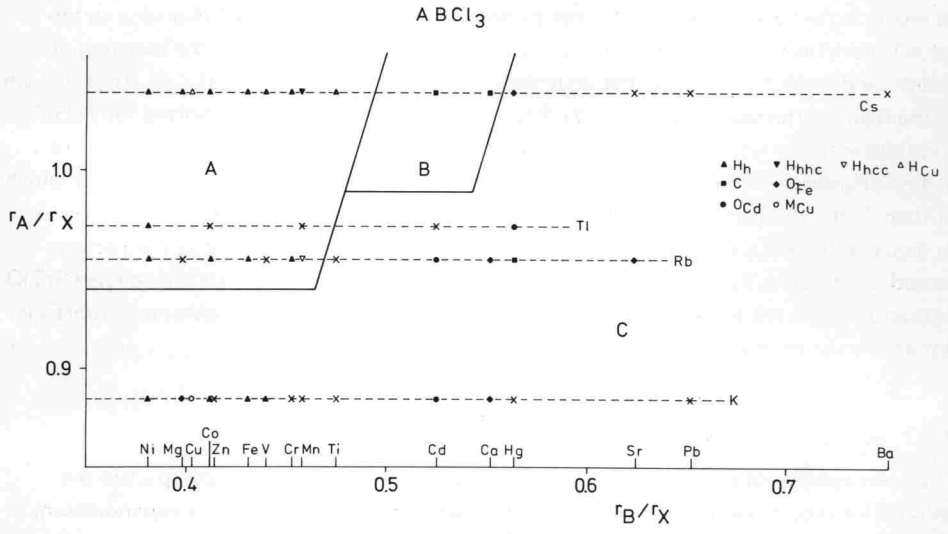

Fig. II.16.

Structure types for $ABCl_3$ compounds at ambient temperature and pressure as a function of r_A/r_X and r_B/r_X-ratios.

H_h = $BaNiO_3$ h-structure
H_{hhc} = $BaRuO_3$ hhc-structure
H_{hcc} = $BaTiO_3$ hcc-structure
H_{Cu} = $CsCuCl_3$ h′-structure
C = $SrTiO_3$ c-structure
O_{Fe} = $GdFeO_3$ c′-structure
O_{Cd} = NH_4CdCl_3 structure
M_{Cu} = $KCuCl_3$ structure
A cross marks an unknown structure type.
The choice of the regions A , B and C is explained in the text.

II.6. Structures of ABX_3 halides at non-ambient temperatures and pressures

II.6.1. Non-ambient temperatures

So far little work has been done on the influence of the temperature on the structure types. Recently, Megaw (138) made an attempt to obtain an insight into the thermal expansion of crystal structures. She considered the expansion of a three-dimensional framework as a result of increasing temperature to be the sum of a bond-length expansion and a tilting effect. We only regard, however, the influence of the temperature on the bond length, which can lead to tilting effects (See, for instance, the derivation of the $KMnF_3$ c′- and $GdFeO_3$ c′-structures in Section II.2.). In the ABX_3 structures that we consider the A-X distances

will increase more strongly with temperature than the B-X distances, since the former bonds are weaker than the latter. We therefore expect for increasing temperature that:

- the fraction of h-stacking increases in the order c , hcc , hhc , h .
- the deformations of the c-stacking disappear in the order $GdFeO_3$ c'-, $KMnF_3$ c'-, $SrTiO_3$ c-structure.
- the NH_4CdCl_3 structure changes into the $SrTiO_3$ c-structure.

Moreover, distortions due to electronic effects of the B ions will disappear with temperature. It is evident that the reverse of these relations is also valid.

The influence of the temperature on the structure types is verified for ABX_3 halides listed in Tables II.14. and 15. As expected the $SrTiO_3$ c-structure deforms with decreasing temperature, the deformations of the $SrTiO_3$ c-structure disappear with increasing temperature and

Table II.14.

Structure types and references for ABX_3 halides below room-temperature. The structures at higher temperatures are given in parentheses and the temperature at which the structure was found is indicated in °K. **C** denotes the $SrTiO_3$ c-structure, $\mathbf{T_{Mn}}$ the $KMnF_3$ c'-structure. See also the caption of Table II.9.

$NaMgF_3$	$NaMgF_3$	$RbZnF_3$	$CsPbF_3$	$KMgCl_3$	$RbCdCl_3$	$RbCdCl_3$	$TlMnCl_3$	$CsCuCl_3$
$t(\mathbf{O_{Fe}})$	$\mathbf{C}(t)$	$\mathbf{H_{hcc}(C)}$	$\mathbf{C}(t)$	$\mathbf{C(O_{Fe})}$	$t(\mathbf{O_{Cd}})$	$\mathbf{C}(t)$	$\mathbf{C}(t)$	$\mathbf{H_h^*(H_{Cu})}$
700-900	900			110-175	140-190	> 190	> 30	> 150
(139)	(139)	(140)	(70)	(85)	(94)	(94)	(108)	(141)
$CsCdCl_3$	$CsGeCl_3$	$CsHgCl_3$	$CsSnCl_3$	$CsSrCl_3$	$CsPbCl_3$	$CsPbBr_3$	$CsPbBr_3$	$CsPbI_3$
$\mathbf{H_{hcc}(C)}$	$\mathbf{C(R_{Ge})}$	$\mathbf{C(O_{Fe})}$	$\mathbf{C(M_{Sn})}$	$\mathbf{C}(t)$	$\mathbf{C}(t)$	$t(m)$	$\mathbf{C}(t)$	$m(\mathbf{O_{Cd}})$
	> 155			> 125	> 47	120	135	305
(116)	(33)	(84)	(128)	(113)	(117)	(129)	(129)	(134)

Table II.15.

Structure types and references for ABX_3 halides above room-temperature. The structures at lower temperatures are given in parentheses and the temperature at which the structure was found is indicated in °C. $\mathbf{H_h}$, $\mathbf{H_{hcc}}$ and **C** indicate the $BaNiO_3$ h-, $BaTiO_3$ hcc- and $SrTiO_3$ c-structures, respectively. $\mathbf{O_{Fe}}$ indicates the $GdFeO_3$ c'-structure, $\mathbf{H_{Cu}}$ the $CsCuCl_3$ h'-structure, $\mathbf{R_{Ge}}$ the $CsGeCl_3$ c'-structure, $\mathbf{O_{Cd}}$ the NH_4CdCl_3 structure and $\mathbf{M_{Sn}}$ the $CsSnCl_3$ structure. See also the caption of Table II.9.

	Co	Fe	Fe	Fe	Mn	Mn
KBF_3	$t(\mathbf{C})$	$r(\mathbf{C})$			$\mathbf{T_{Mn}(C)}$	$m(\mathbf{T_{Mn}})$
	78 (56)	78 (56)			145 (27)	78 (56)
$RbBF_3$	$t(\mathbf{C})$	$t(\mathbf{C})$	$o(t)$	$m(o)$		
	< 101 (66)	86 (68)	87-45 (68)	4.2-45 (68)		

the fraction of h-stacking increases with temperature. The latter is confirmed by $RbZnF_3$ and $CsCdCl_3$. The deformation of the $BaNiO_3$ h-structure for $CsCuCl_3$ and that of the $SrTiO_3$ c-structure for $CsGeCl_3$ due to the electron configuration of the B ions disappear also with increasing temperature.

As to the c_{red}-, a_{red}- and $(c/a)_{red}$-values the relations between these values and the structure types for constant r_A , r_B , r_X (Section II.4.1.) remain valid. Moreover, an additional increase of the c_{red}- and a_{red}-values can be expected for higher temperatures. Since a_{red} is a function of r_A , r_X only and c_{red} of r_B , r_X for the h-structure (Section II.4.1.) and of r_A , r_B , r_X for the hhc- and hcc-structures, the $(c/a)_{red}$-value for the h-, hhc- and hcc-structures is, for the higher temperature modifications, smaller than expected. The $(c/a)_{red}$-value is 0.8165, of course, for the c-structure.
For $RbZnF_3$ $\Delta c_{red}{}^{\circ} = +1.3\%$, $\Delta a_{red} = +\ 1.3\ \%$. For $CsCdCl_3$ $\Delta c_{red} = +1.9\%$, $\Delta a_{red} = +0.7\%$. $\Delta(c/a)_{red}$ is about zero for the c → hcc transition of $RbZnF_3$, positive for that of $CsCdCl_3$ (Fig. II.12.). The above expectations are somewhat ambiguous for the transition c → hcc of these compounds.

The relation between the volumes per formula unit (V) and the structure types for constant r_A , r_B , r_X (Section II.4.2.) remains valid. Moreover, an additional increase of V can be expected for higher temperatures.
In Table II.16. the ΔV-values$^{\circ}$ are reported for the ABX_3 halides at temperatures below and above room-temperature. ΔV is negative for transitions from the $SrTiO_3$ c-structure at room-temperature to a low-temperature deformation of this structure. Generally, ΔV is positive for a transition from a deformed $SrTiO_3$ c-structure at room-temperature to a structure at higher temperatures, as a result of the increase of the temperature. It is, however, negative for $RbCdCl_3$, $TlMnCl_3$, $CsHgCl_3$ and $CsSrCl_3$. For the transition from the h- or c-structure distorted by an electronic effect of the B ion to the undeformed structure at higher temperatures ΔV is always positive. For the transition from the c- to the hcc-structure $\Delta V = +3.9$ and $+3.3\%$ for $RbZnF_3$ and $CsCdCl_3$, respectively. These positive values are expected as a result of the structure transition (Section II.4.2.) and the additional increase of V at higher temperatures.

II.6.2. Non-ambient pressures

We assume the A ions to be more compressible than the B ions, since they have the larger size and the smaller charge. We therefore expect for increasing pressure that:
— the fraction of h-stacking decreases in the order h , hhc , hcc , c .

$^{\circ}$ $\Delta x = 100(x' - x)/x$ = percentual change in x . x' is a variable for structures at non-ambient temperatures, x is a variable for structures at ambient temperature. The variables are c_{red} , a_{red} , $(c/a)_{red}$ or V.

Table II.16.

ΔV-values for modifications of ABX_3 halides below room-temperature (upper part of the table) *or above room-temperature* (lower part of the table). See text.

	Co	Fe	Mn	Mn
KBF_3	t(**C**)	r(**C**)	$\mathbf{T}_{Mn}$(**C**)	m(**C**)
	−1.1	−0.9	−1.2	−0.8

$NaMgF_3$	$NaMgF_3$	$RbZnF_3$	$KMgCl_3$	$RbCdCl_3$	$TlMnCl_3$	
t($\mathbf{O}_{Fe}$)	**C**($\mathbf{O}_{Fe}$)	$\mathbf{H}_{hcc}$(**C**)	**C**($\mathbf{O}_{Fe}$)	t($\mathbf{O}_{Cd}$)	**C**(t)	
9.1	10.4	3.9	4.0	−18.1	−1.0	
$CsCuCl_3$	$CsCdCl_3$	$CsGeCl_3$	$CsHgCl_3$	$CsSnCl_3$	$CsSrCl_3$	$CsPbCl_3$
$\mathbf{H}^*_h(\mathbf{H}_{Cu})$	$\mathbf{H}_{hcc}$(**C**)	**C**($\mathbf{R}_{Ge}$)	**C**($\mathbf{O}_{Fe}$)	**C**($\mathbf{M}_{Sn}$)	**C**(t)	**C**(t)
3.6	3.3	1.7	−5.9	1.3	−0.8	0.1

- the deformations of the c-stacking arise in the order $SrTiO_3$ c-, $KMnF_3$ c'-, $GdFeO_3$ c'- structure for ABF_3 compounds△.
- the $SrTiO_3$ c-structure changes into the $KMnF_3$ c'-, $GdFeO_3$ c'- or NH_4CdCl_3 structure for ABX_3 compounds with X = Cl , Br , I△.

The influence of pressure on structure types is verified for ABX_3 halides listed in Table II.17. The fraction of h-stacking decreases with increasing pressure as expected. Longo & Kafalas plotted the pressure at which the $CsBF_3$ compounds have been prepared against r_B (18). They found that the fraction of h-stacking decreases more rapidly with increasing pressure for $CsMgF_3$ than for $CsBF_3$ compounds with B = a transition metal ion. We plotted the pressure against r_B^3 and used the effective ionic radii of Shannon & Prewitt. $CsMgF_3$ then appears to behave like the other $CsBF_3$ compounds.

The relations between the c_{red}-, a_{red}-, $(c/a)_{red}$-values and structure types for constant r_A , r_B , r_X (Section II.4.1.) remain valid. Moreover, an additional decrease of c_{red} and a_{red} can be expected at high-pressure. Since a_{red} is a function of r_A , r_X only, c_{red} of r_B , r_X for the h-structure and of r_A , r_B , r_X for the hhc- and hcc-structures, the $(c/a)_{red}$-value for the h-, hhc- and hcc-structures is larger than expected by the additional effect at high-pressures. $(c/a)_{red}$ is 0.8165 for the $SrTiO_3$ c-structure.

△ Other structures can be expected, which have not been derived yet.

Table II.17.

Structure types and references for ABX_3 halides at high-pressure. The structures at lower pressures are given in parentheses and the pressure at which the structure was found is indicated in kbars. $\mathbf{H_h}$, $\mathbf{H_{hhc}}$, $\mathbf{H_{hcc}}$ and **C** denote the $BaNiO_3$ h-, $BaRuO_3$ hhc-, $BaTiO_3$ hcc- and $SrTiO_3$ c-structure, respectively.

$RbNiF_3$	$TlNiF_3$	$CsNiF_3$	$CsNiF_3$	$CsMgF_3$	$CsMgF_3$	$CsCoF_3$
C($\mathbf{H_{hcc}}$) 20 (142)	**C**($\mathbf{H_{hcc}}$) <30 (143)	$\mathbf{H_{hhc}}$($\mathbf{H_h}$) 5 (144)	$\mathbf{H_{hcc}}$($\mathbf{H_{hhc}}$) 47 (144)	$\mathbf{H_{hhc}}$ 30 (18)	$\mathbf{H_{hcc}}$($\mathbf{H_{hhc}}$) 40 (18)	$\mathbf{H_{hcc}}$($\mathbf{H_{hhc}}$) 22 (18)
$CsZnF_3$	$CsFeF_3$	$CsMnF_3$	$RbMnCl_3$	$CsMnCl_3$	$CsMnCl_3$	
$\mathbf{H_{hcc}}$ 30 (18)	**C**($\mathbf{H_{hcc}}$) 70 (18)	**C**($\mathbf{H_{hcc}}$) 26 (143)	**C**($\mathbf{H_{hcc}}$) 2 (145)	$\mathbf{H_{hcc}}$($\mathbf{H_{hhc}}$) 5 (145)	**C**($\mathbf{H_{hcc}}$) 30 (145)	

Table II.18.

ΔV-, Δc_{red}- and Δa_{red}-values for high-pressure modifications of ABX_3 halides. See text.

$RbNiF_3$	$TlNiF_3$	$CsNiF_3$	$CsNiF_3$	$CsMgF_3$	$CsCoF_3$
C($\mathbf{H_{hcc}}$)	**C**($\mathbf{H_{hcc}}$)	$\mathbf{H_{hhc}}$($\mathbf{H_h}$)	$\mathbf{H_{hcc}}$($\mathbf{H_{hhc}}$)	$\mathbf{H_{hcc}}$($\mathbf{H_{hhc}}$)	$\mathbf{H_{hcc}}$($\mathbf{H_{hhc}}$)
−3.9	−3.6	−7.7	−5.4	−5.8	−5.9
−1.3	−1.2	−5.1	−2.3	−2.1	−2.7
−1.3	−1.2	−1.4	−1.6	−1.9	−1.7
$CsFeF_3$	$CsMnF_3$	$RbMnCl_3$	$CsMnCl_3$	$CsMnCl_3$	
C($\mathbf{H_{hcc}}$)	**C**($\mathbf{H_{hcc}}$)	**C**($\mathbf{H_{hcc}}$)	$\mathbf{H_{hcc}}$($\mathbf{H_{hhc}}$)	**C**($\mathbf{H_{hcc}}$)	
−3.4	−3.3	−2.6	−2.9	−3.2	
−0.1	−0.5	−1.6	−2.0	−1.4	
−1.6	−1.4	−0.1	−0.1	−0.9	

It is apparent from Table II.18. that the Δc_{red}- and Δa_{red}-values□ are negative for the transitions h → hhc , hhc → hcc and hcc → c , as was expected. Fig. II.12. confirms completely our expectations for the $\Delta(c/a)_{red}$-values.

The relation between the volumes per formula unit (V) and the structure types for constant r_A , r_B , r_X (Section II.4.2.) remains valid. Moreover, an additional decrease of V can be expected at higher pressure.
ΔV□ (Table II.18.) is negative for the transitions h → hhc, and hhc → hcc as expected. It is also negative for the transition hcc → c, due to the additional pressure effect.

□ $\Delta x = 100(x' - x)/x$ = percentual change in x . x' is a variable for structures at high-pressure. x is a variable at lower pressure. The variables are c_{red} , a_{red} , $(c/a)_{red}$ or V.

Conclusions

It was the aim of the present paper to compare the ABX_3 structures derived in Part I with the experimental data on ABX_3 halides. An attempt to calculate c_{red}-, a_{red}-, $(c/a)_{red}$-values and volumes per formula unit failed, although the qualitative agreement between observed and expected structures was satisfactory. However, more work on the derivation of structures with composition ABX_3 has to be done. With some additional assumptions the same approach could be used for structures of compounds at non-ambient temperature and pressure. The $ABBr_3$ and ABI_3 compounds could not be discussed because of scarcity of experimental data. No cation-cation bonding had to be assumed in order to understand the hexagonal and the mixed hexagonal-cubic stackings (6). We conclude that the simple method to derive ABX_3 and A_2BX_6 structures developed in Part I can be used successfully to understand the crystal structures of ABX_3 halides. It can therefore be applied with some confidence to compounds A_2BX_6, $A_2BX_{6-p}Y_p$, and $A_2BX_{6-p'-p''}Y_{p'}Z_{p''}$ (X: halogen; Y, Z = halogen, O, OH, H_2O, N, anion vacancy) in Parts III, IV and V, respectively.

The authors are grateful to drs. C.J.J. van Loon and drs. J.A.R. van Veen for their aid in the study of crystal structures and the pertinent literature, to Miss S. Amadio for the assistance in preparing the manuscript, and to Mr. M. Pison and Mr. J.J. Pot for their aid in the preparation of the figures.

References

1. A.B.A. Schippers, V. Brandwijk and E.W. Gorter, to be published in J. Solid State Chem., Volume **6**, Issue 4 (1973)
2. E.W. Gorter, J. Solid State Chem. **1**, 279 (1970)
3. R.D. Shannon and C.T. Prewitt, Acta Cryst. **B25**, 925 (1969)
4. R.D. Shannon and C.T. Prewitt, Acta Cryst. **B26**, 1046 (1970)
5. E. Parthé, 'Crystal chemistry of tetrahedral structures', Gordon and Breach, Science Publishers, Inc., New York, 1964
6. L. Katz and R. Ward, Inorg. Chem. **3**, 205 (1964)
7. G. Blasse, J. Inorg. Nucl. Chem. **27**, 993 (1965)
8. A.B.A. Schippers and E.W. Gorter, to be published.
9. J.H.N. van Vucht, J. Less-Common Metals **11**, 308 (1966)
10. L. Pauling, J. Am. Chem. Soc. **51**, 1010 (1929)
11. W.H. Baur, Trans. Am. Cryst. Assoc. **6**, 129 (1970)
12. H. Thomas and K.A. Müller, Phys. Rev. Letters **21**, 1256 (1968)
13. J.J. Lander, Acta Cryst. **4**, 148 (1951)
14. P.C. Donohue, L. Katz and R. Ward, Inorg. Chem. **4**, 306 (1965)
15. D. Babel, Z. Anorg. Allgem. Chem. **369**, 117 (1969)
16. A. Hardy, Acta Cryst. **15**, 179 (1962)
17. T. Negas and R.S. Roth, J. Solid State Chem. **3**, 323 (1971)
18. J.M. Longo and J.A. Kafalas, J. Solid State Chem. **1**, 103 (1969)
19. R.D. Burbank and H.T. Evans, Acta Cryst. **1**, 330 (1948)
20. A. Zalkin, K. Lee and D.H. Templeton, J. Chem. Phys. **37**, 697 (1962)
21. J.E. Weidenborner and A.L. Bednowitz, Acta Cryst, **B26**, 1464 (1970)
22. J. Brous, I. Fankuchen and E. Banks, Acta Cryst. **6**, 67 (1953)
23. B. Derighetti, J.E. Drumheller, F. Laves, K.A. Müller and F. Waldner, Acta Cryst. **18**, 557 (1965)
24. H.D. Megaw, Acta Cryst. **A26**, 235 (1970)
25. S. Geller and V.B. Bala, Acta Cryst. **9**, 1019 (1956)
26. L. Rimai and G.A. deMars, Phys. Rev. **123**, 702 (1962)
27. V.J. Minkiewicz, Y. Fujii and Y. Yamada, J. Phys. Soc. Japan **28**, 443 (1970)
28. O. Beckman and K. Knox, Phys. Rev. **121**, 376 (1961)
29. S. Geller, J. Chem. Phys. **24**, 1236 (1956)
30. F. Pompa and F. Siciliano, Ric. Sci. **39**, 370 (1969)
31. A.W. Schlüter, R.A. Jacobson and R.E. Rundle, Inorg. Chem. **5**, 277 (1966)
32. A. Okazaki and Y. Suemune, J. Phys. Soc. Japan **16**, 176 (1961)
33. A. Nørlund Christensen and S.E. Rasmussen, Acta Chem. Scand. **19**, 421 (1965)
34. H. Brasseur and L. Pauling, J. Am. Chem. Soc. **60**, 2886 (1938)
35. C.H. McGillavry, H. Nijveld, S. Dierdorp and J. Karsten, Rec. Trav. Chim. **58**, 193 (1939)
36. R.D. Willett, C. Dwiggins, R.F. Kruh and R.E. Rundle, J. Chem. Phys. **38**, 2429 (1963)
37. Y. Otsubo, Y. Tanaka and M. Miyahara, Nippon Kagakii Zasshi **92A**, 42 (1971)
38. E.J. Harmsen, Z. Krist. **100A**, 208 (1938)
39. A.F. Wells, 'Structural Inorganic Chemistry', Third edition, Oxford University Press, 1962
40. L.E. Orgel, J. Chem. Soc. (1958), 4186
41. F.R. Poulsen and S.E. Rasmussen, Acta Chem. Scand. **24**, 150 (1970)
42. R.E. Rundle and D.H. Olson, Inorg. Chem. **3**, 596 (1964)

43. R.R. McDonald, A.C. Larson and D.T. Cromer, Acta Cryst. **17**, 1104 (1964)
44. D. Mootz and H. Puhl, Acta Cryst. **23**, 471 (1967)
45. E.W. Gorter, to be published.
46. W. Rüdorff and D. Babel, Z. Anorg. Allgem. Chem. **317**, 261 (1962)
47. W. Rüdorff, J. Kändler, G. Lincke and D. Babel, Angew. Chem. **71**, 672 (1959)
48. W. Rüdorff, G. Lincke and D. Babel, Z. Anorg. Allgem. Chem. **320**, 150 (1963)
49. A.G. Tutov and P.P. Syrnikov, Sov. Phys. Cryst. **12**, 619 (1968)
50. A. Tressaud, R. de Pape, J. Portier and P. Hagenmuller, Compt. Rend. **266C**, 984 (1968)
51. M.W. Shafer, Mat. Res. Bull. **4**, 905 (1969)
52. G. Vollmer, Thesis, Tübingen (1966)
53. J.N. Simanov, L.R. Bacanova and L.M. Kovba, Zh. Neorg. Khim. **2**, 2410 (1957)
54. J.D. Donaldson and J.D. O'Donoghue, J. Chem. Soc. (1964), 271
55. J. Portier, A. Tressaud and J.L. Dupin, Compt. Rend. **270C**, 216 (1970)
56. A. Okazaki and Y. Suemune, J. Phys. Soc. Japan **16**, 671 (1961)
57. W.L.W. Ludekens and A.J.E. Welch, Acta Cryst. **5**, 841 (1952)
58. H. Remy and F. Hansen, Z. Anorg. Allgem. Chem. **283**, 277 (1956)
59. K. Knox, Acta Cryst. **14**, 583 (1961)
60. H.A. Klasens, P. Zalm and F.O. Huysman, Philips Res. Rept. **8**, 441 (1953)
61. S. Ogawa, J. Phys. Soc. Japan **15**, 1475 (1960)
62. C. Brisi, Ann. Chim. (Paris) **42**, 356 (1952)
63. E.L. Muetterties, Inorg. Chem. **1**, 342 (1962)
64. R. Hoppe and R. Homann, Z. Anorg. Allgem. Chem. **369**, 212 (1969)
65. L. Goost and G. Bergerhoff, Naturwiss. **54**, 248 (1967)
66. J. Nouet, R. Kleinberger and R. de Kouchkovsky, Compt. Rend. **269B**, 986 (1969)
67. D.S. Crockett and H.M. Händler, J. Am. Chem. Soc. **82**, 4158 (1960)
68. M. Kestigian, F.D. Leipziger, W.J. Croft and R. Guidoboni, Inorg. Chem. **5**, 1462 (1966)
69. J.D. Donaldson, J.D. O'Donoghue and R. Oteng, J. Chem. Soc. (1965), 3876
70. O. Schmitz-Dumont, G. Bergerhoff and E. Hartert, Z. Anorg. Allgem. Chem. **283**, 314 (1956)
71. H.M. Händler, F.A. Johnson and D.S. Crockett, J. Am. Chem. Soc. **80**, 2662 (1958)
72. J. Portier, A. Tressaud, J.L. Dupin and R. de Pape, Mat. Res. Bull. **4**, 45 (1969)
73. J.C. Cousseins and C. Pina Perez, Rev. Chim. Mineral. **5**, 147 (1968)
74. K. Kohn, R. Fukuda and S. Iida, J. Phys. Soc. Japan **22**, 333 (1967)
75. S.A. Kezhaev, A.G. Tutov and V.A. Bokov, Sov. Phys. Solid State **7**, 2325 (1966)
76. D. Babel, Z. Naturforsch. **20A**, 165 (1965)
77. N. Bartlett and J.W. Quail, J. Chem. Soc. (1961), 3728
78. E.L. Boyd, Phys. Rev. **145**, 174 (1966)
79. N.V. Bondarenko, Russ. J. Inorg. Chem. **7**, 714 (1962)
80. I.V. Aleksanyants, N.M. Demido, A.S. Malyugin and A.D. Pogorelyi, Chem. Abstr. **70**, 91237s (1969)
81. M. Kestigian and W.J. Croft, Mat. Res. Bull. **9**, 877 (1969)
82. Z.L. Artem'eva, I.V. Vasil'kova and M.P. Susarev, Chem. Abstr. **70**, 71492t (1969)
83. A. Weiss and K. Damm, Z. Naturforsch. **9B**, 82 (1954)
84. I.N. Belyaev, D.S. Lesnykk and I.G. Eikhenbaum, Russ. J. Inorg. Chem. **15**, 430 (1970)
85. J. Brynestad, H.J. Yakel and G.P. Smith, J. Chem. Phys. **45**, 4652 (1966)
86. H.J. Seifert, Z. Anorg. Allgem. Chem. **307**, 137 (1960)
87. N.P. Luzhnaya and I.P. Vereshchetina, Chem. Abstr. **46**, 4346i (1952)
88. I.V. Vasil'kova, I.I. Kozhina and E.M. Tronina, Chem. Abstr. **72**, 115578y (1970)
89. H.J. Seifert and P. Ehrlich, Z. Anorg. Allgem. Chem. **302**, 284 (1959)

90. H.J. Seifert and K. Klatyk, Z. Anorg. Allgem. Chem. **334**, 113 (1964)
91. W.J. Croft, M. Kestigian and F.D. Leipzig, Inorg. Chem. **4**, 423 (1965)
92. P. Ehrlich and H. Kuknl, Z. Anorg. Allgem. Chem. **292**, 146 (1957)
93. E. Brandenberger, Experientia **3**, 149 (1947)
94. H.F. McMurdie, J. de Groot, M, Morris and H.E. Swanson, J. Res. NBS. **73A**, 621 (1969)
95. I.V. Tananaev, B.F. Dzhurinskii and Y.N. Mikhailov, Zh. Neorg. Khim. **9**, 1570 (1964)
96. I.N. Belyaev and K.E. Mironov, Chem. Abstr. **47**, 2585f (1953)
97. Ch'ih-Fa Li and I.S. Morozov, Zh. Neorg. Khim. **8**, 708 (1963)
98. K. Balasubrahnanyam and L. Nanis, J. Chem. Phys. **40**, 2657 (1964)
99. R.W. Asmussen, T. Kindt-Larsen and H. Soling, Acta Chem. Scand. **23**, 2055 (1969)
100. W. Klemm, K. Beyersdorfer and J. Oryschkewitsch, Z. Anorg. Allgem. Chem. **256**, 25 (1948)
101. A. Engberg and H. Soling, Acta Chem. Scand. **21**, 168 (1967)
102. H.J. Seifert and K. Klatyk, Z. Anorg. Allgem. Chem. **342**, 1 (1966)
103. H.J. Seifert and B. Gerstenberg, Z. Anorg. Allgem. Chem. **315**, 56 (1962)
104. H.J. Seifert and F.W. Koknat, Z. Anorg. Allgem. Chem. **341**, 269 (1965)
105. P. Ehrlich and R. Schmitt, Z. Anorg. Allgem. Chem. **308**, 91 (1961)
106. H.C. Gaur and W.K. Behl, Chem. Abstr. **57**, P12104d (1962)
107. F.K. Mikhailov and Z.K. Zubakhina, Russ. J. Inorg. Chem. **13**, 618 (1968)
108. M. Kestigian, Mat. Res. Bull. **5**, 263 (1970)
109. I.I. Il'yasov and A.G. Bergman, Zh. Neorg. Khim. **4**, 913 (1959)
110. J. Huart, Bull. Soc. France, Mineral. Crist. **88**, 65 (1965)
111. Yu. P. Afinogenov and A.D. Lemesh, Russ. J. Inorg. Chem. **12**, 896 (1967)
112. G.N. Tischenko, Chem. Abstr. **50**, 16251g (1956)
113. D.J.W. IJdo, Thesis, Leiden (1960)
114. H. Soling, Acta Chem. Scand. **22**, 2793 (1968)
115. M. Kestigian, W.J. Croft and F.D. Leipziger, J. Chem. Eng. Data **12**, 97 (1967)
116. S. Siegel and E. Gebert, Acta Cryst. **17**, 790 (1964)
117. C.K. Møller, Nature **180**, 981 (1957)
118. Z.A. Mateiko, E.S. Yagub'yan and G.A. Bukhalova, Zh. Neorg. Khim. **11**, 2405 (1966)
119. G. Kellner, Z. Anorg. Chem. **99**, 165 (1917)
120. I.I. Il'yasov, V.N. Mirsoyapov and Yu.V. Korotkov, Zh. Neorg. Khim. **4**, 909 (1959)
121. I.N. Belyaev and K.E. Mironov, Chem. Abstr. **47**, 2585h (1953)
122. I.I. Il'yasov, G.G. Shchemeleva and A.G. Bergman, Russ. J. Inorg. Chem. **5**, 606 (1960)
123. I.I. Koshina and D.V. Korol'kov, J. Struct. Chem. **6**, 84 (1965)
124. I.I. Il'yasov, S.D. Dionis'ev and A.G. Bergman, Zh. Neorg. Khim. **7**, 625 (1962)
125. G. Stucky, S.D. Agostino and G. McPherson, J. Am. Chem. Soc. **88**, 4828 (1966)
126. G. Natta and L. Passerini, Gazz. **58**, 472 (1928)
127. S.V. Náray-Szabó, Structure Reports **11A**, 456 (1947/48)
128. J.F. Dorrian and R.E. Newnham, Personal Communication (1968) in 'J.B. Goodenough and J.M. Longo, Crystallographic and magnetic properties of perovskite and perovskite-related compounds', Landolt-Börnstein, New Series III/4a, Springer-Verlag, Berlin-Heidelberg-New York, 1970
129. C.K. Møller, Kgl. Danske Videnskab. Selskab, Mat. Fys. Medd. **32**, no. 2, 1 (1959)
130. I.I. Il'yasov and S.D. Dionis'ev, Zh. Neorg. Khim. **10**, 1681 (1965)
131. I.I. Il'yasov and A.G. Bergman, Chem. Abstr. **50**, 15315h (1956)
132. I.I. Il'yasov and A.G. Bergman, Zh. Neorg. Khim. **2**, 2771 (1957)
133. I.I. Il'yasov and A.G. Bergman, Zh. Neorg. Khim. **9**, 1416 (1964)

134. C.K. Møller, Kgl. Danske Videnskab. Selskab, Mat. Fys. Medd. **32**, no. 1, 1 (1959)
135. V.M. Goldschmidt, T. Barth, G. Lunde and W. Zachariasen, Die Gesetze der Krystallochemie. Skrifter Vidensk.-Akad. Oslo, I. Mat.-Nat. Klasse no. 2 (1926) (1)
136. R.W.G. Wyckoff, 'Crystal Structures', Vol. 2, p. 430, Second Edition, Interscience, New York, 1964
137. C.J.J. van Loon and G.C. Verschoor, to be published.
138. H.D. Megaw, Mat. Res. Bull. **6**, 1007 (1971)
139. E.C.T. Chao, H.T. Evans jr., B.J. Skinner and C. Milton, Am. Mineralogist **46**, 379 (1961)
140. D. Babel, Thesis, Tübingen (1961)
141. C.J. Kroese, J.C.M. Tindemans- Van Eyndhoven and W.J.A. Maaskant, Solid State Comm. **9**, 1707 (1971)
142. J.A. Kafalas and J.M. Longo, Mat. Res. Bull. **3**, 501 (1968)
143. Y. Syono, S. Akimoto and K. Kohn, J. Phys. Soc. Japan **26**, 993 (1969)
144. J.M. Longo and J.A. Kafalas, J. Appl. Phys. **40**, 1601 (1969)
145. J.A.R. van Veen, Mat. Res. Bull. **6**, 1269 (1971)

CHAPTER III

THE EFFECT OF PRESSURE ON A_2BX_6 HALIDES, CONTRARY TO THE EFFECT OF PRESSURE ON ABX_3 HALIDES

V. Brandwijk and D.L. Jongejan.
Dept. of Solid State Chemistry, Gorlaeus Laboratories, P.O. Box 75, Leiden, The Netherlands.

Abstract

The compounds Cs_2GeF_6, Rb_2SiF_6 and Cs_2ZrCl_6 with K_2PtCl_6 c-structure transform under the influence of pressure to phases with K_2MnF_6 hc-structure. The respective lattice constants of the unit cells are
$a = 6.124 \pm 0.006$ Å, $c = 10.021 \pm 0.007$ Å.
$a = 5.90 \pm 0.02$ Å, $c = 9.59 \pm 0.03$ Å.
$a = 7.37 \pm 0.01$ Å, $c = 12.02 \pm 0.02$ Å.
The fraction of hexagonally stacked AX_3-layers thus increases with pressure contrary to what was found for ABX_3 halides.

III.1. Introduction

It was found experimentally for ABX_3 halides with X=F (1,2,3,4) and Cl (5,6) that the fraction of hexagonally (h) stacked 'close-packed' AX_3-layers with triangular order of the A ions (T-pattern) (7) decreases with increasing pressure. In an extensive paper (8) it is derived for halides ABX_3 in which A is a large cation, B a small one and X a halogen ion that this could be expected from a model based on mainly qualitative electrostatic bonding rules. For A_2BX_6 halides, however, it is predicted (9) that the fraction of h-stacked AX_3-layers with T-pattern increases with pressure. Because of the lack in literature of experimental data to prove this prediction we investigated some easily prepared compounds, *viz.* Rb_2SiF_6, Cs_2GeF_6 and Cs_2ZrCl_6 with K_2PtCl_6 c-structure, which have a r_A/r_B-ratio close to that of structures with h-stacked layers (see Tables III.1. and III.2., taken from Ref. 9.).

III.2. Experimental

The A_2BF_6 compounds with B=Si, Ge were prepared by dissolving ACl in a 40% HF solution, slowly adding BO_2 and evaporating the solution to dryness by heating carefully for one day. Cs_2ZrCl_6 was prepared (13) by dissolving $ZrOCl_2.8H_2O$ in a 20% aqueous solution of hydro-

Table III.1.

Structure types of $A_2B^{4+}F_6$ compounds at ambient temperature and pressure.

H_h = K_2GeF_6 h-structure (10).
H_{hc} = K_2MnF_6 hc-structure (11).
C = K_2PtCl_6 c-structure (12).

	Si	Ni	Co	Mn	Ge	Cr	V	Ti
K	H_{hc}	C		H_h	H_h	H_{hc}	H_h	H_h
Rb	C	C		H_{hc}	H_h	H_{hc}	H_h	H_h
Cs	C	C	C	C	C	C	H_h	H_h

Table III.2.

Structure types of $A_2B^{4+}Cl_6$ compounds at ambient temperature and pressure.

	Hf	Zr	Pb	Te	Bk	Pu	Ce	Np	U	Pa	Th
K	C	C									
Rb	C	C	C	C							
Cs	C	C	C	C	H_{hc}	H_h	H_h	H_h	H_h	H_h	H_h

chloric acid and adding CsCl to the almost boiling solution. The Cs_2ZrCl_6 precipitate was filtered off from the hot solution on a glass filter, washed with a hot 20% aqueous HCl solution and dried in a vacuum desiccator over concentrated sulfuric acid. The high-pressure experiments were carried out in an opposed-anvil apparatus as described by C.J.M. Rooymans (14).

Structural analysis was carried out with a Philips X-ray powder diffractometer using monochromatic (LiF-crystal) CuKα radiation.

III.3. Results and discussion

The results are summarized in Tables III.3. and 4. Cs_2GeF_6 and Rb_2SiF_6 with K_2PtCl_6 c-structure do transform to the K_2MnF_6 hc-structure, but we did not obtain hc-patterns free from reflections due to the c-structure.

The experiments on Cs_2GeF_6 show no obvious relationship between the fraction of the hc-phase formed and pressure, temperature or time. We assume that the material partly reverts to the c-structure after release of pressure, because an X-ray pattern, taken after one week on a sample containing a large proportion of hc-phase, was purely cubic. For Cs_2ZrCl_6 no phase transformation occured at 30 kbars under various conditions, but the hc-phase was almost pure after application of a pressure of 55 kbars. The prediction that the fraction of hexagonal stacking increases with pressure for A_2BX_6 halides contrary to the behaviour of ABX_3 halides has thus been confirmed by the experimental data.

Table III.3.
Preparative conditions and stacking-type.

	pressure in kbars	temperature in °C	time in hours	stacking type [a]
Cs_2GeF_6 c	40	25	1	c(s), hc(s)
	40	400	1	c(s), hc(w)
	40	400	3	c(s), hc(s)
	50	25	1	c(s), hc(w)
	55	400	1	c(s), hc(s)
	55	400	4	c(s), hc(s)
		250	1	
Rb_2SiF_6 c	55	400	1	c(s), hc(w)
	30	25	48	c
	30	300	24	c
Cs_2ZrCl_6 c	30	300	1	c
		25	24	
	55	450	1	c(w), hc(s)

[a] s and w denote strong and weak reflections in the X-ray pattern.

Table III.4.
Lattice constants of the unit cells, c/a-values and references.

	c in Å	a in Å	c/a	reference
Cs_2GeF_6 c	–	8.99	–	15
Cs_2GeF_6 c	–	9.008 ± 0.003	–	[a]
Cs_2GeF_6 hc	10.021 ± 0.007	6.124 ± 0.006	1.636	[a]
Rb_2SiF_6 c	–	8.446	–	16
Rb_2SiF_6 c	–	8.461 ± 0.002	–	[a]
Rb_2SiF_6 hc	9.59 ± 0.03	5.90 ± 0.02	1.625	[a]
Cs_2ZrCl_6 c	–	10.407	–	12
Cs_2ZrCl_6 c	–	10.420 ± 0.006	–	[a]
Cs_2ZrCl_6 hc	12.02 ± 0.02	7.37 ± 0.01	1.631	[a]

[a] This paper

One of us (V.B.) is grateful for permission to carry out part of the experiments at the Philips Research Laboratories, N.V. Philips Gloeilampenfabrieken, Eindhoven, The Netherlands.

References

1. J.A. Kafalas and J.M. Longo, Mat. Res. Bull. **3**, 501 (1968).
2. J.M. Longo and J.A. Kafalas, J. Solid State Chem. **1**, 103 (1969).
3. J.M. Longo and J.A. Kafalas, J. Appl. Phys. **40**, 1601 (1969).
4. Y. Syono, S. Akimoto and K. Kohn, J. Phys. Soc. Japan **26**, 993 (1969).
5. J.M. Longo and J.A. Kafalas, J. Solid State Chem. **3**, 429 (1971).
6. J.M. Longo, J.A. Kafalas, N. Menyuk and K. Dwight, J. Appl. Phys. **42**, 1561 (1971).
7. A.F. Wells,'Structural Inorganic Chemistry', Third Edition, Fig. 121(a), p. 376. Clarendon Press, Oxford, 1967.
8. V. Brandwijk, A.B.A. Schippers and E.W. Gorter, 'Derivation and discussion of crystal structures of compounds ABX_3 and A_2BX_6, Part II. Structural chemistry of ABX_3 halides', to be published.
9. V. Brandwijk, A.B.A. Schippers and E.W. Gorter, 'Derivation and discussion of crystal structures of compounds ABX_3 and A_2BX_6. Part III. Structural chemistry of A_2BX_6 halides', to be published.
10. J.L. Hoard and W.B. Vincent, J. Am. Chem. Soc. **61**, 2849 (1939).
11. H. Bode and W. Wendt, Z. Anorg. Allgem. Chem. **269**, 165 (1952).
12. G. Engel, Z. Krist. **90A**, 341 (1935).
13. G.M. Toptygina and I.B. Barskaya, Russ. J. Inorg. Chem. **10**, 1226 (1965).
14. C.J.M. Rooymans, Philips Res. Reports **23** (Suppl.), 129 (1968).
15. W. Schütz, Z. Phys. Chem. **B31**, 292 (1936).
16. J.A.A. Ketelaar, Z. Krist. **92A**, 155 (1935).

SAMENVATTING

In dit proefschrift werd een poging gedaan om op systematische wijze kristalstructuren af te leiden van verbindingen met samenstelling ABX_3 en A_2BX_6 door uit te gaan van een basisrooster en door hoofdzakelijk kwalitatieve regels, gebaseerd op een elektrostatisch model, te gebruiken (A is een groot kation dat de plaats kan innemen van een anion, B is een klein interstitieel kation, X is een halogeen ion). Eerst werden ideale structuren waarin A en X dezelfde diameter hebben afgeleid voor hypothetische AX_3 verbindingen. Er werd aangetoond dat, als A-A contacten niet zijn geoorloofd in een stapeling van trigonale netten ("dichtstgepakte" lagen), elke laag de samenstelling AX_3 en hetzelfde ordeningstype (patroon) moet hebben. Bovendien mag dit patroon slechts zijn opgebouwd uit de motieven "T" (triangular) of "R" (rectangular) of combinaties ervan. Uitgaande van deze AX_3 structuren werden ABX_3 a en A_2BX_6 structuren afgeleid. De meeste structuren konden worden uitgesloten op grond van een elektrostatisch ongunstige omringing van het anion. Ook afwijkingen van de ideale ABX_3 en A_2BX_6 structuren door variatie in de grootte van de A , B en X ionen werden bekeken.
De afgeleide ABX_3 structuren waarin het A ion groter of gelijk is aan het X ion werden vergeleken met die welke experimenteel werden gevonden voor ABX_3 halogeniden. Ze bleken kwalitatief goed overeen te stemmen. Het was niet nodig om kation-kation binding in te voeren om de verschillende gemengd hexagonaal-kubische stapelingen te verklaren. Voor ABX_3 verbindingen met A ionen die kleiner zijn dan de X ionen bleken de afgeleide structuren ongeveer overeen te komen met de structuren gevonden voor $KMnF_3$ en $GdFeO_3$. De laatste structuur kon echter niet in detail worden begrepen. Voor ABX_3 verbindingen met A ionen die kleiner zijn dan de X ionen kon geen structuur worden afgeleid voor grote en polariseerbare X ionen. In dit gebied was de structuur van NH_4CdCl_3 reeds experimenteel gevonden. Misschien kan deze structuur van een ander basisrooster worden afgeleid. Andere structuren die ook tot dit gebied behoren, maar waarin de B ionen bovendien nog een voorkeur voor een afwijkende coördinatie vertonen, zijn de structuren gevonden voor NH_4HgCl_3 en $CsSnCl_3$. De structuren van $CsCuCl_3$, $KCuF_3$ en $CsGeCl_3$ konden worden verklaard door de bijzondere elektronenconfiguratie van het B ion in aanmerking te nemen. Berekening van de afstanden tussen en in de dichtstgepakte lagen, gereduceerde c/a-waarden en volumes per formule eenheid met behulp van de stralen van Shannon & Prewitt leidde niet tot goede overeenstemming met de experimenteel gevonden waarden. De in de literatuur vermelde structuren voor ABX_3 halogeniden, met inbegrip van de lagere en hogere temperatuur en hogere druk fasen, bleken in de stabiliteitsgebieden te liggen die ruwweg werden aangegeven.

De afgeleide kristalstructuren werden ook vergeleken met de experimentele gegevens over A_2BX_6 halogeniden. Dit werk werd echter niet meer in dit proefschrift opgenomen. Ook hier is de overeenstemming tussen afgeleide en gevonden structuren goed. Aangezien hierin werd voorspeld dat voor A_2BX_6 halogeniden de fractie hexagonaal gestapelde lagen met T-patroon toeneemt met toenemende druk (dit in tegenstelling tot de ABX_3 halogeniden) en hierover geen experimentele gegevens bekend waren, werden door ons enkele hogere druk modificaties van A_2BX_6 halogeniden bestudeerd. De verwachting werd bevestigd.
Concluderend kan worden gezegd dat de in dit proefschrift geschetste methode veelbelovend is om meer inzicht te krijgen in kristalstructuren van anorganische verbindingen en in hun onderlinge samenhang.

OVERZICHT VAN STUDIE

1956-1962	*Gymnasium β, Christelijk Lyceum, Dordrecht.*
1962-1965	*Studie voor kandidaatsexamen Scheikunde, letter F (hoofdvak: Scheikunde, bijvakken: Natuurkunde, Wiskunde, Mineralogie), Rijksuniversiteit, Leiden. Examen op 21 september 1965.*
1965-1968	*Studie voor het doctoraal examen met hoofdvak Anorganische Scheikunde (Prof.dr. E.W. Gorter, dr. W.J.A. Maaskant), bijvakken Theoretische Natuurkunde (Prof.dr. P.W. Kasteleyn) en Godsdienstwijsbegeerte (Prof.dr. H.J. Heering), Rijksuniversiteit Leiden. Examen op 25 november 1968.*
1968-1972	*Promotieonderzoek in de Scheikunde van de Vaste Stof (Prof.dr. E.W. Gorter), Rijksuniversiteit, Leiden. Promotie op 22 november 1972.*

Tijdens mijn studie was ik kandidaat-assistent (1966-1968) en doctoraal assistent (1970-1972) aan de Afdeling Anorganische Scheikunde van de Gorlaeus Laboratoria der Rijksuniversiteit te Leiden.

Het werk in dit proefschrift beschreven is voor het merendeel ontstaan uit langdurige schermutselingen tussen Guus (drs. A.B.A. Schippers) en mij. Verschillende anderen, zoals Rob (drs. J.A.R. van Veen) en Stan (drs. C.J.J. van Loon), die dit werk theoretisch en experimenteel voortzetten, hebben ook in dit proefschrift hun sporen achtergelaten. De vaak moeilijke figuren hebben hun definitieve vorm gekregen onder de handen van de heren M. Pison en J.J. Pot.